A MODEL OF THE MICROCLIMATE IN POROUS SHADE HOUSES

A THESIS SUBMITTED TO THE GRADUATE DIVISION OF THE UNIVERSITY OF HAWAII IN PARTIAL FULFILLMENT OF THE REQUIREMENTS FOR THE DEGREE OF

MASTER OF SCIENCE
IN
AGRONOMY AND SOIL SCIENCE

MAY 1994

By

Haifeng Xia

Thesis Committee:

Elizabeth A. Graser, Chairperson
Richard E. Green
Goro Uehara

We certify that we have read this thesis and that, in our opinion, it is satisfactory in scope and quality as a thesis for the degree of Master of Science in Agronomy and Soil Science.

THESIS COMMITTEE

Elizabeth A Graser

Chairperson

R E Green

Jose Chilvers

This thesis is dedicated to my family.

ACKNOWLEDGMENTS

Financial support from the Governor's Agricultural coordinating Committee is gratefully acknowledged. The support of the Hawaii Anthurium Industry and the cooperation of three commercial anthurium operations, Puna Flower, Hawaii Heart, and Shiroma Farm also are appreciated.

I wish to express my sincere appreciation to Dr. Elizabeth A. Graser for her kind patience and excellent guidance and advice in my course work and research, and friendly and continuous support throughout my academic study and the development of this thesis. I also wish to thank her husband Mr. Barry Lindsey for his assistance in the data collection, building instruments, and his kindly teaching in tool using skill.

Many thanks are given to Joanne Imamura Lichty, University of Hawaii, Hilo for assistance in arranging transportation, and loading and unloading equipment during the field measurements.

Special thanks are given to Drs. Richard Green and Goro Uehara for serving as members of the advisory committee. Their aid and suggestions were invaluable in the completion of this thesis.

I also thank Dr. Ikawa, Mr. Jun Zhu and Mr. Rodolfo Martinez for their assistance in data collection.

Finally, thanks to the Chairman of Graduate Program Dr. Silva and the department secretaries Gayle, Susan, Kathy and Lynne for their kindly assistance in my academic study and research.

ABSTRACT

The first shade-house microclimatic model was developed based on the energy and moisture balances of four shade-house system components -- the shade cloth, inside air, canopy, and soil surface. The transport is parameterized by resistances for small-scale turbulence and by intermittent refreshment for large-scale non-local gusts. The temperature and humidity in a semi-infinite shade house are predicted when the six coupled differential equations based on the energy and moisture balances are simultaneously solved. The model includes liquid-water balances for surfaces. The model requires only weather data, and, if desired, measured shade-house characterization data. Weather data for running the model, inside temperature and humidity data for verifying the model, and energy balance and turbulence data for further development of the model processes were collected in a large commercial shade house near Pahoa, Hawaii from 10 January to 25 March 1992.

TABLE OF CONTENTS

LIST OF TABLES

LIST OF FIGURES

LIST OF SYMBOLS USED IN THE MODEL

Symbols	Explanation	Unit
A_{D1}	amplitude of daily soil surface temperature	°C
a_c	absorption of shortwave radiation by shade cloth	--
A_c	shade cloth fiber area per unit area	m^2
a_f	absorption of shortwave radiation by canopy	--
A_f	projected area of crop on unit area	m^2
A_g	area of soil surface per unit area	m^2
c	subscript for the shade cloth	--
C_a	heat capacity of air	$J\ m^{-3}K^{-1}$
$C_{c,dry}$	heat capacity of shade cloth	$J\ m^{-3}K^{-1}$
$C_{f,dry}$	heat capacity of dry foliage	$J\ m^{-3}K^{-1}$
C_g	heat capacity of the soil	$J\ m^{-3}K^{-1}$
c_w	specific heat of water	$J\ kg^{-1}K^{-1}$
D	drainage for a unit area of the soil layer	kg
D_1	surface soil layer depth	m
D_2	depth of second soil layer	m
D_a	density of air	$kg\ m^{-3}$
dt	time interval	s
D_f	density of the plants	$kg\ m^{-3}$
D_w	density of water	$kg\ m^{-3}$
E_{cia}	water-vapor flux between cloth and inside air	$kg\ s^{-1}$
E_{coa}	water-vapor flux between cloth and outside air	$kg\ s^{-1}$
E_f	evaporation rate of the liquid-water on foliage	$kg\ s^{-1}$
E_{faia}	water-vapor flux between canopy and inside air	$kg\ s^{-1}$
E_{ffa}	water-vapor flux between foliage and canopy air	$kg\ s^{-1}$
E_{gfa}	water-vapor flux between soil surface and canopy air	$kg\ s^{-1}$
E_{iaoa}	water-vapor flux between the inside air and outside air	$kg\ s^{-1}$
es	saturated vapor pressure	kPa
Etr	foliage transpiration rate	$kg\ s^{-1}$
f	subscript for foliage of canopy	--
fa	subscript for air in canopy	--
F_c	area fraction of shade cloth	m^2m^{-2}
Fex	fraction of the volume of inside air that is exchanged	--
F_f	area fraction of crop canopy	m^2m^{-2}
F_g	area fraction of soil surface	m^2m^{-2}
g	subscript for the soil surface	--
G_b	soil heat flux between the surface and the subsoil	W
H	sensible-heat flux	W
H_{cia}	sensible-heat flux between the shade cloth and inside air	W

symbols	Explanation	Unit
H_{coa}	sensible-heat flux between the shade cloth and outside air	W
H_{faf}	the sensible heat flux to the foliage to allow evaporation	W
H_{faia}	sensible-heat flux between the canopy and the inside air	W
H_{gfa}	sensible-heat flux between the soil surface and canopy air	W
H_{iaoa}	sensible-heat flux between inside and outside air	W
ia	subscript for inside air	--
IR	irrigation rate	kg $m^{-2}s^{-1}$
IR_f	irrigation intercepted by a unit area of canopy	kg s^{-1}
IR_g	irrigation intercepted by a unit area of soil surface	kg s^{-1}
k_g	soil thermal diffusivity	m^2s^{-1}
K_g	soil thermal conductivity	$Wm^{-1}oC^{-1}$
L	latent heat of vaporization at T = 20 °C	J kg^{-1}
LA	leaf area	m^2
oa	subscript for outside air	--
P	precipitation	kg $m^{-2}s^{-1}$
P_c	precipitation intercepted by cloth	kg s^{-1}
P_f	precipitation intercepted by canopy	kg s^{-1}
P_g	precipitation intercepted by soil surface	kg s^{-1}
PEC	active surface fraction of shade cloth	--
PEF	active surface fraction of canopy	--
PEG	active surface fraction of soil surface	--
PPT	precipitation	m s^{-1}
q_a	specific humidity of air	kg kg^{-1}
q_c	specific humidity of shade cloth	kg kg^{-1}
q_f	specific humidity of crop canopy	kg kg^{-1}
q_{fa}	specific humidity of air in crop canopy	kg kg^{-1}
q_g	specific humidity of soil surface	kg kg^{-1}
q_{ia}	specific humidity of air in shade house	kg kg^{-1}
q_{oa}	specific humidity of air outside shade house	kg kg^{-1}
$q_s(T)$	saturation specific humidity at temperature	kg kg^{-1}
r_c	albedo of the shade cloth	--
R_c	liquid water runoff from a unit area of shade cloth	kg
r_f	albedo of the crop canopy	--
R_f	liquid water runoff from a unit area of foliage	kg
r_g	albedo of the soil surface	--
r_{hcoa}	resistance to heat transfer from shade cloth to outside air	s m^{-1}
r_{hcia}	resistance to heat transfer from shade cloth to inside air	s m^{-1}

Symbols	Explanation	Unit
r_{hfaia}	resistance to heat transfer from canopy to inside air	s m^{-1}
r_{hgfa}	resistance to heat transfer from soil surface to canopy air	s m^{-1}
r_{hiaoa}	resistance to heat transfer from inside air to outside air	s m^{-1}
RH_{oa}	relative humidity of outside air	%
Rl	longwave radiation	W
Rl_{cs} Rl_{cf} Rl_{cg}	longwave radiation from shade cloth	W
Rl_{gs} Rl_{gc} Rl_{gf}	longwave radiation from soil surface	W
Rl_{fs} Rl_{fc} Rl_{fg}	longwave radiation from crop canopy	W
Rl_{sc} Rl_{sf} Rl_{sg}	sky longwave radiation	W m^{-2}
r_s	stomatal resistance	s m^{-1}
Rs	solar radiation flux	W
R_{sc}	solar radiation flux to shade cloth	W
R_{scf}	solar radiation flux to canopy foliage	W
R_{scfg}	solar radiation flux to soil surface	W
R_{scfgf}	solar radiation reflection from soil surface to canopy foliage	W
R_{scfgfc}	solar radiation reflection from soil surface to shade cloth	W
$R_{scfgfcs}$	solar radiation reflection from soil surface to sky	W
RS	solar radiation flux density	W m^{-2}
RSmean	mean solar radiation flux density	W m^{-2}
RS_{max}	maximum solar radiation density	W m^{-2}
r_{wcia}	resistance to water-vapor transfer from shade cloth to inside air	s m^{-1}
r_{wcoa}	resistance to water vapor transfer from shade cloth to outside air	s m^{-1}
r_{wfaia}	resistance to water-vapor transfer from canopy air to inside air	s m^{-1}
r_{wffa}	aerodynamic resistance to water vapor transfer from foliage to canopy air	s m^{-1}
r_{wgfa}	resistance to water vapor transfer from soil surface to canopy air	s m^{-1}
r_{wiaoa}	resistance to water vapor transfer from inside air to outside air	s m^{-1}
s	subscripts for sky	--
ΔStE_{fa}	water-vapor storage of canopy air	J s^{-1}
ΔStE_{ia}	water-vapor storage of inside air	J s^{-1}
ΔStH_{c}	sensible-heat storage of shade cloth	J s^{-1}
ΔStH_{faf}	sensible-heat storage of canopy air	J s^{-1}

Symbols	Explanation	Unit
ΔStH_g	sensible-heat storage of surface soil	$J\ s^{-1}$
ΔStH_{ia}	sensible-heat storage of inside air	$J\ s^{-1}$
$\Delta StLE_{fa}$	latent-heat storage of canopy air	$J\ s^{-1}$
$\Delta StLE_{ia}$	latent-heat storage of inside air	$J\ s^{-1}$
t	time	s
t_0	shift time	s
T	temperature	°C
T_2	temperature of subsoil layer	°C
T_a	air temperature	°C
t_c	transmission of the shade cloth	--
T_c	temperature of the shade cloth	°C
t_f	transmission of the canopy	--
T_f	temperature of the foliage	°C
T_{fa}	temperature of air in crop canopy	°C
T_g	soil surface temperature	°C
T_{ia}	temperature of air inside shade house	°C
T_{oa}	temperature of air outside shade house	°C
T_s	apparent sky temperature	°C
U	horizontal wind speed	$m\ s^{-1}$
V_c	volume of shade cloth for a unit area	m^3
V_f	plant volume in the crop canopy	m^3
V_{ia}	volume of the inside air	m^3
W_c	amount of liquid water on the shade cloth	kg
W_{cmax}	water-holding capacity for a unit area of shade cloth	kg
W_f	mass of liquid water on a unit area of foliage	kg
W_{fmax}	water-holding capacity for a unit area of canopy	kg
W_g	mass of liquid water in soil for a unit area	kg
W_{gmax}	water-holding capacity of soil for a unit area	kg
z	height or depth	m
z_f	height of the crop canopy	m
z_{sh}	height of the shade house	m
ϵ_c	emissivity of shade cloth	--
ϵ_f	emissivity of foliage	--
ϵ_g	emissivity of soil surface	--
ϵ_s	emissivity of sky	--
σ	Stefan-Boltzman constant	$W\ m^{-2}K^{-4}$
ß	switch function ß = 0 for condensation ß = 1 for evaporation	--
ω	angular frequency	s^{-1}
Θ_{vFC}	volumetric water content at field capacity	$m^3\ m^{-3}$
Θ_v	volumetric water content	$m^3\ m^{-3}$
ψ_g	soil water potential	MPa

CHAPTER 1
INTRODUCTION

1.1 BACKGROUND ON SHADE HOUSES

1.1.1 The Use of Shade in Crop Production

Shading has been commonly employed in the production of nursery, flowering (for example, anthurium and orchid), foliage (for example, tobacco), and root (for example, ginseng) plants to reduce the unfavorable effects of high sunlight for horticultural crops with high value (Barden, 1987). The shade cloth protects plants from excess sunlight, wind, desiccation, and insects, and helps make shade-loving plants flourish (Waggoner et al., 1959). Black or white shade cloth, which is available to provide from minimal to 95% shade, is commonly used for shading.

Shading in this study means the artificial shading from shade cloth, which is made of saran (one kind of thermoplastic resin derived from vinyl compounds) or plant fibers. Various terms have been applied to shading: shade tent, shelter tent, cheesecloth tent, shade canopy, shade cloth, and shade house. The name shade cloth will be used in this thesis for the shading materials which provide the shading; the name shade house will be used to represent the structure of the shading which is made of the shade cloth and some other construction materials.

1.1.2 The Study of Shading Effects on the Microclimate

In the absence of microclimatic data, people have expected various effects from shade cloth. Shade cloth is often expected to reduce temperature and radiation levels during the day, to keep the temperature warmer at night, as well as to increase the humidity level. From the point of view of micrometeorology, shading materials modify the microclimate in the shade house by absorbing and reflecting the incident solar energy and reducing the solar energy load received in the shade house, and by reducing air exchange with the atmosphere. This modification will help to reduce the radiation energy load on the crop leaf, and reduce crop transpiration rates and soil evaporation rates, so presumably the heat and moisture stress on plants will be reduced. Because the growing conditions under shade cloth can enhance crop yield and quality, agrometeorologists have been interested in investigating the modification of the microclimate in shade houses for a long time (Jenkins, 1900; Frear, 1906; Stewart, 1907; Street, 1934; Purdy, 1933; Waggoner et al., 1959; Allen, 1975; Aylor and Taylor, 1982; Stathers and Bailey, 1986; Graser and Amiro, 1991; Graser and Xia, 1994a and 1994b).

Many investigations have found that shade houses increase the inside temperatures while other studies show the opposite. Most investigations of the shade-house microclimate have found that the humidity of the inside air is higher than that outside (for example, Frear, 1906; Purdy,1933;

Waggoner et al., 1959; Allen, 1975; Aylor and Taylor, 1982); soil moisture is increased and soil temperature is decreased by the shade cloth (for example, Frear, 1906; Waggoner et al., 1959; Aylor and Taylor, 1982; Stathers and Bailey, 1986); wind speed is significantly reduced beneath the shade cloth (for example, Waggoner et al., 1959; Aylor and Taylor, 1982; Stathers and Bailey, 1986; Graser and Amiro, 1991; Graser and Xia, 1994a and 1994b); and evaporation and transpiration are less in the shade house (for example, Waggoner et al., 1959; Stathers and Bailey, 1986; Graser and Xia, 1994a and 1994b). These studies, however, vary in the purpose of the research, characteristics of the shade house such as the height and size, the location of the shade house, and the type and the usage of the instruments. As a result of these differences, the different studies are not unanimous in their conclusions about the effect of a shade house on the microclimate.

A number of studies found elevated temperatures in shade houses. Frear (1906) reported that, on days with bright sunshine, the temperature inside the shade house (about 2-m high, size of the shade house was not indicated) was higher than outside. A difference between the inside and outside temperature of 10 °C appeared at 1500 h on 5 September. Stewart (1907) found that the temperature within a shade house (dimensions were not given) was 0.5 to 3 °C warmer at midday than the temperature outside. Stathers and Bailey (1986) studied a ginseng shade house (135 by 155 m, 2

m high) and concluded that air temperature beneath the shade cloth is up to 6 °C higher during the day and 2 °C higher at night than an adjacent open area. According to the microclimatic data in a porous shade house between 10 January and 25 March 1992 on the Big Island of Hawaii, Hawaii, Graser and Xia (1994b) found that the temperature in a shade house (230 by 154 m, 3 m high) was 2.3 °C higher on average than that outside during the midday.

In contrast, other studies found depressed temperatures in shade houses. Purdy (1933) found that on very warm days shade cloth (dimensions were not given) decreased the air temperatures by 1 to 3 °C, but on cool days there was no temperature difference between inside and outside. Waggoner et al. (1959) compared the microclimatic conditions in a tobacco shade house (45 by 55 m, 2.7 m high) with those in an adjacent open area. On a clear day, the house slightly decreased the temperature during the day and decreased the temperature 1.5 to 2 °C at night compared to an adjacent open area. On a cloudy day, the temperature was nearly equal inside and outside. Valli and Young (1963) reported that the mean monthly air temperature was reduced about 1 °C by shade cloth. Allen (1975) reported that the temperature at a 0.40 m height under shade cloth (dimensions were not given) was 3 °C lower than that in open air on 22 August 1971. Frear (1906) and Stewart (1907) reported the night-time air temperature was slightly lower than that in an adjacent open area. Graser

and Xia (1994) also found that the average temperature is 0.6 °C lower than that outside during the night.

Unlike most investigations which report that the humidity of the inside air is higher than that outside, our data show that humidity is lower in the shade house than that at the weather station upwind of the site during the day (Graser and Xia, 1994a and 1994b). Because the conclusions of the other studies are based on the relative humidity which depends strongly on the temperature and no data were presented in the reports, we cannot make a conversion to allow a comparison based on the vapor pressure or other conservative measures of atmospheric humidity.

How does the microclimate in a shade house differ during the day and at night from open air conditions? How does temperature modification by the shade cloth differ among different shade houses? Early work on the microclimate in shade house was limited by the meteorological theory and the observational instruments. Waggoner et al. (1959) said "We shall see if the advances in meteorological theory and instruments will permit a better description of the climate and understanding of the physics of the shade tent." With further developments in meteorological theory and instrumentation, it should now be possible to describe the microclimate of shade houses.

In order to know the effect of shade cloth on the microclimate in a shade house on a physical basis, the energy and mass (water vapor) balance

analysis approach is applied to investigate the solar energy distribution in the shade-house system (Stathers and Bailey, 1986). They conclude that the solar and net radiation were reduced by up to 75% beneath the shade cloth during the day; most of the net radiation was dissipated as sensible heat both above and below the shade cloth; ventilation was also significantly reduced in the shade house. Graser and Amiro (1991) studied the effect of shade cloth on the heat and moisture exchange between inside and outside air in a porous shade house and found that the shade cloth reduces the air turbulence by 2/3 of outside air turbulence in terms of the variance in the vertical velocity σ_w, which was constant with height in the shade house.

1.1.3 Disease Problems in Shade Houses

Recently, the microclimate in shade houses has been hypothesized to favor the development of some crop diseases. For example, the tobacco blue mold, caused by the fungus *Peronospora tabacina* Adam, is stimulated by cool moist microclimatic conditions (Aylor and Taylor, 1982). Aylor and Taylor (1982) suggested that when a plant disease is introduced, it may thrive and become epidemic or decline and disappear depending largely upon the microclimate.

Stathers and Bailey (1986) reported that in commercial operations where a large area is covered by shade cloth, the root zone soil or straw mulch remains wet for extended periods, allowing fungal diseases to become

established and cause extensive damage to the crop.

The anthurium blight epidemic at Hilo, Hawaii caused by the bacterium *Xanthomonas campestris pv. diffenbachiae* (for example, Graser and Amiro, 1991; Graser and Xia, 1994b) has been suspected to result from a warm and humid microclimatic condition in the shade houses. The questions that anthurium flower growers are quite concerned about are: What size and height of a shade house are suitable for growing anthurium flowers, that is, what dimensions result in a microclimate which provides the minimum risk of promoting anthurium blight? What will be the temperature and humidity in a specific size shade house? Are the temperatures and humidities in shade houses near the optimum for blight? To answer these questions we need first to understand how the weather and shade-house design affect the microclimate in shade houses.

1.1.4 Crop Production in Shade Houses

Crop production in shade houses is promoted if the microclimatic conditions are near the optimum for the particular crop.

1.2 NEED FOR A SHADE-HOUSE MODEL

1.2.1 The Need for a Microclimatic Model for Management of Commercial Shade Houses

To make more efficient use of water and to manage the shade-house microclimate to optimize crop yield and quality, a physically based process

model of the shade-house system is needed to predict the outcome of management changes and to serve as the basis for management decisions. These needs cannot be addressed experimentally, because the number of potential management options and year-to-year weather variability exceeds field-based research possibilities. A physically based, process model is necessary so the model will be flexible enough to handle changes in the shade-house system. The model needs to be able to predict based on common meteorological data such as solar radiation, wind speed, air temperature, and humidity to allow widespread use.

An example of how a model could enhance shade-house environment modification and control and the efficient use of resources is in the management of irrigation. High daytime temperatures in shade houses can promote anthurium blight development, and sprinkler irrigation can be used to decrease the high temperature. If the irrigation system is controlled based on a microclimatic simulation model and the irrigation is only given when it is needed, the irrigation water and the energy used for irrigation are used more efficiently than with a clock-based irrigation schedule.

Using the microclimatic model in the management of the shade houses can be expected to bring benefits as use of greenhouse models in the control of greenhouse microclimates has. For example, the microclimate model can be used in the control of the microclimate in greenhouses for calculating the energy requirement so that the energy usage is more

efficient, and for providing a suitable growth environment appropriate for the requirements of valuable crops.

Until this time, no microclimatic simulation model has been developed for shade-house management.

1.2.2 The Need for a Microclimatic Model for Shade-House Design

Because the various factors such as size and height and the properties of the shade cloth that affect the shade-house microclimate can be tested in a well developed shade-house microclimatic simulation model and, not easily by other means, a simulation model of the microclimate of shade-houses microclimate is needed to aid design of shade houses.

1.2.3 The Need for a Microclimatic Model for Shade-House Research

Shade houses are complex systems which consist of many components, processes, and linkages. The energy and mass transfer processes between the components of the system -- the roof, air, crop, and soil -- determine the dynamic and static behavior of shade houses. To represent all components in the system, to describe the exchange processes between these components, and to make accurate predictions of the microclimate, simulation modelling on computers is the only realistic approach.

With a simulation model, the processes in a shade house can be explored in a way not possible in a real system, for example, individual or select groups of variables can be varied and alternate approaches to modeling the system can be studied. This is important because investment in research is often limited.

1.3 OBJECTIVES OF RESEARCH

Although the shade-house microclimate has been studied off and on for almost 100 years and a number of investigations have considered the effects of shade cloth on the microclimate with the purpose of improving the performance of the shade-house system, still the shade-house microclimate has not been investigated and understood thoroughly; and, especially, it has not been described theoretically by mathematical modeling to the extent of the greenhouse microclimate.

Fig. 1.1 shows that the temperature in the middle of the shade house we studied reached a plateau where the horizontal temperature gradient was small, and, thus, the horizontal heat movement was small. Because the horizontal heat movement at the center of the shade house can be neglected, one-dimensional models can be applied to describe the heat and water-vapor exchange in the vertical direction in the plateau area. At the edge of a large shade house or throughout a small shade house in which the temperature does not reach a plateau, a two- or three-dimensional model will

be needed to catch both the horizontal and vertical exchanges of heat and water vapor.

The objective of this study is to:

Develop a component-type simulation model, that can simulate the average temperature and humidity of the shade-house components in semi-infinite, porous-cloth shade houses, based on energy- and mass (water) balance principles, with energy and moisture transfer in the vertical direction between the components of the shade-house system and with average weather data as the input.

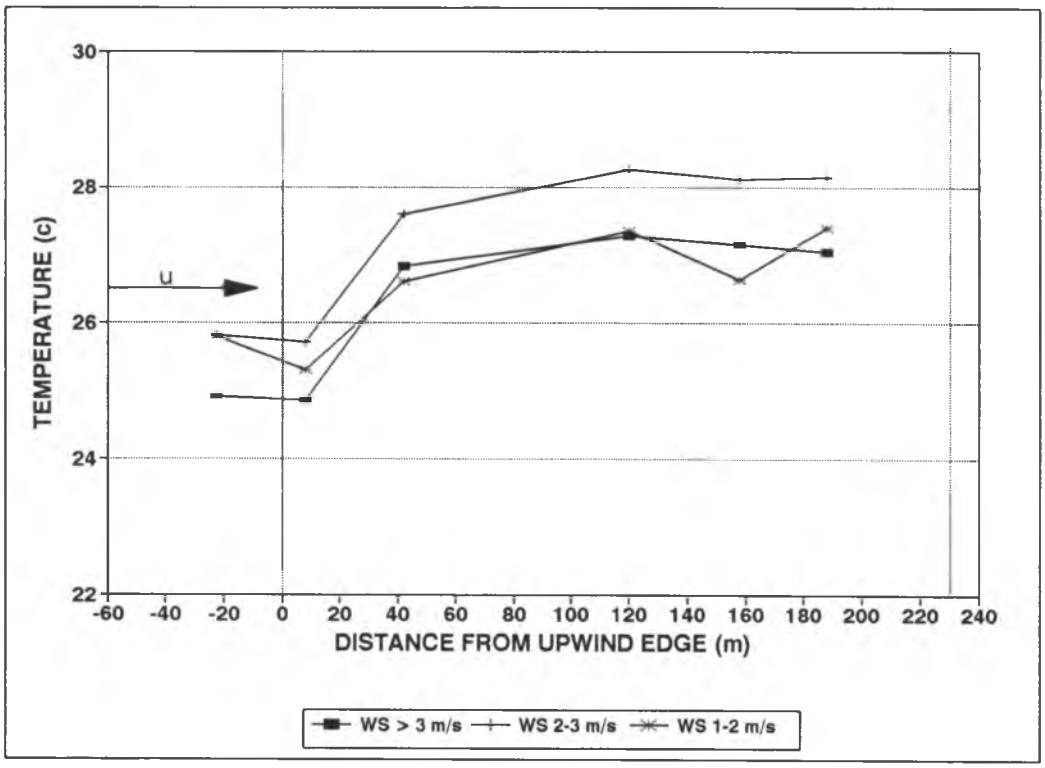

Fig. 1.1 Temperature distribution in a porous shade house (Graser and Xia, 1994a). Solar radiation was greater than 600 W/m² and the wind direction was between 15 and 65° from N. Data were collected between 10 January and 25 March 1992 (see Chapter 3).

CHAPTER 2
LITERATURE REVIEW

2.1 A PHYSICALLY BASED APPROACH TO MODELING

Physically based modeling can allow the mathematical description of the state of a system over time as well as the interaction between components in the system at any specific time. The processes of the interaction among the system components can be described by physically based equations allowing the prediction of the state variables of the components. The shade-house microclimatic model will be based on this approach to simulation modeling. The shade-house system components will be defined; the processes of interaction among the components will be described; and the state variables, such as temperature, water-vapor content, etc., will be predicted.

Physically based models offer the advantage of applicability to systems and regions beyond the system studied. Their development, however, requires detailed knowledge of the processes active in the system. Because there are many previous works on greenhouse models and crop-canopy models, but not on shade-house models, as a starting point for developing a shade-house model, we will consider physically based approaches taken to modeling greenhouses, and crop and forest canopies.

2.2 MICROCLIMATE MODELS FOR GREENHOUSES

2.2.1 Models of the Energy Balance of Greenhouses as a Whole Unit

The energy and moisture balance approach is based on the balance between energy and/or mass flowing into and out of a system. If the fluxes are equal, the system is in steady state; if either the input is greater than the output or the output is greater than the input, the system state will change, that is, storage in the system will change.

Greenhouse microclimatic models involving different amounts of mathematical simplification represent the microclimate of real greenhouse systems. The simplest approach to modeling the greenhouse microclimate is to consider the whole greenhouse as a unit with average conditions. These simple models may also only consider some of the energy-balance components such as the heat gained by solar radiation and the heat lost by convection and conduction due to the temperature difference between the inside and the outside of the shade house.

Udink (1984) gives an example of this simple approach. He considers the greenhouse as well mixed and describes the change in the greenhouse temperature by a heat-storage term. His model can be conceptually expressed as

Heat storage = short-wave radiation

+ heat exchange through roof with the outside air

+ ventilation heat loss

+ heating

Udink did not directly include latent-heat flux, long-wave radiation, and soil heat flux in his analysis, but he thought that the coefficients in his model compensate for them.

2.2.2 Model of the Energy and Moisture Balances of Multiple Greenhouse-System Components

A more detailed modeling approach to the greenhouse microclimate is to consider the energy balance of the greenhouse components separately (for example, Iwakiri and Uchijima 1971; Kimball 1973; Van Bavel et al., 1980, 1981; Alabiso et al., 1984; Arinze et al., 1984). In these approaches, the greenhouse system is often divided into the roof, the inside air, the crop, and the soil. The energy and moisture balance equations, as described for the greenhouse as whole unit in the previous section, are now developed for each of the greenhouse components. Additional energy-balance components such as net radiation, sensible-heat and latent-heat flux are included in these models. In some cases, the soil and crop canopy are divided into several layers when the canopy or soil energy balance is computed (for example, Arinze et al., 1984). In some cases a detailed model of radiative heat transfer is included.

Arinze et al. (1984) establish a greenhouse simulation model based on the assumptions that the air inside the greenhouse is well mixed and the temperature gradients in the inside air are negligible and that soil heat transfer in the soil layer is only in the vertical direction. Their model can be given conceptually as:

Heat storage = solar radiation
+ long-wave radiation
+ convective heat transfer from the inside air
to active or passive thermal storage
+ convective heat transfer from the canopy
to the inside air
+ floor edge and corner heat loss
+ heat loss by ventilation
+ heating

Multiple-component models exist which do not assume the green house is uniform and which handle temperature and moisture gradients (for example, Alabiso et al., 1984).

2.2.3 Modeling the Turbulent or Aerodynamic Flow in Greenhouses

Unlike the energy and moisture balance approach, models of turbulent or aerodynamic flow predict the conditions in greenhouses based on air movement and transport of energy and water vapor. Newton's First Law

states that the motion of a body is determined by forces exerted on it. Starting from the momentum equation, the movement of air and wind turbulence in greenhouses is described based on the balance of the forces on the unit mass of air.

Okushima et al. (1989) give an example of this modeling approach for a greenhouse system. Their model is for an incompressible, three-dimensional turbulent flow in greenhouses with natural ventilation. The model, which predicts the distribution of air flow, that is, the velocity field, and which includes a temperature and gas concentration submodel, can predict the spatial distribution of temperature and humidity or gas concentration for various types of greenhouse structures including with different arrangements of ventilator openings and plants. With the small-scale motions which occur in greenhouses, air movement is predicted by

Local rate of change of wind =

momentum transfer in horizontal direction

+ turbulent kinetic energy

+ pressure

+ vorticity from wind shear

+ buoyancy due to heat forcing

+ friction from the crop canopy

To predict the velocity distribution, the model requires the upstream boundary (the weather conditions in the upwind direction outside of the

greenhouse), the downstream boundary, the side boundary, the upper boundary, the wall boundary at ground level, and the wall boundary of the greenhouse. The submodel of temperature and gas concentration is conceptually given by

Local rate of change of temperature =

Heat transfer by horizontal wind

+ Heat transfer by diffusion

Local rate of change of gas concentration =

Gas transfer in horizontal direction

+ Gas transfer by diffusion

+ Gas source term

+ Gas sink term

2.2.4 Implications of Greenhouse Models for Modeling a Porous Shade House

Although greenhouse models are distinct from shade houses, since they lack the predominate natural ventilation experienced by shade houses, the energy and mass balance approach, particularly considering multiple uniform components with vertical fluxes between them, is applicable to modeling shade houses.

In the middle of a shade house, we can consider the house uniform as Udink did, but there are other problems with applying this model to a shade

house. Natural ventilation through the porous walls is too complicated to be described by ventilation heat loss and a roof resistance.

Similar to a multiple-component model of a greenhouse, a shade-house system also can be divided into the shade cloth, inside air, crop, and soil; each of the components can be described. This will allow us understanding how the behavior of the components affects the shade-house microclimate and how much each component contributes to the shade-house energy and moisture balance. The multiple-component energy- and moisture-balance approach will be applied to develop the shade-house microclimatic model.

Although the aerodynamic turbulent flow model is based on physical principles, it theoretically could describe the wind speed well, it is three dimensional and can handle horizontal transport of heat and gas, and it can handle some natural ventilation, it is not currently considered a practical basis for shade-house modeling. It has several disadvantages. Most important, the turbulent flow model does not model the energy input or output, but instead describes the temperature distribution in terms of a constant field of temperature, so it is not possible to predict the temperature change over time without adding an energy balance to the model. It also requires kinematic and thermodynamic parameters which are unavailable.

2.3 MICROCLIMATE MODELS FOR CROP AND FOREST CANOPIES

2.3.1 The Energy- And Mass-Balance Approach to Models

A common approach to energy and mass balances of vegetative systems is to consider the canopy as a "big" uniform leaf or, similarly, a single component or zero-dimensional object. The energy balance, such as the radiation, sensible-heat, and latent-heat exchange, and the water-vapor balance are developed based on the ideal simplified "big leaf". The temperature is directly solved from the energy balance of the canopy. An advantage of the big-leaf approach is that the canopy model is easy to establish and solve because details of the canopy physical structure, such as the leaf angle distribution and the vertical distribution of the leaf area, are not considered. A disadvantage of the big-leaf approach is that the details about the canopy structure are hidden, and thus the model cannot simulate the profile of the microclimate in the vegetative canopy. Some examples of the big-leaf approach are Arinze et al. (1984) and Deardorff (1978).

Deardorff (1978) presents a microclimatic model for the soil surface with a layer of vegetation based on available temperature and moisture models. The model predicts the microclimatic behavior of the canopy system, such as the canopy temperature, soil temperature, soil moisture, amount of liquid water on the leaves, etc. Conceptually, his one-dimensional energy balance of the soil temperature model can be described by

Heat storage = Energy input - Energy output

where the rate of change in temperature is calculated from the heat storage. Because the soil heat flux at the bottom of the subsoil is assumed negligible, the subsoil temperature model only has one term. The approach for describing the soil surface temperature is called the force-restore method because the soil surface-temperature is forced or driven by the soil heat flux term that connects the soil temperature to the environmental conditions through the soil surface energy balance and it is restored by the term which contains the deep soil temperature. The soil heat flux G is determined from the soil surface energy balance:

$$- G = NR_g + H_g + LE_g$$

where NR_g is the net radiation received by the soil surface, H_g is the sensible-heat flux density from the soil surface, and LE_g is the latent-heat flux density from the soil surface. This method predicts surface temperature well without many soil layers as utilized by many other soil temperature models. Because the method of predicting the soil temperature is based on the energy balance, it should apply at any place and any condition if the energy balance of the soil surface and the soil physical properties are available. A problem with the approach is that the same soil heat flux term is used in both the surface and the subsoil temperature equations. This may be inaccurate because some heat energy would be stored by the surface soil layer.

Although Deardorff's model emphasizes the soil surface temperature, it also includes the soil moisture and canopy water balances, as well as the canopy layer energy balance, because these variables can also affect the soil temperature. The soil-moisture balance includes precipitation arriving at the soil, soil-surface evaporation, water uptake by plants, and water movement between the soil layers. Liquid water on the crop canopy is simply expressed as the balance of precipitation intercepted by the leaf, condensation (dew), and evaporation and transpiration from the leaf. Deardorff gives a scheme to describe the extent of liquid water on the leaf surfaces (this is described in detail in Section 4.1.5). The temperature of the canopy foliage is predicted by solving for the foliage temperature in the long-wave radiation term of the canopy foliage energy balance.

Because of the non-uniformity in the physical structure of the vegetative canopy, a one-dimensional approach to modeling vegetative canopies describes the energy balance for each horizontal layer of the system. Usually the effects of the variation in the incident solar radiation and the wind speed on the energy and mass balances and exchanges are considered. An advantage of the one-dimensional approach is that the radiation balance and the sensible-heat and latent-heat exchanges are calculated for each layer, so the temperature and water-vapor profile in the canopy can be predicted. A disadvantage of this approach is that the velocity profile through the canopy, the stomatal resistance for all layers,

and the canopy structure need to be known (Norman, 1979); these requirements add complexity to the model, so the model is difficult to establish and solve. Inaddition, horizontal energy and mass fluxes are ignored. Some examples of one-dimesional canopy models are Goudriaan (1977), Norman (1979), and El-kilani (1991).

Horizontal advection of sensible-heat and latent-heat fluxes is usually neglected in energy-balance studies in microclimatology because of the difficulty of including it. This necessitates selection of systems to model where the horizontal gradient of temperature and moisture will be negligible. If a large temperature difference exists between the canopy and the surrounding air, the horizontal sensible-heat and latent-heat transfer are large when the surrounding air flows through the crop canopy such as at the edges. For a horizontal temperature gradient $\partial T/\partial x$ of 1 °C per 100 m, the horizontal sensible-heat flux density H may be as large as 100 W m^{-2} based on a wind speed U of 2 m s^{-1} and according to the equation (Thom, 1975; Kanemasu et al., 1979)

$$H = \int_0^{z_R} \partial(C_a\, U\, T)/\partial x \approx z_R\, C_a\, U\, \partial T/\partial x$$

where z_R is the reference height of 4 m above the surface; C_a is the heat capacity of air of 1.25 J m^{-3} K^{-1}.

Because the horizontal energy transport is not necessarily negligible in a vegetative canopy, three-dimensional energy exchange models have been

developed for within canopies to take into account both vertical and horizontal heat exchange (for example, Martsolf and Panofsky, 1975; Kanemasu et al. 1979). The basic equation in this type of model is

$$C_a\,\partial T/\partial t + C_a\,\partial uT/\partial x + C_a\,\partial vT/\partial y + C_a\,\partial wT/\partial z = NR + H + LE + G + J$$

where T is the temperature (°C); x, y, and z are the coordinate directions along and across the prevailing wind direction and the height; u, v, and w are the x, y, and z components of the wind vector; NR is the net radiation flux; H and LE are sensible-heat and latent-heat fluxes in the vertical direction; G is the soil heat flux; J is the source or sink term which includes the heat storage rate in canopy and the latent-heat and sensible-heat storage in the air.

2.3.2 Approach to Modeling Transport in Crop Canopies

2.3.2.1 Gradient Diffusion and Resistance Approaches

Air movement plays an important role in heat, water vapor, and momentum transfer in a crop canopy. The vegetative canopy also has a significant influence upon the exchange processes. In studies of the air movement and the exchange processes of scalars within vegetative canopies, a common approach (for example, Goudriaan, 1978) to describing the exchange of scalars in the vertical direction, gradient diffusion, has been applied in terms of exchange coefficients (k theory)

$$F = -k(z)dC/dz$$

where F is the vertical flux density of the scalar, k(z) is the exchange coefficient at height z, and C is the scalar concentration (heat, vapor density, carbon dioxide concentration, etc.) or in terms of resistance by analog with Ohm's Law (for example, Monteith, 1973; Campbell, 1977)

$$F = [C(z_1) - C(z_2)]/r_a$$

where r_a is the aerodynamic resistance to transport between the path endpoints.

These equations can be used in canopy models to simulate the scalar transport between multiple layers in vertical direction along the gradient of the scalar, if the scalar concentration profile and the profile of the exchange coefficients or the aerodynamic resistances are known. For example, El-Kilani (1991) describes the canopy by three layers. The heat and water-vapor transport between each component is described by the local transport resistance. When the temperature and water-vapor content difference and the resistance to transport between the layers are known, the fluxes of the heat and water-vapor between the layers can be calculated by the above equation.

The resistance approach is often written such that one of the concentrations is at the surface where, for sensible heat flux,

$$H = C_a(T_a - T_s)/r_a$$

where T_a and T_s are the air and the surface temperatures, and r_a is the

boundary-layer resistance to the transfer of the sensible heat, or, for water-vapor flux from a leaf,

$$E = D_a(q_a - q_s(T_s))/(r_w + r_s)$$

where D_a is the density of the air; q_a is the specific humidity of air; $q_s(T_s)$ is the saturated specific humidity at the surface temperature; r_w is the boundary-layer resistance to the transfer of water vapor; r_s is the stomatal resistance. The water-vapor equation assumes the stomatal cavity is saturated at the surface temperature and that the stomata control the loss of this water vapor from the surface.

Various approaches have been used to determine aerodynamic resistances. As an example, the resistance to heat transfer r_h has been measured in laminar forced convection as established in a wind tunnel for a flat plate (Campbell, 1977) as given by

$$r_h = D/[0.66Dh(Re)^{1/2}(\upsilon/Dh)^{1/3}]$$

where D is the characteristic dimension (length) of the surface, Dh is the diffusivity of heat, υ is the kinematic viscosity, and $Re = DU/\upsilon$ is the Reynolds number, U is the horizontal wind speed. This equation can be simplified by substituting the value of thermal diffusivity of air at 20 °C, $21.5 * 10^{-6}$ m^2 s^{-1}, and the υ value of $151 * 10^{-7}$ m^2 s^{-1} as

$$r_h = 307(D/U)^{1/2}$$

The constant 0.66 in the original equation is obtained in the wind tunnel; in the natural atmosphere, the average value is about 1.1 because the

turbulence of air is larger than that in a wind tunnel (Goudriaan, 1977). The aerodynamic resistance in the atmosphere is about 60 to 70% of that predicted from the wind-tunnel equation (Rosenberg et al, 1983). With the value of 1.1 and same values of the Dh and *u*, the resistance to heat transfer in natural atmosphere is given by

$$r_h = 180(D/U)^{1/2}$$

It should be pointed out that the gradient approach and resistance approach are actually the both flux-gradient approaches, where

$$r = \int_{z_1}^{z_2} k(z)\, dz$$

where r is the resistance to heat and water-vapor transport, k is the exchange coefficient, and z is height (Monteith and Unsworth, 1990). The exchange coefficient k can be converted to the resistance r with the assumption that the k is not the function of height, but is an average value in the specific layer for which r is considered, according to

$$r = \Delta z/k$$

where Δz is the thickness of the layer.

It is now clear that the gradient-diffusion approach is often not suitable for vegetative canopies, because countergradient flow cannot be explained by gradient diffusion. In addition, gradient diffusion models provide little insight into the nature of the turbulent diffusion processes within the plant canopy (Campbell 1977). Research into alternative

approaches to transfer processes in vegetative canopies has been an important research direction in the recent years (Wilson and Shaw, 1977; Campbell, 1977; Raupach, 1989). Some examples will be given in the following sections.

2.3.2.2 Turbulent Closure Approaches

Assuming steady-state conditions and horizontal homogeneity in the plant canopy, Wilson and Shaw (1977) expanded the mean flow equation, or the basic momentum equation, in which the Coriolis force is neglected, in terms of mean and fluctuating components and then applied various closure assumptions to get a canopy flow model which can predict the average horizontal wind speed, the momentum transport in vertical direction, and the variance of the wind components in each coordinate direction in the crop canopy. Others have expanded on this approach (such as PawU, 1989, 1985; Meyers, 1987, 1986). Because the method is complicated, it requires turbulence characteristics of the system which are often unavailable, and it needs many closure assumptions to solve the equation, it has not been used widely for modeling energy and water-vapor transfer.

2.3.2.3 Lagrangian Approach

Raupach (1989) and others (for example, Baldocchi, 1990) have applied the Lagrangian 'Localized Near-Field' theory to calculating scalar

transfers in vegetative canopies. The approach to energy and mass transport has been an active area of research in recent years. The concentration distribution C(z) at some distance from a source with a known vertical source strength S(z) is calculated based on system turbulence properties, such as Lagrangian time scale T_L, the variance of the vertical velocity σ_w, and the mean horizontal wind speed u. The basic idea of this approach is that scalars such as heat and water vapor in a canopy are emitted from a large number of vertically distributed point sources, for example, the individual leaves. The motion of the 'marked fluid particles' released from the point sources is individually tracked and the numerous paths are ensemble-averaged to indicate the spread of the scalar. For an ensemble of independent marked particles released at time t_0 ($t = 0$), the effects of persistence are divided into the near field and the far field by the ratio of the travel time t of the ensemble to the Lagrangian time scale T_L. The near field is the region where t much less than T_L and dispersion is dominated by persistence. The far field is the region where t is much greater than T_L and the dispersion is dominated by randomness. Raupach assumed that dispersion in the far-field can be calculated from a gradient-diffusion equation, while near-field or persistence effects can be treated by assuming the turbulence to be locally homogeneous.

2.3.2.4 Non-local Transport and A Parameterization of Gusts With an Exchange Coefficient

Turbulent transport is intermittent with gusts active over short time intervals and much less activity between these events. Because large-scale gusts are responsible for long-distance transport, they can force the transport of heat and water vapor against the local gradient such as a gust can push above-canopy air into a crop canopy against an inverted temperature profile during the day.

The flux gradient (or k theory) approach includes some but not all of the contribution of large length scales (El-kilani, 1991). As a way to take account of the countergradient transport and the intermittency of the turbulent transport within canopy, Goudriaan (1989) and El-kilani (1991) created a new intermittent refreshment approach which parameterizes large-scale non-local gusts with an abruptly changing exchange coefficient, the value of which depends on if a large-scale gust is occurring. The local transport is handled by the flux gradient approach. The relationship between local and non-local transport was described by El-kilani: "A gust comes in and replaces all the air in the canopy with fresh air from above and then a build-up of the temperature and vapor pressure of the air follows due to the delivery of sensible and latent heat from the leaves into the inter-canopy air stream." El-kilani concludes that the build up between gusts is necessary to create a realistic gradient for local transport. He uses a gust frequency of 1/90 Hz in the daytime and of 1/360 Hz at night. El-kilani exchanged a 1 or

0.5 fraction of the air when a gust is in process. The exchange coefficient for local transport within the canopy is determined by

$$K_m = A\, K_{mh} \exp(-n(1-z/h))$$

where K_m is the exchange coefficient within the canopy; K_{mh} is the value of K_m above the canopy ($z = h$); n is an empirical constant, with a typical value of 2 to 3; z is the height; h is the height of the canopy; A is constant to convert between the exchange coefficient for momentum and heat (Goudriaan, 1977), which El-kilani lets be 1. K_{mh} can be calculated from

$$K_{mh} = k\, u^* (z - d)$$

where k is the Von Karman constant, u^* is the friction velocity, and d is the zero-plane displacement. In this model u^* is a function of the time of the day with a minimum constant value during the night of 0.05 m s^{-1} and with a maximum value at noon of 0.28 m s^{-1};

2.3.3 Implications of Crop Models for a Porous Shade-House Modeling

As mentioned in Section 2.2.4, the energy balance approach to predicting the temperature of the shade-house system over time will be used. The intermittent refreshment approach (Goudriaan, 1989 and El-kilani, 1991) is selected for development of the shade-house microclimatic model although the closure and Lagrangian approaches can also handle countergradient flow; the other approaches can be tried later when the model is improved further.

The model will be developed in terms of resistance rather than exchange coefficients because with a component-type model the differences in state between the uniform components is known rather than the gradient along a path through the shade house.

Some of Deardorff's parameterizations and approaches will be adopted to simplify the processes in a way expected to be applicable in a shade-house system: the description of surface water distribution and its evaporation, and the approaches to soil heat flux and the soil water balance.

Large-scale gusts have an important role in the heat and moisture transport in shade houses, like crop canopies. The air exchange with outside air is suppressed by the shade cloth and by a strong, daytime inverted temperature profile below the shade cloth. A large-scale gust is necessary to break through these barriers and transport air between the outside and inside air.

2.4 MICROCLIMATE MODELS FOR SHADE HOUSES

There are not any complete shade-house models in the literature, however, one paper (Aylor and Taylor, 1982) predicts the wind speed in a tobacco shade house using outside wind speed in order to estimate the effect of wind speed on spore transport. Aylor and Taylor investigated the effect of the shade house upon wind with no plants in the shade house and with 2.6 tobacco plants per m^2 (about 1-m tall and with a leaf- area index of

2.0). Wind speed was measured by Thornthwaite sensitive cup anemometers, three mutually perpendicular Gill propeller anemometers, and Anemotherm hot-wire anemometers inside or outside of the tobacco shade house (40 by 50 m, 3 m high).

Aylor and Taylor (1982) described the spatial variation in the average horizontal wind speed in the tobacco shade house by

$$u(x,z) = u_0[1 + \exp(-ßx)] \qquad 0 \leq z \leq 0.4\ z_f$$

$$u(x,z) = u_0[1 + \exp(-ßx)]\exp(\Gamma(z - 0.4\ z_f)) \qquad 0.4\ z_f \leq z \leq z_{sh}$$

where u_0 is half of the wind speed u at $x = 0$, x is the horizontal distance measured from the upwind edge of the shade house, z_f and the z_{sh} are the heights of the crop canopy and the shade cloth (3m), ß and Γ are the empirical constants for which no values were given and no information is available to allow their estimation.

These equations indicate that, as the wind penetrates into the house, due to the effect of friction from crop canopy, horizontal wind will decrease as the distance from the upwind edge increases. Wind in the canopy is assumed to be constant with height, but between the canopy and the shade cloth, wind speed increases with height. Aylor and Taylor think that as the wind penetrates the vegetation within the house, the horizontal wind will slow and this slowing will be compensated for by an average vertical upward wind speed w(x,z) as required by continuity

$$\partial u/\partial x + \partial w/\partial z = 0$$

From the three equations, the vertical wind speed was derived.

Aylor and Taylor did not show how well their wind model works, suggesting it was not based on their data. The relationship between w and u as described by the continuity equation is not appropriate because the resistance from the plant canopy is not considered: the momentum in the x direction cannot be completely converted into the momentum in the z direction because part of the momentum in the x direction is lost when air flow moves through the crop canopy and u decreases. Neither the variance in the vertical velocity σ_w, measured in a porous shade house by Graser and Amiro (1991), which was constant with height nor smoke candle observations show an exponential decrease in wind speed with distance into the house as the equations indicated.

2.5 RELEVANCE OF THE LITERATURE TO SHADE-HOUSE MODELING

Although there is no previous experience with shade-house microclimate modelling, the basic principles and approaches for greenhouses and some crop canopies may be appropriate for modeling a shade house; however, because the purpose or origin of the structures and the materials of which they are made are different, there are some major differences between shade houses and greenhouses and between shade houses and vegetative canopies.

Despite the similarities, a greenhouse has many obvious differences from a shade house. The most obvious difference is that a greenhouse is often a closed system, which is well mixed by fans and hence relatively uniform. The ventilation and heating systems, which act through specific openings, can be treated as non-turbulent duct flow (or simple pipe flow) and these artificial energy-balance components can be very dominant in magnitude making some otherwise important energy-balance components negligible. This keeps the greenhouse more steady, and distinct from outside conditions than a shade house.

A crop or forest canopy is distinct from a shade house in that the leaf area is usually distributed smoothly over height while the shade cloth is an abruptly distributed momentum sink.

A shade house is a modified open system. The shade-house microclimate is more closely coupled to the environment than the greenhouse microclimate. The porous roof and walls allow the creation of a unique microclimate distinct from an open system, similar to how a crop or forest canopy results in a microclimate distinct from an open system but coupled to the atmosphere above. Because the shade-house microclimate depends strongly on the weather conditions and the porous material for constructing the roof, the microclimate in shade houses is less steady and less uniform than in greenhouses. Canopy approaches may be more appropriate for shade houses.

The boundary conditions of a shade-house microclimate simulation model will be quite different from that of a greenhouse model or a canopy model. For example, the boundary conditions of a greenhouse wall or roof for wind speed can be described by $u=0$, $v=0$, and $w=0$, and the ventilation only happens at specific openings, but these boundary conditions will not be appropriate for a porous shade-house wall or roof. When borrowing ideas from greenhouse and canopy models for use with shade houses, we will need to pay particular attention to the assumptions made for the greenhouse and vegetative canopy. We need to determine if the assumptions made in the greenhouse models and the canopy models apply to the shade-house systems.

An energy- and mass-balance model is needed to predict the microclimate over time. As with vegetative canopies, all the energy balance components may be important and need to be considered. The environmental variables, such as short-wave and long-wave radiation, wind, and outside air temperature, will be used to predict the state variables, such as temperature and water-vapor content.

Since greenhouses typically are uniform, they often can be accurately modeled by component-type or one-dimensional models. Similarly, uniform vegetative canopies can be accurately modelled by component or one-dimensional models, although non-uniform canopies, for example, with a wide-row spacing cannot. A two- or three-dimensional model may be

needed to completely or adequately model the microclimate in a shade house with a strong edge effect. Although the edge effect has important management significance, this model will be a component-type model. It will consider only the heat and water-vapor exchange between components in the vertical direction; the horizontal heat and water-vapor exchanges will be ignored. This model will be considered a first step toward developing a multi-dimensional shade-house model capable of addressing all conceivable questions commercial growers or researchers may be interested in.

The approach to modeling energy transfer by sensible and latent heat is one of the main distinguishing aspects among the models and it determines the precise system-state behavior and its agreement with reality. The intermittent refreshment approach offers a simple, conceptually attractive approach for modeling non-local transport in a component-type or one-dimensional model.

CHAPTER 3
MATERIALS AND EXPERIMENTAL METHODS

3.1 STUDY SITE

The shade house studied is located on the Island of Hawaii, Hawaii. It is near the town of Pahoa, where the elevation is near sea level. It is 3.5 hectares in area, with dimensions of 230 m long, 153 m wide, and 3 m high. The ceiling and sidewalls are made of black woven saran shade cloth. The house is constructed with the panels of shade cloth attached to cables which are supported by metal posts; the interior of the house is open and free of obstructions. The shade cloth is considered to provide 80% shade: its measured transmission is reported in Section 3.2.2.1. There is an air gap of about 1 m at both the roof and ground junctions of the sloping side wall for ventilation. The center line of the shade house is oriented 30° from N, near the direction of the prevailing winds, which varied from 345 to 45 ° from N during the day during the study. There is little upwind obstruction and the site is nearly level.

The anthuriums (*Anthurium andraeanum*) are about 0.2-m tall for the new plants to 1.5-m tall for mature plants and the crop is relatively uniform in horizontal distribution. The plants look healthy and strong. The average leaf size is about 0.2 m in diameter. The anthurium plants are estimated to cover about a 0.7 fraction of the surface, and the walkways and roads

together are estimated to cover a 0.3 fraction of the surface. The plant bed is built with volcanic cinder, which is about 0.1- to 0.2-m height above the surface of the walkways.

3.2 MEASUREMENT AND INSTRUMENT ARRANGEMENT

3.2.1 Weather Data For Input Into the Model

The arrangement of the instruments at the study site is shown in Fig. 3.1. A weather station was located at location 1 which is 23 m from the upwind wall. This is the weather data, much of which are needed for input into the model. At the weather station, two 3-cup anemometers (Model 2012, Qualimetrics, Inc., Sacramento, CA 95843) were located at 1.5- and 4.0-m heights, and a low-threshold wind vane (Model 2005, Qualimetrics, Inc.) was mounted at about a 4.5-m height. The precipitation was measured by a tipping-bucket rain gage (TE525 Tipping bucket rain gage, Campbell Scientific, Inc., Logan, UT 84321). The solar radiation was measured with a pyranometer (LI-200SZ, LI-COR, Ltd., Lincoln, Nebraska 86504) at a 4-m height. Temperature and relative humidity were measured at 1.5- and 4.0-m heights by a combination temperature and relative-humidity sensor (HMP 35A, Vaisala, Helsinki, Finland, with modifications by Campbell Scientific, Inc.). 12-plate Gill radiation shields were used to protect the temperature and relative-humidity sensors from solar radiation and rain. Leaf wetness was measured as described in Section 3.2.3. Of this data, neither the wind

direction and leaf wetness, nor the wind speed, temperature and humidity at 1.5 m are necessary model inputs; all of the other weather data are. All sensors at the weather station were connected to a datalogger (Model 21X, Campbell Scientific, Inc.) with a 10-s scanning rate. Thirty-min averages were calculated. A multiplexer (Model AM416 4 x 16 Relay Multiplexer, Campbell Scientific, Inc.) was used in between the datalogger and the temperature and humidity and the leaf wetness sensors.

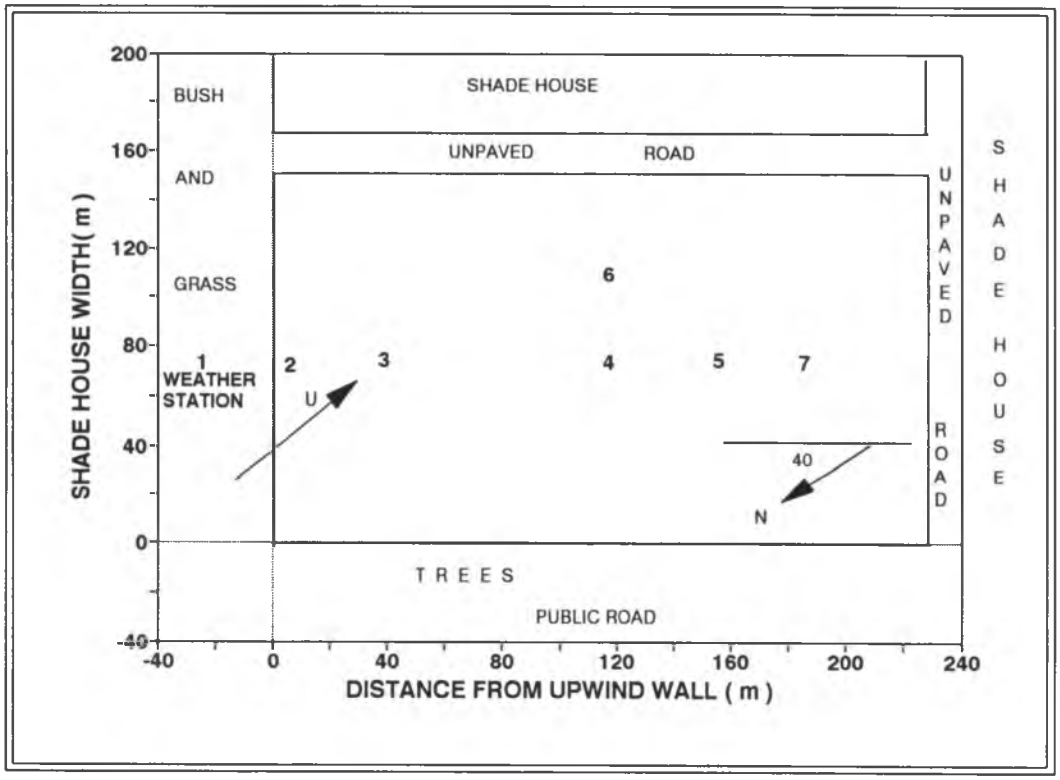

Fig.3.1 Shade-house size and instrument locations.

3.2.2 The Shade-House-System Characteristics for Input into the Model

3.2.2.1 The Characteristics of the Shade Cloth

The characteristics of the shade cloth for use in the model are listed in Table 3.1; an explanation of how this data was determined follows.

Table 3.1 The characteristics of the shade cloth.

t_c	r_c	ϵ_c	V_c m^3 $*10^{-5}$	$C_{c,dry}^*$ $Jm^{-3}K^{-1}$ $*10^6$	W_{cmax} kg $*10^{-2}$	z_{sh} m
0.17	0.06	0.91	1.75	0.5	9.6	3.0

* An equation is given in the text for the wet-cloth case

In Table 3.1, t_c and r_c are the transmittance and the reflectance of the shade cloth measured by a downward facing Eppley pyranometer (Model 8-48, Eppley Black and White Pyranometer, The Eppley Laboratory, Inc. 12 Sheffield Ave., Newport, R. I. 02840, U.S.A.) above the house (RS_{cs}) and a Licor pyranometer above the shade house (RS) for short-term measurement of reflectance and an Licor pyranometer both above (RS) and below the cloth (R_{in}) for long-term measurement of transmittance.

$$t_c = R_{in}/RS$$

$$r_c = RS_{cs}/RS$$

where RS is the measured solar radiation flux density at the weather station; R_{in} is the measured solar radiation flux density in the shade house at station 4; RS_{cs} is the measured solar radiation reflected from shade cloth back to the sky. The reflectance measured above the shade RS_{cs} house is not just

the reflectance of the cloth, because the radiation received by the sensor includes both the radiation reflected from the shade cloth and the radiation reflected from the surfaces beneath the shade cloth. (Stacked layers of cloth would give a better value than shade cloth in situ).

ϵ_c is the emissivity of the shade cloth. It was measured over the house with a downward-facing infrared thermometer (Model 4000, Everest Infrared Transducer, Interscience Inc., Tustin, CA) and a thermocouple (Type T, copper-constantan, 0.0001 m or Gauge 30, Omega Engineering, Inc., One Omega Drive, Box 4047, Stamford, CT 06907). According to the Stephan-Boltzman law

$$RI_c = \sigma \epsilon_c T_c^4$$

where RI_c is the long-wave radiation from the shade cloth; σ is Stefan-Boltzman constant; ϵ_c emissivity of the shade cloth; T_c is the temperature of the shade cloth, and

$$RI_{c+f+g} = \sigma T_{IRT}^4$$

where RI_{c+f+g} is the longwave radiation from the cloth, ground, and foliage viewed by the infrared thermometer; 1 is the emissivity used to estimate the shade-cloth temperature by the infrared thermometer; T_{IRT} is the shade-cloth temperature measured by infrared thermometer. If the longwave radiation from the cloth is assumed to be all the infrared thermometer sees ($RI_c = RI_{c+g+f}$) and the cloth temperature is assumed to be precisely measured

by the thermocouple (see Section 3.2.3 where thermocouple precision is discussed),

$$\sigma\epsilon_c T_c^4 = \sigma T_{IRT}^4$$

so the emissivity of the shade cloth is given by

$$\epsilon_c = (T_{IRT}/T_c)^4$$

This measurement includes errors both due to the longwave radiation the infrared thermometer receives from the canopy and the ground below the porous shade cloth instead of the cloth and due to the radiation error associated with the large thermocouple used to measure the cloth temperature. Nevertheless, 0.91 seems to be a reasonable ϵ_c when compared with published values for other surfaces. (Stacked layers of cloth would give a better value than shade cloth in situ).

V_c is the volume of the shade cloth for a unit of horizontal area. It was measured by water displacement with a graduated cylinder. When the shade cloth was in the water, the cylinder was shaken or stirred for a few minutes to release the air on the cloth. The increase in the volume of water after the cloth was inserted is the volume of the shade cloth.

The estimated heat capacity of the dry shade cloth $C_{c,dry}$ is $0.5*10^6$ J m^{-3} K^{-1}; this value is similar to plastics or peat soil. The heat stored by the shade cloth per unit rate of temperature change $\Delta StH_c/(dT_c/dt)$ must be calculated depending on the amount of liquid water standing on the cloth W_c according to

$$\Delta StH_c/(dT_c/dt) = A_g W_c c_w + C_{c,dry} V_c$$

where A_g is a unit area and c_w is the specific heat of water, $4.18*10^3$ J kg^{-1} K^{-1}.

W_{cmax} is the water-holding capacity of the shade cloth. It was measured by weighing the cloth after it was wetted and allowed to drain briefly and without disturbance. In situ, W_{cmax} may be less than the value measured in the laboratory due to the effect of wind.

z_{sh} is the height of the shade house.

3.2.2.2 The Characteristics of the Crop Canopy

The characteristics of the crop canopy for use in the model are given in Table 3.2; an explanation of how these data were determined follows.

Table 3.2 The characteristics of the crop canopy.

t_f	r_f	ϵ_f	V_f m^3m^{-2} $*10^{-2}$	$C_{f,dry}$[a] $Jm^{-3}K^{-1}$ $*10^6$	LAI $m^{-2}m^{-2}$	z_f m	Wfmax kg $*10^{-2}$
0.36	0.20	0.95	0.33	3.85	1.7	1.2	4.3

a An equation is given in the text for the wet foliage case

If the vertically projected area of the anthurium plants is estimated to cover about a 0.7 fraction of the surface and the walkways and roads together are estimated to cover a 0.3 fraction of the surface (Section 3.1), the average transmittance of the anthurium canopy is calculated by

$$t_f = I/I_0 * 0.7 + 0.3$$

where I and I_0 are the radiant flux density below and above the crop canopy as measured by an Eppley pyranometer in a short-term test to give the transmittance through the canopy gaps.

The reflectance of the canopy r_f was measured by the Eppley pyranometer in a short-term test.

The emissivity of the crop canopy, ϵ_f is adopted from the literature (Deardorff, 1978; Oke, 1991).

V_f is the volume of plants per unit ground area. It is estimated by

$$V_f = FW_f / D_f$$

where FW_f is the fresh plant weight per unit ground area which is estimated to be 3 kg; D_f is the density of plants and it was determined by weighing and water displacement for a plant sample to be 920 kg m^{-3}.

The heat capacity of the crop when the leaf surfaces are dry, $C_{f,dry}$ is calculated by

$$C_{f,dry} = D_f c_w$$

where c_w the specific heat of water, since the anthurium plant is composed mainly of water. The heat stored by the foliage per unit rate of T change $\Delta StH_{fa}/(dT_{fa}/dt)$ must be calculated as a function of the amount of liquid water standing on the foliage W_f according to

$$\Delta StH_{fa}/(dT_{fa}/dt) = D_f c_w V_f + A_g W_f c_w$$

The leaf area index of the anthurium crop, LAI, was estimated by the Beer-Bougher Law (Rosenberg et al., 1983) based on the crop transmittance t_f

$$LAI = -\ln(t_f)/k_f$$

where k_f is the extinction coefficient for the plant leaves with a value of 0.3 to 0.5 for plants with vertical leaves, or a value of 0.7 to 1.0 for plant with horizontal leaves (Rosenberg et al., 1983). A value of $k_f = 0.6$ was used in the estimation of LAI.

The height of the anthurium canopy z_f was the plant height at the middle of the shade house at location 4 in Fig. 3.1, where the energy balance instruments were located. The canopy height varied from 0.2 to 1.5 m at other locations (Section 3.1).

The surface water-holding capacity of anthurium plants W_{fmax} was determined from data for an individual plant by

$$W_{fmax} = W_{pmax} / LAp * LAI$$

where LAp is the leaf area of the individual anthurium plant measured by a leaf area meter (Model LI 3100, Licor, Ltd., Lincoln, Nebraska 86504); and W_{pmax} is the maximum mass of liquid water which can stand on the test plant's leaves; and LAI is the leaf area index.

3.2.2.3 The Characteristics of the Soil Surface

The characteristics of soil surface for use in the model are given in Table 3.3; an explanation of how these data were determined follows.

Table 3.3 The characteristics of the soil surface.

r_g	ϵ_g	$\Theta_v(t_0)$ $m^3\ m^{-3}$	Θ_{vFC} $m^3\ m^{-3}$	C_g $Jm^{-3}K^{-1}$ $*10^6$	K_g $Jm^{-1}s^{-1}K^{-1}$	k_g m^2s^{-1} $*10^{-6}$	d m	A_{D1} °C
0.03	0.95	0.259	0.271	1.50[a]	1.486[b]	0.67	0.135	4.12

a Value of C_g for $\Theta_v(t_0)$; Equation: $C_g(\Theta_v) = 4.16*10^5 + 4.186*10^6*\Theta_v$
b Value of K_g for $\Theta_v(t_0)$; Equation: $K_g(\Theta_v) = 0.4186 + 1.6744*\Theta_v^{1/3}$

The "soil" in the shade house is not soil in the usual sense (although we will use the word soil to describe it), but fresh cinders imported from a volcanic area. There is no organic fraction and most of the material is greater than 0.002 m in size, sometimes reaching several centimeters across. Cinder is the media commonly used in shade houses.

r_g is the reflectance of the soil-surface layer, which was measured with an Eppley pyranometer in a short-term study; the emissivity of the soil ϵ_g is from the literature (Deardorff, 1978; Oke, 1991).

According to laboratory measurements in which the soil was saturated and allowed to drain for a few minutes (n = 5), the average volumetric water content at field capacity for the volcanic cinder, Θ_{vFC}, is 0.271 ± 0.017 $m^{-3}\ m^{-3}$. Soil samples were taken from the shade house in the morning on 14 January 1992. Because the soil is loose and coarse, we pushed the moisture can into the soil, removed the soil from around the can, and cut the soil at the lip of the can. The height of the can is 0.05 m and the diameter is 0.069 m. Six samples at depth 0 to 0.05 m and six at depth

0.05 to 0.10 m were taken for measurement of the soil water content and the soil bulk density. The soil bulk density D_b is 500 kg m^{-3} and the volumetric water content Θ_v was 0.259 $\pm$ 0.025 m^3 m^{-3} (n = 12). Since irrigation is applied several times a day and rain occurs frequently in this area, the soil water content in the shade house is near to that at field capacity. This measured value of volumetric water content is thought to represent the usual wet state of the soil due to the daily afternoon irrigation. This value is used to initiate the model, $\Theta_v(t_0)$.

Based on the measured bulk density 500 kg m^{-3} and the estimated particle density of the mineral fraction D_m 3000 kg m^{-3} (assuming Fe, Al, and Mn content) (G. Uehara, Personal communication), the pore fraction of the cinder soil is calculated by

$$x_{pore} = 1 - D_b/D_m$$

which yields 0.833.

The heat capacity of the soil, C_g can be calculated by

$$C_g = x_w C_w + x_m C_m + (x_{pore} - x_w) C_a$$

where x_w and x_m are the volume fractions of the water and the mineral components of the soil; C_w, C_m, and C_a are the heat capacities of the water, the mineral, and the air. The "soil" did not have an organic component. The heat capacity of the mineral component for the volcanic cinder is 2.49 $*10^6$ J m^{-3} K^{-1} (calculated from the specific heat is 830 J kg^{-1} K^{-1} (G. Uehara,

Personal communication) and the particle density). The contribution of the air component is negligible.

$$C_g = 4.186*10^6\ \Theta_v + 0.167*2.49*10^6$$

$$= 0.416*10^6 + 4.186*10^6\ \Theta_v$$

Due to its large porosity, the heat conductivity of the volcanic cinder soil K_g will largely depend on its water content. Deardorff (1978) pointed out that the soil properties used in his soil temperature model appear to depend more upon soil moisture than soil type and empirically he expressed the heat conductivity as a function of the soil water content,

$$K_g = 0.4186 + 1.6744\ \Theta_v^{1/3} \quad [J\ s^{-1}\ m^{-1}\ K^{-1}]$$

This equation, based on a comparison with the data of van Duin (1963 from Jury, 1991), is closest to values for sand (Fig. 3.2).

Two methods will be used to estimate the soil heat diffusivity, k_g. The first method to determine the k_g is by using the measured maximum and minimum soil temperatures at two different depths according to a method presented by Jury (1991). The principle of the method is that the amplitude of soil temperature decreases as the depth into the soil increases. The formula for calculating k_g is given by

$$k_g = \pi\ d^2/86400$$

where d is the damping depth,

$$d = (z2 - z1)/\ln[(Tmax(z1) - Tmin(z1))/(Tmax(z2) - Tmin(z2))]$$

where Tmax(z) and Tmin(z) are the maximum and minimum daily soil

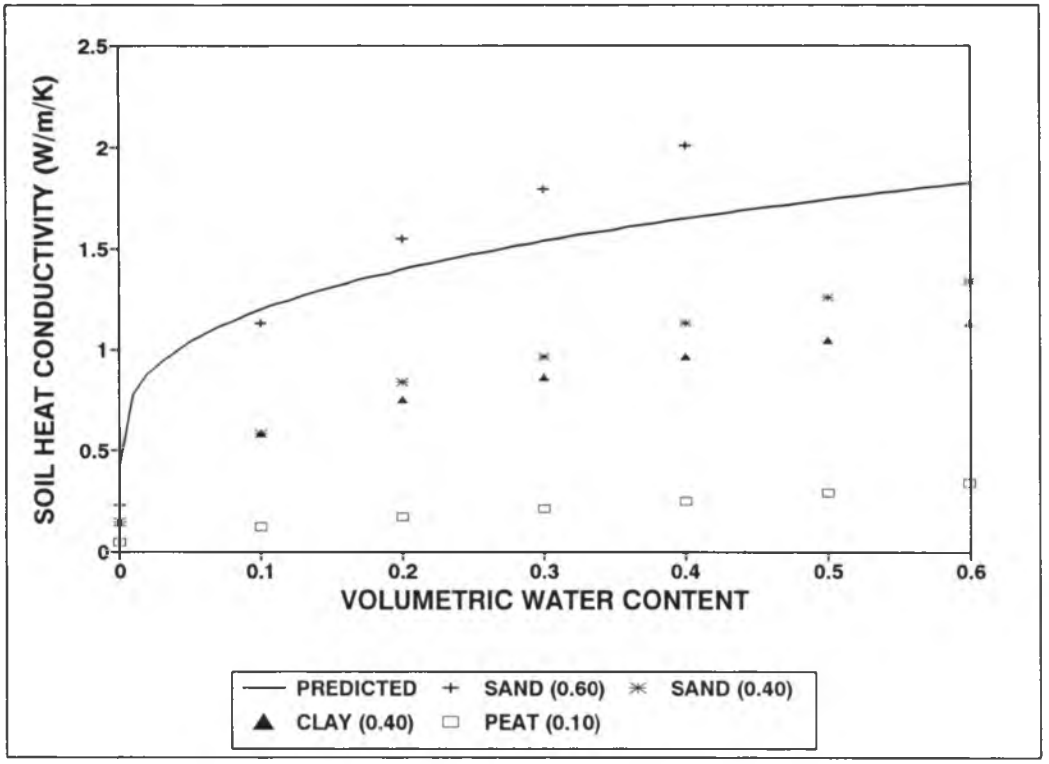

Fig. 3.2 Soil heat conductivity calculated as a function of water content using a generic equation developed by Deardorff (1978) and the heat conductivity of various soil types (data of van Duin from Jury, 1991 with correction). The numbers in parentheses refer to the volume fraction of the solid phase.

temperature at depth z. For measured maximum and minimum soil temperatures at depths of 0.005 and 0.03 m on 12 January 1992,

$$T_{max}(0.005\ m) = 24.1\ °C \quad T_{max}(0.03\ m) = 23.2\ °C$$

$$T_{min}(0.005\ m) = 15.8\ °C \quad T_{min}(0.03\ m) = 16.3\ °C$$

The damping depth and the heat diffusivity for the volcanic cinder soil are

$d = 0.135$ m

$k_g = 0.67 * 10^{-6}$ m^2 s^{-1}

The second method to calculate k_g is to use estimates of the soil heat conductivity, K_g, and soil heat capacity, C_g, according to

$k_g = K_g/C_g$

For a volumetric water content of 0.259 m^{-3} m^{-3} and using the heat capacity and the heat conductivity equations, the thermal diffusivity for the cinder soil in the shade house is

$k_g = 0.99 * 10^{-6}$ $m^2 s^{-1}$

Both approaches to determining k_g give very similar values, suggesting that the value for thermal diffusivity is reliable and also suggesting that the method for calculating the thermal conductivity is reliable for this soil.

The average amplitude of the soil surface temperature, A_{D1}, is obtained from the soil temperature measured at the depth of 0.005 m under the anthurium crop canopy according to

$A_{D1} = \{\Sigma 0.5[Tmax(0.005\ m) - Tmin(0.005\ m)]\}/n$

where Tmax(0.005 m) and Tmin(0.005m) are the maximum and the minimum temperature during the day, n is the number of days (n = 69).

3.2.3 Monitoring Data In the Shade House For Testing the Model

Monitoring data were collected in the shade house at six locations between 10 January and 25 March 1992 (Fig. 3.1). At each location, the temperature and humidity sensors (same as the sensors at the weather station), protected by a 12-plate radiation shield, were at a 1.5-m height above the ground. The temperature and humidity at location 4 is appropriate for the model testing because it is well away from edge effects (Section 1.3; Fig. 1.1).

A leaf wetness sensor (Model 237, Leaf Wetness Sensor, Campbell Scientific, Inc., Logan, UT 84321, painted with white latex primer) was installed at a 1.2-m height to measure wetting time. The angle between the vertical and the normal to the plane of the leaf wetness sensor was 45° so the wetting time for the sensors is similar to the wetting time of the leaves. These sensors were not field calibrated and were not quantitative.

The temperature, humidity, and leaf wetness in the shade house were monitored with the same datalogger as that at the weather station (Section 3.2.1).

The temperature profile was measured near location 4 at the center of the shade house where temperature is uniform horizontally. Fourteen thermocouple (Type T, copper-constantan, Omega Engineering, Inc.) were installed: three thermocouple with a 0.00003-m diameter (0.001 inch) were positioned 1.5, 1.0, and 0.5 m above the shade cloth; one thermocouple

with a 0.0001-m diameter (Gauge 30) was attached with adhesive (Scotch Super Strength Adhesive) to the underside of the cloth; six thermocouples with a 0.00003-m diameter were evenly distributed between the shade cloth and the top of the canopy at 2.4, 2.1, 1.8, 1.5, 1.2, and 0.9 m; four thermocouple with a 0.0001-m diameter were used to measure soil temperature at 0.005-m and 0.03-m depths in a walkway and under the plants. The temperature profile data were collected by another datalogger (Model 21X) with a scan rate at 10-s; 30-min means were calculated.

Thermocouple of the same size as those used to measure the temperature profile were thoroughly tested to determine the magnitude of radiation error to be expected. The test results show that the thermocouples with a diameter of 0.00003 m do not have a radiation error when they are exposed to direct solar radiation over a range of wind speeds as experienced in an outdoor test, and the thermocouple with a diameter of 0.0001 m has a radiation error of 0.5 to 1 °C depending on the wind speed. Because the thermocouple used to measure the cloth temperature was underneath the shade cloth, which has a transmittance of 0.17, the radiation error should be much smaller than under direct solar radiation. In addition, the thermocouple was securely attached with adhesive to the shade cloth, so the heat conductivity between the cloth and thermocouple should keep the thermocouple near the cloth temperature. The soil thermocouple, of course, are not subject to radiation error.

The temperature measured by the HMP 35A temperature sensor at location 4 did not have an error because it agreed well with the temperature measured by a thermocouple with a 0.00003-m diameter at the same place (the average temperature difference between 22 and 25 March 1992 was only 0.15 °C), although it did not agree well with the temperature at a 1.5-m height in the temperature profile near to location 4 (the average temperature difference between 22 and 25 March 1992 was 0.74 °C).

In short, the cloth temperature and air temperature are reliable indicators of the shade-house conditions and are appropriate for model testing.

3.2.4 Turbulence Characteristics For Model Development

Sonic anemometers were occasionally used to measure the instantaneous horizontal and vertical wind speed and temperature in and around the shade house from which turbulence properties can be calculated. Three one-dimension sonic anemometers were used in 1991 (Model CA27 Sonic Anemometer and Fine Wire Thermocouple, Campbell Scientific, Inc., Logan, UT 84321), and two three-dimensional sonic anemometers were used in 1992 (Three-Axis Sonic Wind System SWS-211/3V, Applied Technologies, Inc., Boulder, CO 80301). Data collected in 1991 are mentioned in the literature review. Noise in the 1992 data (due to

manufacture grounding problems which were corrected later) made a number of the data sets less reliable and of limited usefulness.

Smoke candles were occasionally used to visualize the movement of air in the shade house, although it is not a quantitative measurement. The smoke candles were used outside of the upwind wall, inside the shade house and above the shade house to see how the air passes the shade cloth in horizontal and vertical directions, and to determine the approximate speed of air movement in the shade house.

3.2.5 Energy-Balance Measurements for Model Development

The energy balance above and within the shade house was measured by the eddy correlation method during the monitoring data collection period on 11 and 14 January 1992 and 24 March 1992. Within the shade house, a net radiometer (Model Q6, Radiation and Energy Balance Systems, Inc. P.O. Box 15512, Seattle, WA 98115-0512) was located at a 2.5-m height. The instrument could be located near the uniform cloth, but it needed sufficient height to view an average surface with the strong surface row pattern of anthuriums and soil. A one-dimensional sonic anemometer (Model CA27, Sonic Anemometer and Fine Wire Thermocouple, Campbell Scientific, Inc.) and a Krypton hygrometer (KH20 Krypton Hygrometer, Campbell Scientific, Inc.) were located at the same height as the net radiometer to measure the sensible-heat and latent-heat flux densities within the shade

house. A second set of the same instruments were located 1.5 m above the shade cloth to measure the energy fluxes outside of the shade house.

The combination method (Tanner 1963) was used to measure the surface soil heat flux under the plants and in the walkway to obtain a good spatial average. At each position, two thermocouples (described in Section 3.2.3) were used to measure the temperature at 0.005- and 0.03-m depths to calculate the heat storage in the soil. Soil-heat-flux plates (Heat Flow Transducer 1, Radiation and Energy Balance Systems, Inc.) were placed at a 0.05-m depth at each position. The measured soil heat flux together with the surface heat storage gives the soil heat flux according to

$$G_0 = C_g [\Delta z_1 (T_{z1,t+dt} - T_{z1,t}) + \Delta z_2 (T_{z2,t+dt} - T_{z2,t})]/dt + G_{plate}$$

where z_1 is the depth of the thermocouple in the surface soil layer or 0.005 m, z_2 is the depth of the thermocouple in the subsoil layer or 0.03 m; Δz_1 and Δz_2 are the thicknesses of the surface soil layer, or 0.01 m, and the subsoil layer, or 0.04 m; G_{plate} is the measurement by the soil heat flux plate at the depth of 0.05 m; C_g is the soil heat capacity.

Three infrared thermometers (Everest Model 4000, IR Transducer, Interscience Inc., Tustin, CA) were used to measure the average crop canopy and soil temperature, the shade cloth temperature viewed from below, and the apparent sky temperature, respectively. (It is now realized that due to the atmospheric window this is not a reliable approach to

determining the apparent sky temperature). Unfortunately, the sensors were damaged by rain and did not provide any data.

The energy-balance sensors were monitored with dataloggers (Model 21X, Campbell Scientific, Inc., Logan, UT 84321) at a 10-Hz scanning rate for w, T, and qv, and a scan rate at 1-Hz for net radiation, soil heat flux, and the infrared thermometers. The datalogger covariance subroutine was used for calculations. Ten-min means were calculated.

CHAPTER 4
DESCRIPTION OF THE MICROCLIMATIC MODEL

4.1 MODEL SYSTEM DESCRIPTION

4.1.1 General Overview of the Model

The purpose of this model is to predict the temperature and humidity of the four uniform shade-house components -- shade cloth, inside air, plant canopy, and soil surface -- over time for a semi-infinite, porous-cloth shade house. This model is based on the energy and mass balances of the components using only normal weather data and shade-house descriptions as the model inputs. The system of coupled differential equations for the temperature and humidity of each shade-house component is solved simultaneously by the Runge-Kutta numerical integration method.

Because transport can be countergradient in porous shade houses (Graser and Amiro, 1991), the heat and water-vapor transport is simulated by the resistance approach for local transport by small-scale turbulent diffusion exchange along gradients (for example Goudriaan, 1977) and by intermittent refreshment by large-scale gusts for long-distance transport as described by Goudriaan (1989) and El-kilani (1991). The long-distance transport is only used to transport the heat and water vapor between the inside air and the outside air above the shade cloth. Periodic step changes in the resistance cause this transport to be intermittent. Since the equations

in the model system are coupled, the gust effect reaches other system components because the gradient of temperature and humidity between those components and the inside air is increased when the gust is in process. As the gradients between the inside air and the other system components become small between gusts, the exchange of heat and water vapor gradually becomes smaller. The long-distance transport causes the periodically large temperature and humidity gradients; and its intermittency increases the magnitude of the sensible-heat and latent-heat exchange and its reach to other system components.

4.1.2 Definition of System Components

The shade-house system is represented by four components: the shade cloth (in the model, it will be represented by the lowercase letter c), the inside air (ia), the crop canopy (f for the foliage surface, and fa for the air in the foliage), and the soil surface (g for ground). This model will not describe variation in the horizontal and vertical dimensions, such as edge effects or temperature and humidity profiles, but it will assume each of the components are internally uniform. As the driving forces, the environmental factors of outside air (oa) and sky (s) also are included in the model.

The definition of the shade-house model system components are given below:

The **SHADE CLOTH** (c) is the top boundary of the shade-house

system. As controlled by its porosity, it reduces the air exchange between the inside air and the outside air. It is assumed that the shade cloth has uniform temperature and that there is no heat movement horizontally within the fibers of the shade cloth. The shade cloth is considered to include liquid water when it is wet; it is not considered to contain air in the pores, but, instead, the pore air is associated with the outside and inside air. No latent-heat (or, equivalently, water-vapor) storage is considered to be associated with the shade cloth. The humidity of the pore air is considered associated with the humidity of the outside or inside air depending on which is being considered.

The **INSIDE AIR** (ia) is between the shade cloth and the crop surface in the shade house. Its properties, for example temperature and specific humidity, are assumed to be uniform in all direction in this model. The inside air is important as the mobile fluid in the shade-house system for non-radiative energy and mass transfer between the shade-house components.

The **PLANT CANOPY** is considered uniform horizontally and vertically. The roads and the regularly spaced walkways between the plant rows will not be considered separately but as averaged with the plants. The plants are assumed to be of one age, one size, one variety, one height, and one leaf size. The plant canopy includes the foliage surface (f) and the air in the plant-canopy space (fa). The foliage and air are treated as having the same properties for the energy balance. The foliage is recognized as a source for

the humidity balance. Assuming the temperature of the foliage and air are equal eliminates one coupling between the energy and water-vapor balances (Section 4.2.2).

The **SOIL SURFACE** (g) is the bottom boundary of the shade-house system. It is considered to be underlying a uniform plant canopy and to be uniform itself. The surface layer represents the very surface of the soil and, consequently, it must be as thin as possible to represent the greater range of temperature and water content experienced by the surface itself than by a thick soil layer. A thickness of between 0.001 and 0.01 m is thought to be thin enough for this layer to respond similar to the very surface and yet thick enough to realistically represent coarse cinder fragments. Because the soil surface is very thin, the latent-heat (and, equivalently, water-vapor) storage is very small and will be neglected.

The **OUTSIDE AIR** (oa) and **SKY** (s) are the external environmental factors in the shade-house model. They are also considered uniform. The outside air will represent the air which is exchanged with the air inside the shade house. The sky above shade house will represent the external environment with which the shade house is in longwave exchange. The characteristics of the outside air and sky are considered to be those at the weather station, where temperature, humidity, wind speed and direction, solar radiation, and rainfall are collected. The weather data collected in this study were measured at a 4-m height, 1 m above the shade house. If such

data are not available, some modification in the model parameterization will be needed.

4.1.3 Sign Convention

The sign convention in the shade-house microclimatic model is that positive values of fluxes indicate that energy or water flows to a system component, and negative values of fluxes indicate that energy or water flows away from a system component. Since energy or water moves between the system components, a flux will simultaneously be positive relative to the component toward which it is flowing and negative relative to the component from which it is flowing. In the figures (Fig. 4.1 and 4.2), the arrows and the subscript order show the direction of the flux being considered; the symbol does not indicate the sign (which varies over time), but as the fluxes are expanded the sign convention is followed.

4.1.4 Energy Balances of the Shade-House Components

The energy balances of the shade-house system components which are considered in this model are illustrated in Fig. 4.1. The energy balance of each system component determines if heat storage occurs and the temperature changes. The component's energy balance is solved for storage and the equations for storage of sensible heat are solved with equations for

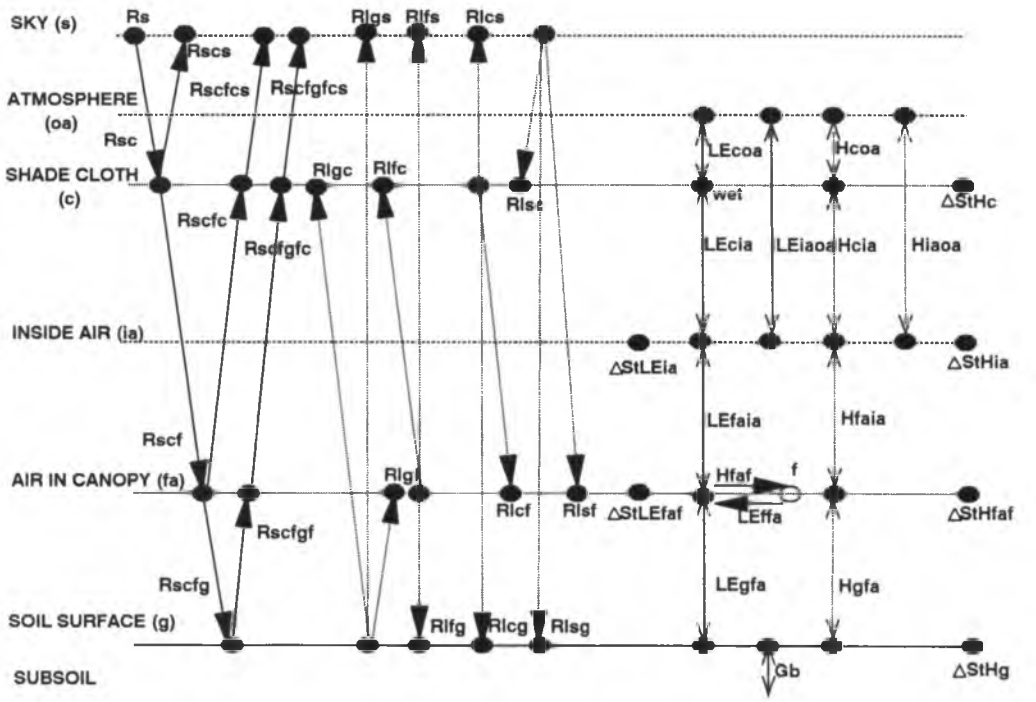

Fig. 4.1 Shade-house system energy balance. Rs is solar radiation or shortwave radiation flux; Rl is longwave radiation flux; H is sensible-heat flux; LE is latent-heat flux; ΔStH is the stored sensible heat; ΔStLE is stored latent heat; s, c, f, oa, ia, fa, and g are the subscripts for sky, shade cloth, crop surfaces, outside air, inside air, air in canopy, and soil surface. Each horizontal line represents a shade-house component or the external environment. Energy fluxes begin and end in the system component designated with a dot. In the absence of a dot, the energy (radiation) passes through the component. The circle is the crop foliage which is the moisture source. For convective transport, indicated by double-headed arrows, the subscripts in the symbol are ordered to indicate first the component to which the sign convention refers; the symbol for only one direction is shown.

storage of water vapor (Section 4.1.5) to determine the temperature change over time. Each component equation will be given and expanded in a later section.

Only the first reflection of solar radiation is taken into account in the model (Fig. 4.1): this is as if reflected radiation goes straight back to its origin without being scattered and only being intercepted by the components though which it passes. All radiation is accounted for. This simplifies the radiation part of the model and introduces only small errors. For instance, if the solar radiation flux density is 1000 W m^{-2} above the shade cloth, the transmittances of the shade cloth and the canopy are each 0.2, and the reflectances of the canopy and the soil are each 0.1, then the radiation flux densities arriving at the canopy and the underlying soil are 200 W m^{-2} and 40 W m^{-2}, respectively. The first reflection from each is 20 W m^{-2} from the canopy up to the shade cloth, and 4 W m^{-2} from the soil surface to the canopy. When this radiation is reflected again, the second reflections will be much less than the first reflections (less than 1 W m^{-2}).

Transmittance in the model means the proportion of solar radiation which passes through the pore (that is, between the fibers) of the shade cloth or the spaces between the leaves. The actual transmittances of the cloth fibers and the anthurium leaves are not considered because the components are considered uniform, but are included in the model's bulk average transmittance terms t_c and t_f. The surface fraction (also called

shading fraction or cover) is 1 - t_c or F_c, 1 - t_f or F_f, and 1 or F_g. Thus, the radiative properties of the surfaces only apply to the surface fraction, where $r + a = 1$ because the transmittances of the surfaces are considered zero.

In the model the components of the shade house are simply described by the surface fraction F or the surface area A when they interact with longwave and shortwave radiation and the liquid water. A_g is the soil area associated with a unit horizontal surface area and its value is 1 m^2. A_c is the fiber area associated with a unit surface area. A_f is the projected area of the crop associated with a unit surface area. The soil surface fraction, F_g, is defined as A_g/A_g and its value is 1. The surface fraction of the cloth, F_c, is defined as A_c/A_g; it is equal to 1 - t_c. The surface fraction of the canopy, F_f, is defined as A_f/A_g; it is equal to 1 - t_f.

This same area, measured in terms of shortwave radiation (Section 3.2.2), is where shortwave radiation is received, longwave radiation is assumed to be emitted and received, and liquid water (rain or dew) is assumed to be intercepted. A slightly different transmitting area would probably be appropriate for each of these fluxes. The transmittance of the cloth for shortwave and longwave presumably varies for these different wavebands, and a liquid water drop is expected to be transmitted differently than light. When radiation passing through the shade house is modeled with bulk transmittances, this assumes that the radiation can be modelled by parallel rays. For example, shortwave radiation received from the cloth and

reflected by the ground goes to the cloth and foliage in proportions according to t_f; and longwave radiation emitted from the ground goes to the cloth and foliage in proportions according to t_f. Some research (for example, Dickinson, 1983 and Sutherland and Bartholic, 1977) indicate a cavity effect makes this approximation not strictly correct.

All the sensible and latent heat fluxes in Fig. 4.1 are along the local gradient, except LE_{iaoa} and H_{iaoa} which represent large-scale gusts and which may occur with or against the local gradient at the shade cloth.

In summary, the energy balances of the four shade-house components will be used to develop equations for predicting the temperature variation over time of the four shade-house-system components (in Section 4.2).

4.1.5 Moisture Balances of the Shade-House Components

The moisture balance of the shade-house system includes the water-vapor balances and the liquid-water balances. These are illustrated in Fig. 4.2. Water-vapor content is expressed in terms of the specific humidity because it is conservative and it relates directly to mass fluxes.

Because the shade-cloth fibers, canopy foliage, and the soil surface can story liquid water and, therefore, are the sources or sinks of water vapor in the air through the processes of condensation and evaporation, their liquid-water balances are needed in order to determine when there is a source and to provide a sink for the water-vapor balances. Irrigation, rain,

drainage, evaporation and condensation, and air exchange with the atmosphere are the factors that influence the liquid-water balance of the shade house. The inside air and the air in the crop canopy do not store liquid water, and liquid-water balances are not needed for these shade-house components.

Water-vapor balances are determined for the inside air and the air in the crop canopy. The changes in water-vapor content of these shade-house components are determined by the evaporation from and the condensation onto the surfaces, and the transport in the air between the components. The other shade-house components, the cloth and the soil, do not have water-vapor balances, because their air layers are extremely thin and have negligible storage.

When the surfaces are wet (as indicated by the liquid-water balances), the water-vapor content of the shade cloth, the canopy leaves, and the soil surface (the first approach in Section 4.2.3) will be a combination of the water-vapor content of the air adjacent to the surface and the saturated water-vapor content calculated based on the surface temperature. The proportion of the saturated and air water-vapor content used in this combination approach is based on the amount of surface covered by liquid water and, for the canopy, the stomatal resistance. The water-vapor content at the soil surface is calculated based on the soil water content (the second approach in Section 4.2.3). When it is dry, the water-vapor content

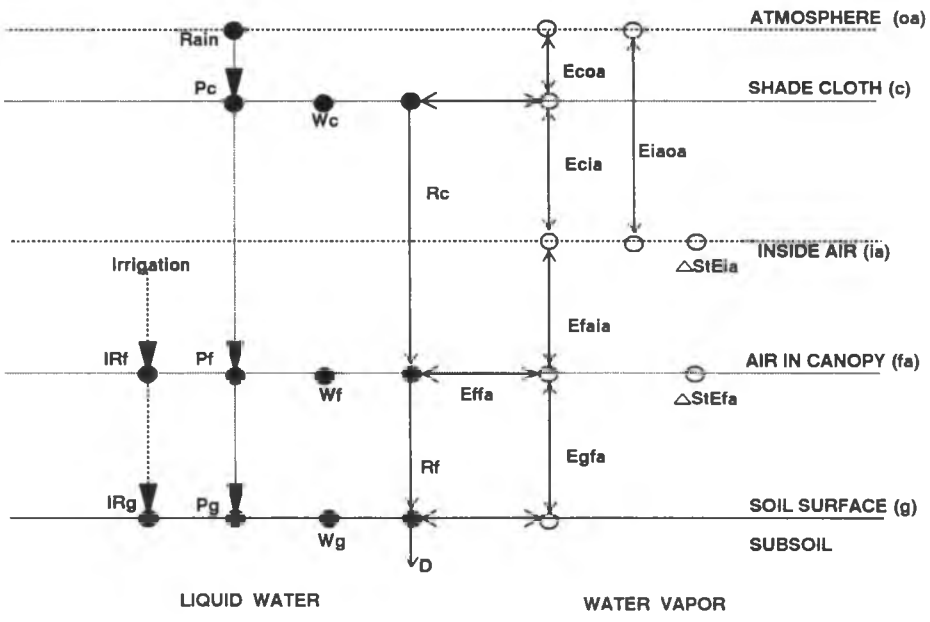

Fig. 4.2 Shade-house moisture balance. P_c, P_f, and P_g are the rain intercepted by the shade cloth, the crop canopy, and the soil surface; IR_f and IR_g are the irrigation intercepted by the crop canopy and the soil surface; R_c and R_f are the liquid water runoff from the shade cloth and crop canopy; D is the drainage; E is the water-vapor exchange between the components in the system; ΔStE is the water-vapor storage; W is the amount of liquid water stored by the component (the absolute amount not the amount stored during the time interval); c, f, oa, ia, fa, and g are the subscripts for shade cloth, crop surface, outside air, inside air, air in canopy, and soil surface. Each horizontal line represents a shade-house component or the external environment. Liquid-water fluxes begin and end in the system component designated with a dot. Water-vapor fluxes begin and end in the system component designated with a circle. The shade cloth only has its own water-vapor content when wet; when dry it has the water-vapor content of the inside air when considered from the inside and of the outside air when considered from the outside. In the absence of a circle or dot, the water vapor or liquid water passes through the component. A horizontal arrow between a dot and a circle represents a water phase change. For convective transport, indicated by double-headed arrows, the subscripts in the symbol are ordered to indicate first the component to which the sign convention refers; the symbol for only one direction is shown.

of the shade cloth will be that of the inside air when considered from the inside and that of the outside air when considered from the outside (it does not have its own storage and, when dry, there is no evaporation). The water-vapor content at the leaves and the soil are determined with the same approach when dry as when they are wet.

This approach for calculating the specific humidity of the surfaces in the shade house is given by Deardorff (1978) for leaf and ground surfaces

$$q = PE\ qs(T) + (1 - PE)\ q_a$$

where q is the specific humidity at the surface; q_a is the specific humidity of the nearby air; PE is the active surface fraction (where PE is the potentially evaporating surface fraction); qs(T) is the saturated specific humidity at the surface temperature T, which is calculated by (Rosenberg et al.,1983)

$$q = 0.622\ e/(P - 0.378\ e)$$

where P is the air pressure (a value of 100 kPa can be used at sea level if no data is available), and where

$$es = 0.61078\ \exp[17.269\ T/(T + 237.3)]$$

PE is an approach to represent the fraction of the surface which is active, that is, to represent liquid water as depositing over the entire surface during condensation, but occupying only a fraction of the surface during evaporation. The stomatal resistance is included in the equation for PE for the crop surface, as described later (Section 4.2.2), so a dry leaf can continue to be a water-vapor source. PE is expanded as

$$PE = 1 - ß[1- (W/W_{max})^{\alpha}]$$

where W is the amount of liquid water on the surface (kg m^{-2}); W_{max} is the water holding capacity of the surface (kg m^{-2}); ß is a switch for evaporation and condensation, so during condensation, that is, when qs(T) is less than q_a and ß is 0, PE is 1, meaning condensation can occur over the entire surface; and during evaporation, that is, when qs(T) is greater than q_a and ß is 1, PE varies from 0 to 1 according to the amount of liquid water on the surface. When W/W_{max} equals 1 and PE equals 1, meaning that the entire surface is wet, the specific humidity of the surface is equal to the saturated specific humidity; when W/W_{max} equals 0 and PE equals 0, meaning the surface is dry, the specific humidity of the surface equals the specific humidity of the nearby air.

α affects the evaporation rate by representing how the surface water is distributed (Fig. 4.3): with α equal to 1, Deardorff found the dew never quite disappears; with α equal to 0, evaporation is too fast and the dew is represented as a continuous thin film which becomes evenly thinner as the water evaporates. Although the value of α is expected to be different for different surfaces with different surface characteristics, an α of 0.667, used by Deardorff for crop canopies, is chosen for shade-house surfaces -- the cloth, the foliage, and the soil surface (approach 1). Because the shade cloth usually is dry, even if this value for α is in error, it will not produce a

large error in the model results. If the depth and surface area of water on the cloth were measured, α could easily be determined for shade cloth.

The energy and water-vapor balances of the shade-house components are coupled through the evaporation or condensation terms which transport water vapor and latent energy between the system components so the water transported by the water-vapor exchange (E terms in Fig. 4.2) is identical to that transported by the latent-heat fluxes (LE terms in Fig. 4.1). When the water-vapor and temperature equations are coupled between water-vapor and temperature, among the water-vapor equations, and among

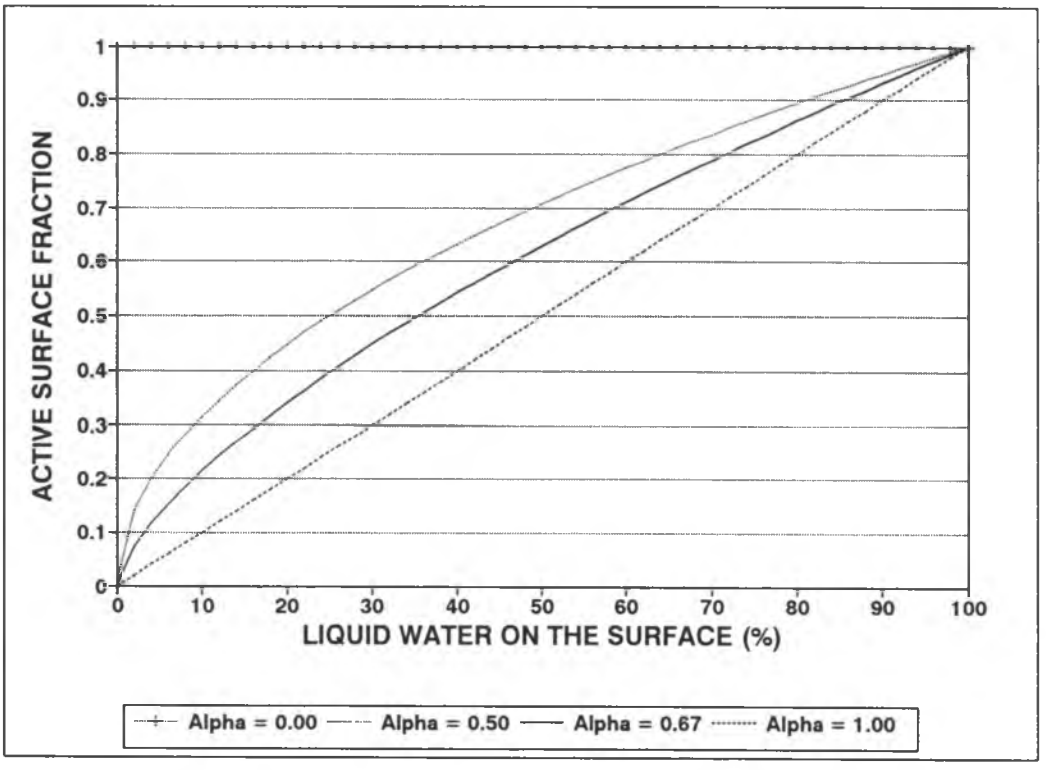

Fig. 4.3 Active surface fraction of the surface (PE) as the function of liquid water on the surface (W).

the temperature equations, and solved simultaneously, the changes in the water-vapor content or temperature of one system component causes changes in other components in the system.

In summary, the two water-vapor balances for two shade-house components, the inside air and the air in canopy, will be used to develop equations for predicting the humidity variation over time of the shade-house--system components; and three liquid-water balances for the shade cloth, the crop foliage, and the ground surface will be developed.

4.1.6 Resistance to Heat and Moisture Transfer in the Model System

In this model, the convective fluxes will be expanded in terms of resistances. The resistances along pathways of sensible heat and water-vapor (and latent-heat) exchange (as shown in Fig. 4.1 and 4.2) for the shade-house model system are illustrated in Fig. 4.4. This discussion will begin with local transport and then will cover non-local transport.

Theoretically, the resistances to sensible-heat and water-vapor exchange can be considered for subincrements of these paths so that, for example, for sensible-heat transport, the laminar-boundary-layer resistance, $r_{h,b}$, and the bulk aerodynamic resistance, $r_{h,a}$, would be in series along paths between the surface and the air

$$r_h = r_{h,b} + r_{h,a}$$

and, analogously, for water-vapor exchange,

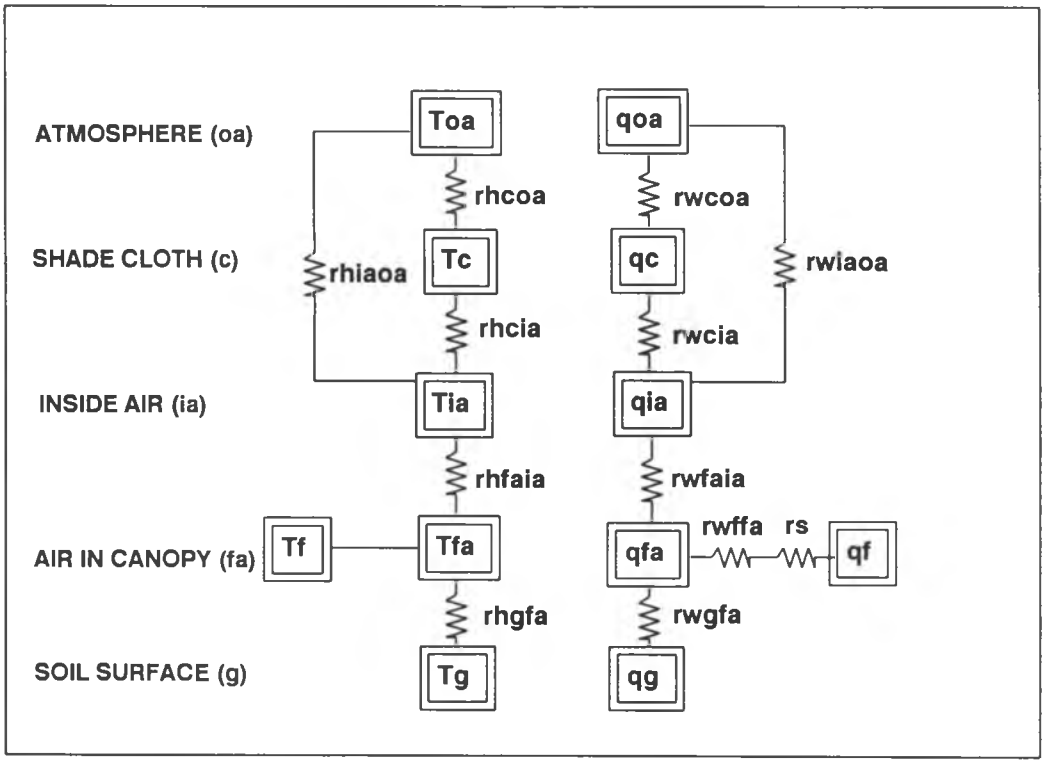

Fig. 4.4 Resistances to sensible heat and water-vapor (and, equivalently, latent-heat) exchange in the shade-house system. q_c, q_{ia}, q_f, q_{fa}, and q_g, are the specific humidities of the cloth, the inside air above the canopy, the foliage, the canopy air, and the soil surface; T_c, T_{ia}, T_f, T_{fa}, and T_g are the temperatures of the shade cloth, the air above the canopy, the plant canopy, the air in the canopy, and the soil surface.

$$r_w = r_{w,b} + r_{w,a}$$

and, for the crop-canopy surface, the stomata resistance, r_s would be taken into account

$$r_w = r_{w,b} + r_{w,a} + r_s$$

In choosing values for resistances for a greenhouse model, Van Bavel et al. (1981) point out that "Values of the heat exchange resistance for the roof interior and the canopy are estimates that vary widely among investigators and will not be constant." They handle the resistances to heat

transfer from the roof to the air and the canopy to the air in a greenhouse by a constant (250 s m^{-1}) based on the assumption that the resistance is independent of wind speed and the temperature gradient between the surface and the air. Rosenberg et al. (1983) indicate that for a vegetated surface, "The resistance r_a may vary from near zero in very turbulent air to about 300-400 s m^{-1} in still air." Oke (1991) gives some representative values of the aerodynamic resistance and canopy resistance for different surface types.

Table 4.1 Representative values of the aerodynamic (r_a) and canopy resistance (r_{canopy}) for different surface types (from Oke, 1991).

Surface	r_a(s m^{-1})	r_{canopy}(s m^{-1})
Open water	200	0
Short grass (pasture)	70	70
Crops	20-50	50
Forests	5-10	80-150

The references cited above indicate that the resistances to heat and water-vapor exchange among the shade-house components and the atmosphere are difficult to estimate appropriately. Therefore overall resistances (except stomatal resistance) will be used for the heat and water-vapor exchange along the model paths. In order to give further basis for selecting reasonable magnitudes for the resistances, resistances for molecular diffusion, resistances from the logarithmic wind profile equation, and the resistances measured for laminar forced convection are compared below based on wind speeds of 0.2 m s^{-1} and 4 m s^{-1}.

For diffusion, the resistance to heat and moisture movement is given by (Campbell, 1977)

$$r_j = L / D_j$$

where L is the distance from the source to the point at which the heat or moisture is measured; and D_j is the diffusivity of heat or water vapor at an air temperature of 20 °C and an air pressure of 100 kPa, which is $21.5*10^{-6}$ $m^2\ s^{-1}$ for heat, D_H, and $24.2*10^{-6}$ $m^2\ s^{-1}$ for water vapor, D_V. If the heat and moisture are measured at a distance of 0.6 m from the source, i.e. the midpoint in the crop canopy in shade house, or L = 0.6 m, the diffusion resistance to heat transfer is

$$r_h = 0.6\ m / 21.5*10^{-6}\ m^2\ s^{-1} = 27910\ s\ m^{-1}$$

From the wind-profile equation in neutral stability, the aerodynamic resistance for the heat and moisture exchange above a surface is described by (Monteith and Unsworth, 1990; Rosenberg et al., 1983)

$$r_h = \{\ln[(z-d)/z_0]\}^2/[k^2 u_z]$$

where u_z is the wind speed at height z (4 m); d is the zero-plane displacement; k is 0.41, the Von Karman constant; and z_0 is the roughness height. Although the shade house with the momentum sink, the shade cloth, at a single height is distinct from the type of system, to which this equation is usually applied such as crop canopies with leaves distributed over height, we apply it to the roof of the shade house. The zero-plane displacement height, d, is the mean level of the momentum absorption.

Since in the shade house, the height of the shade cloth is that of maximum absorption of the momentum (personal communication between E. A. Graser and B. Amiro), a value of 3 m will be used for d. In the absence of wind-profile data, there is no basis for the selection of z_0. If we assume z_0 is 0.01 m, then

$$r_h = \{\ln[(4\ m - 3\ m)/0.01\ m]\}^2/[0.41^2 u_z] = 126.1 / u_z$$

For $u_z = 0.2\ m\ s^{-1}$, $r_{ha} = 630\ s\ m^{-1}$; for $u_z = 4\ m\ s^{-1}$, then $r_{ha} = 31.5\ s\ m^{-1}$.

The resistance to heat exchange for a flat plate with laminar forced convection in a wind tunnel is given by (Campbell, 1977; Rosenberg et al, 1983)

$$r_h = 307(D/U)^{1/2}$$

where r_h is the resistance to heat exchange in $m\ s^{-1}$; D is the characteristic dimension of the object in m; U is the wind speed (in $m\ s^{-1}$) near the surface of the object. Because the turbulence is greater under natural conditions, the resistance to heat exchange is about 60% of the resistance measured in a wind tunnel (Rosenberg et al., 1983; Goudriaan, 1978)

$$r_h = 180(D/U)^{1/2}$$

The characteristic dimension of the anthurium leaves is 0.2 m. When U is $0.2\ m\ s^{-1}$, r_h is $180\ s\ m^{-1}$; when U is $4\ m\ s^{-1}$, r_h is $9\ s\ m^{-1}$.

Measured data provides another basis for selecting resistance values. Using the temperature profile and the sensible-heat-flux-density data

measured above the shade cloth on 11 and 14 January 1992, r_h can be calculated by

$$r_h = C_a (T_c - T_{oa})/H_{coa}$$

where H_{coa} is the sensible-heat flux measured by a one-dimensional sonic anemometer; T_c and T_{oa} are the shade-cloth temperature and the outside air temperature at a 1-m height above the shade cloth. The results shown in Fig. 4.5 indicate that the resistance to heat transport is about 15 s m^{-1} during the day with little dependence on wind speed or solar-radiation levels.

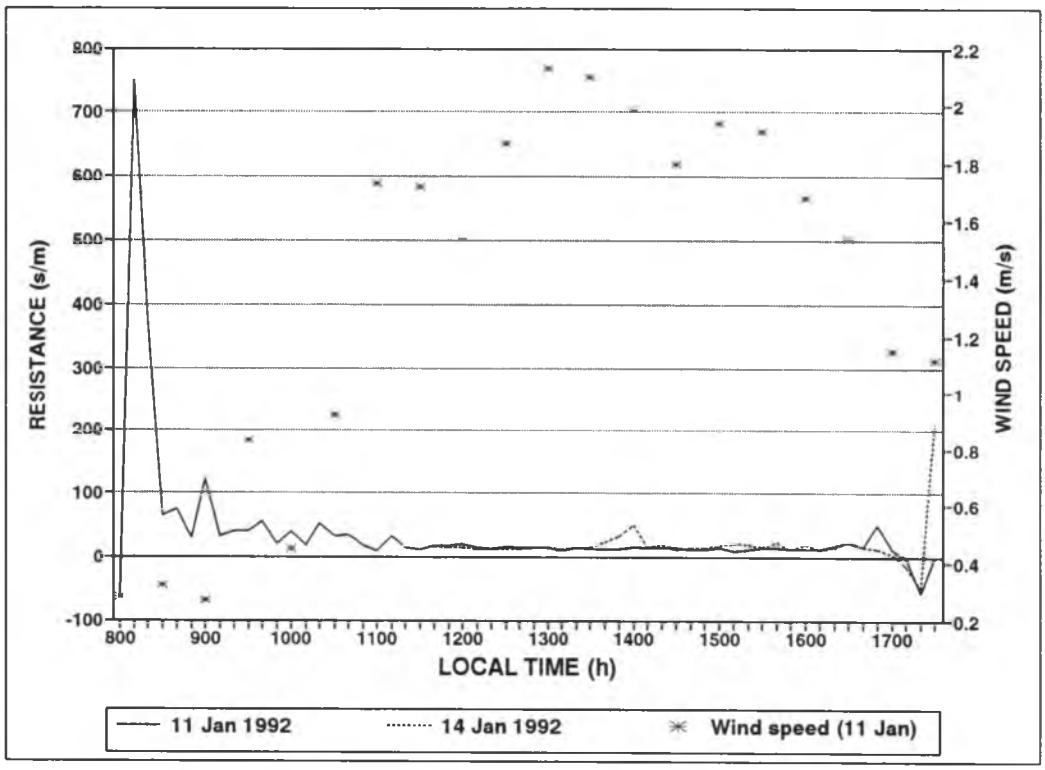

Fig. 4.5 Variation of the resistance to heat transport above the porous shade house on 11 (clear) and 14 (cloudy) January 1992.

The above calculated and measured resistances are similar to or fall into the range of the resistances given by Rosenberg et al., Oke, and Van Bavel et al.. The important role of wind and buoyancy in the exchange of heat and water vapor in the shade house is evident because the resistance is 50 to 60 times smaller when they are effective than with pure molecular diffusion even when the wind speed is only 0.2 m s^{-1}.

In an attempt to provide reasonable resistances for heat and water-vapor transfer for the model pathways shown in Fig. 4.4, which are consistent with the literature and measurements, which are wind-speed dependent, and which include obvious differences in resistance throughout the shade-house system, equations are created with the following characteristics: r_{hcoa} and r_{wcoa} agree to some degree with the logarithmic wind profile for neutral conditions. r_{hcia} and r_{wcia} are 3 times the values for above the shade house since σ_w is reduced by 1/3 by the shade cloth (Graser and Amiro, 1991). r_{hfaia} and r_{wfaia} show more resistance is expected in the crop canopy. More resistance is expected near the crop surfaces, r_{wffa}, and the ground surface, r_{hgfa} and r_{wgfa}, where wind speeds are lowest. The equations for the shade-house model are:

$$r_{wcoa} = r_{hcoa} = 50 - 3.33u$$

$$r_{wcia} = r_{hcia} = 3\, r_{hcoa} = 150 - 10u$$

$$r_{wfaia} = r_{hfaia} = 200 - 10u$$

$$r_{wffa} = 300 - 10u$$

$$r_{wgfa} = r_{hgfa} = 400 - 10u$$

where u is the wind speed at a 4-m height. There is no heat exchange between the canopy foliage and the air in the canopy because we assume their temperature is the same. Because these equations for resistance are mere "educated guesses", the numbers in the equations need to be adjusted to optimize fit when the model results are compared with real data.

These equations cover all the shade-house resistance pathways (Fig. 4.4) which are considered to follow the gradient-diffusion approach. Because the air exchange with the outside air is suppressed by the shade cloth, because a strong, daytime inverted temperature profile occurs below the shade cloth, and because the air exchange can be countergradient and as cool air passes the hot shade cloth in the daytime and is driven primarily by large-scale gusts of wind, the gradient diffusion approach is unable to describe the air exchange between the outside and the inside air in the shade house. Another approach is needed to handle the two remaining pathways with resistances, r_{hiaoa} and r_{wiaoa}, for non-local transport.

The non-local air exchange by large-scale gusts is handled according to the intermittent-refreshment approach Goudriaan (1989) and El-kilani (1991) described for a crop canopy. The air exchange in the shade-house system is envisioned as follows: the shade cloth suppresses the energy and moisture exchange with the outside air; heat and moisture builds up in the shade-house system and the water-vapor content becomes distinct from the

outside air (Graser and Xia (1994a and 1994b) indicate inside water-vapor levels are lower than those outside); eventually a gust breaks through the shade cloth, and comes in replacing some air in the shade house with fresh air from above the shade house and forcing old air out of the shade house. Initially, inside fluxes are promoted by the greater gradients the fresh air causes, but gradually the inside gradients decrease and fluxes decline until the next gust comes in. Through the use of long-distance exchange and a varying resistance to parameterize gusts allows modelling this vision.

This model will continue to work in terms of resistances and not exchange coefficients as El-kilani does. Even though the "gust resistance" is being used in resistance-type equations, the temperature or humidity difference between the endpoints of the path is not the driving force behind the flux and hence this approach only looks like a resistance or a flux-gradient approach. Along the path, the local temperature or humidity difference is unrelated to the non-local flux and can even be opposite in sign. The difference only gives the energy transported between the endpoints.

El-kilani (1991) modelled the gust transport between crop canopy and the atmosphere by introducing non-local transport and parameterizing the transport with a large constant value of the exchange coefficient when a gust is active, and with a small value for the exchange coefficient between gusts; the exchange coefficient changed at a constant frequency (1/300 Hz at night and 1/90 Hz in the day time). The advantage to parameterizing the

local and non-local transport separately, as done by El-kilani, is that the effects of intermittent large-scale transport, that is, large-scale gusts which can occur counter to the gradient, on local small-scale transport, that is, small-scale gusts which follow gradients between large-scale gusts, can be simulated much as it actually happens in the atmosphere; however, because gusts do not actually occur at a constant frequency and a constant intensity, this parameterization of gusts is imperfect.

To determine an appropriate resistance for large-scale gusts for the shade-house model, a simple system is considered conceptually in which the heat stored in the system (in) changes only when part of its air is removed and exchanged with the same volume of outside air (out) at a different temperature. The energy balance of this system indicates that the amount of the energy moved by the exchange (H_{outin}) is the same as the change in the heat storage of the system (ΔStH):

$$\Delta StH = H_{outin}$$

$$C_a V \Delta T_{in}/\Delta t = A C_a (T_{in} - T_{out})/r_{hiaoa}$$

where Δt is the time for the air to be exchanged, that is, the gust duration. With a complete air exchange of the inside air,

$$C_a V (T_{in}-T_{out})/\Delta t = A C_a (T_{in} - T_{out})/r_{hiaoa}$$

If only a fraction of the volume of inside air was exchanged (Fex), the new temperature would be related to the volume of air that was exchanged

$$C_a Fex V (T_{in}-T_{out})/\Delta t + C_a(1-Fex) V (T_{in}-T_{in})/\Delta t = A C_a (T_{in} - T_{out})/r_{hiaoa}$$

Solving for the resistance,

$$r_{hiaoa} = A\, C_a(T_{in} - T_{out})\Delta t/[V\, C_a\, Fex\, (T_{in} - T_{out})]$$

$$= A\, \Delta t/(Fex\, V)$$

$$= \Delta t/(ht\, Fex)$$

where ht is $z_{sh} - z_f$.

This resistance would be appropriate for shade-house gusts, r_{hiaoa} and r_{wiaoa}, although the shade-house system would have other energy exchanges occurring; however, when other energy exchanges are occurring besides H_{iaoa}, the change in inside air temperature, ΔT_{ia}, would be determined by the energy balance of the inside air.

According to the instantaneous vertical wind data from the porous shade house at noontime on 5 August 1992 (see Fig. 4.6), if a vertical wind speed of about 0.3 m s^{-1} is chosen to indicate a non-local gust, then the average non-local gust frequency is about 1/90 Hz, that is, a gust occurs about every 90 seconds. This vertical wind speed threshold yields the same gust frequency as used by El-kilani. Although this frequency is dependent on an untested threshold for defining a non-local gust, it is a useful starting point for selecting an appropriate gust frequency.

For this model, the frequency of gusts will be made dependent on the half-hour mean wind speed u, according to u/180 Hz where the average wind speed between 11 January and 25 March 1992 at the porous shade house of 2.1 m s^{-1} during the day and 0.9 m s^{-1} at night corresponds to an

average frequency of gusts of 1/86 Hz during the day and 1/200 Hz at night.

During gusts with a gust duration of 2 s and an air-exchange fraction, Fex, of 0.2, the gust resistance is

$$r_{hiaoa} = 2 \text{ s}/(0.2*1.8 \text{ m}) = 5.6 \text{ s m}^{-1}$$

Between gusts, the gust resistance is considered to be infinite and no transport occurs.

The gust resistance changes over time, and, thereby, affects the gradient in the house; however, if it had a constant value, for this scenario

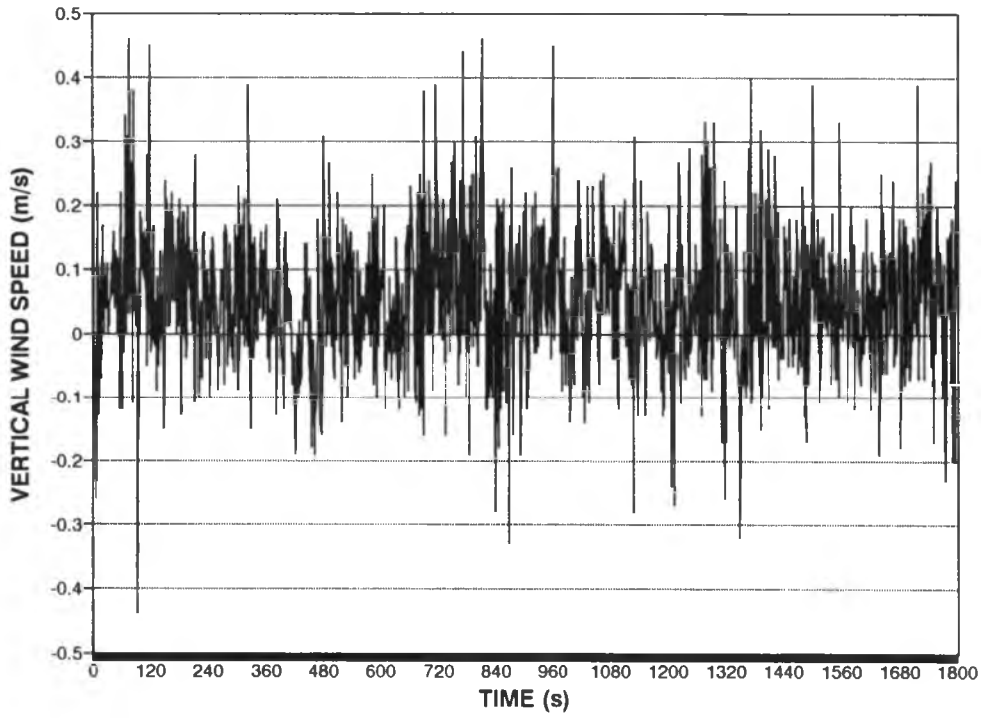

Fig. 4.6 Vertical wind speed in the porous shade house. Data were collected from 1140 h to 1210 h on 5 August 1992 by a 3-dimensional sonic anemometer at a 10-Hz rate. The data time interval in the plot is 1 s, although data were collected at 10 Hz.

with a time interval between gusts of 90 s and an air exchange fraction, Fex, of 0.2, it would be given as:

$$r_{hiaoa} = 90 \text{ s}/(0.2*1.8 \text{ m}) = 250 \text{ s m}^{-1}$$

4.2 BASIC EQUATIONS IN THE SHADE-HOUSE MICROCLIMATIC MODEL

4.2.1 Shade-Cloth Energy Balance

As shown in Fig. 4.1, the energy balance for the shade cloth is described by

$$\begin{aligned} -\Delta StH_c = {} & Rs_c + Rs_{cs} + Rs_{cf} + Rs_{cfc} + Rs_{cfcs} + Rs_{cfgfc} + Rs_{cfgfcs} \\ & + Rl_{sc} + Rl_{gc} + Rl_{fc} + Rl_{cs} + Rl_{cf} + Rl_{cg} \\ & + H_{cia} + H_{coa} + LE_{cia} + LE_{coa} \end{aligned}$$

The equation indicates that the shade cloth influences the energy balance of the shade-house system by absorbing incident solar radiation (that is, the balance of $Rs_c + Rs_{cs} + Rs_{cf}$); by absorbing reflected solar radiation from the canopy ($Rs_{cfc} + Rs_{cfcs}$) and the soil ($Rs_{cfgfc} + Rs_{cfgfcs}$); by absorbing the longwave radiation from the sky (Rl_{sc}), the soil (Rl_{gc}), and the canopy (Rl_{fc}); by emitting longwave radiation upward from the surface to the sky (Rl_{cs}), downward from the surface to the canopy (Rl_{cf}) and the soil (Rl_{cg}); when the shade cloth is wet due to the dew formed at night, by exchanging latent heat with the inside air (LE_{cia}) and the outside air (LE_{coa}); by exchanging sensible heat with inside air (H_{cia}) and outside air (H_{coa}) due to the natural ventilation; and by sensible-heat storage (ΔStH_c). The

combination of letters in the subscripts of the radiation terms indicates the pathway of the radiation in the system. The subscripts of the sensible-heat and latent-heat fluxes indicate between which shade-house components the energy exchange is occurring; the exchange could be in either direction.

Expanding these terms with expressions relating the energy flux densities to measurable properties (according to Section 3.2.2.1),

$$\Delta StH_c = -(W_c c_w + C_{c,dry} V_c)\, dT_c/dt$$

where c_w is the specific heat of water; W_c is the liquid water storage on the shade cloth; $C_{c,dry}$ is the heat capacity of the dry cloth (MJ m^{-3} K^{-1}); V_c is the volume of shade cloth (m^3); T_c is the temperature of the shade cloth.

$$Rs_c + Rs_{cs} + Rs_{cf} = (Rs - F_c r_c Rs - (1 - F_c)Rs) = (1 - r_c)F_c Rs = a_c F_c Rs$$

$$Rs_{cfgfc} + Rs_{cfgfcs} = a_c F_c r_g t_c t_f^2 Rs$$

$$Rs_{cfc} + Rs_{cfcs} = a_c F_c r_f t_c Rs$$

$$Rs = A_g RS$$

where a_c is the absorption of the shade-cloth fibers for shortwave radiation; A_g is the unit area of the soil surface (m^2); F_c is the surface fraction of the cloth; t_c and t_f is the transmissivity of the shade cloth and the crop canopy; r_g, r_f, and r_c are the reflectances of the soil, the canopy, and the shade cloth; RS is the measured solar radiation flux density at the weather station.

$$Rl_{cs} + Rl_{cf} + Rl_{cg} = -2A_c \epsilon_c \sigma (T_c + 273.15)^4$$

$$Rl_{gc} = A_c \epsilon_c (1 - F_f) F_g \epsilon_g \sigma (T_g + 273.15)^4$$

$$Rl_{fc} = A_c \epsilon_c F_f \epsilon_f \sigma (T_f + 273.15)^4$$

where A_c is the cloth fiber area per unit area of the shade cloth (m^2); T_g and T_f are the temperatures of the soil surface and the crop canopy (°C); ϵ_g, ϵ_f, and ϵ_c are the emissivities of the soil surface, the crop canopy, and the shade cloth; F_f and F_g are the surface fractions for the canopy and the ground; and σ is the Stefan-Boltzman constant ($5.6705 * 10^{-8}$ W m^{-2} K^{-4}).

$$RI_{sc} = A_c \epsilon_c RI_s$$

where the longwave radiation from the sky is calculated from the sky temperature

$$RI_s = \epsilon_s \sigma (T_s + 273.15)^4$$

where ϵ_s is emissivity of the sky, and its value is 1; and Ts is the apparent sky temperature (hereafter called sky temperature). The sky temperature can be estimated from the outside air temperature T_{oa} measured at the weather station with a separate equation for a clear sky or cloudy sky (Goudriaan, 1977; Monteith, 1973)

$$T_s = T_{oa}(1 + 0.2) - 21 \qquad \text{clear}$$

$$T_s = T_{oa} - 2 \qquad \text{cloudy}$$

where all temperatures are in °C. The original references use temperature at a 2-m height, but here, the temperature at a 4-m height is used in the calculation of sky temperature. The cloudiness of the sky during the day can be recognized by the comparing the measured solar radiation, RS, to the theoretical solar radiation for the latitude, day of the year, and time (for example, Oke, 1991), or to the mean solar radiation curve for that season

and location. As an example of determining cloudiness for calculation of sky temperature, Fig. 4.7 shows the comparison of measured solar radiation on 11 January 1992 (clear) and on 15 January 1992 (cloudy) to the mean solar-radiation curve during the period from 10 January to 25 March 1992 for the Hilo, Hawaii area. The comparison is only made between 800 h and 1600 h because, with low radiation values before 800 h and after 1600 h, the seasonal effects on the mean can make the comparison inappropriate; for example, clear mornings in January may have similar solar radiation to

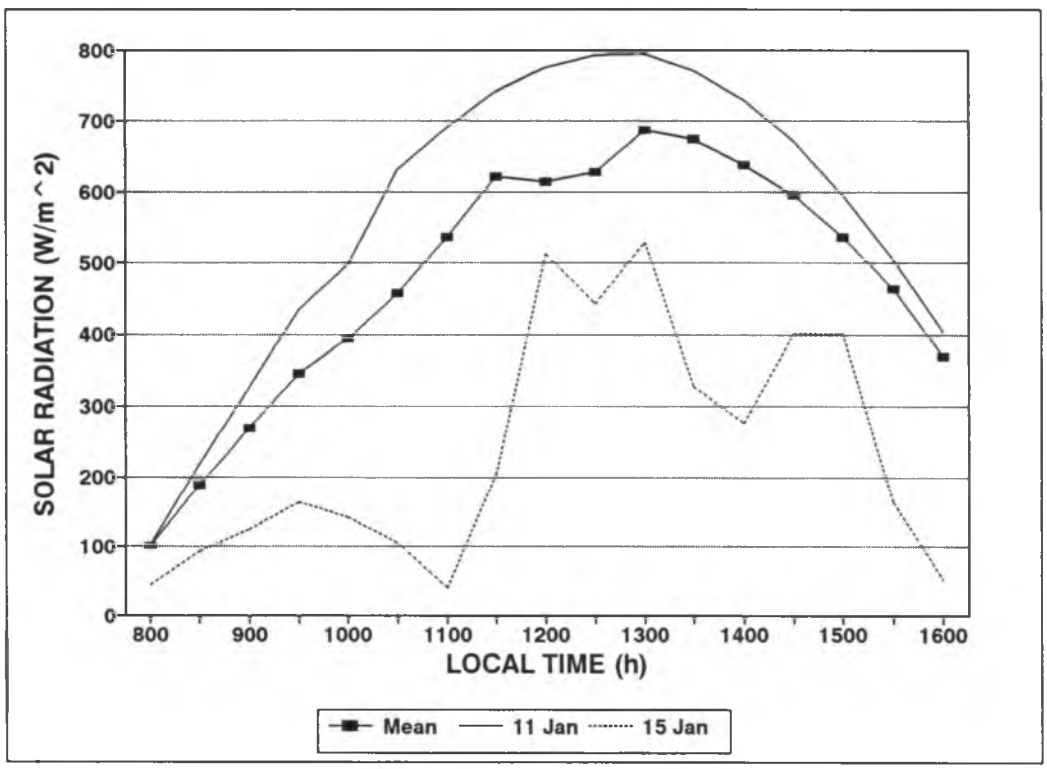

Fig. 4.7 Comparison of the solar radiation on a clear day (11 January 1992) and on a cloudy day (15 January 1992) to the mean solar radiation curve between 10 January and 25 March 1992 for the Hilo, Hawaii area.

cloudy mornings in March. If the ratio of RS(t) to RSmean(t) is greater than a critical value, such as 1 in this case (since the mean contains many cloudy days), then the sky temperature is calculated using the clear sky temperature equation; otherwise, the sky temperature is calculated with the cloudy sky temperature equation.

According to the resistance approach (for example, Campbell, 1977; Goudriaan, 1977), the sensible-heat and latent-heat flux can be calculated by

$$H_{cia} = - C_a A_g (T_c - T_{ia})/r_{hcia}$$

$$H_{coa} = - C_a A_g (T_c - T_{oa})/r_{hcoa}$$

where C_a is the heat capacity of air (J m^{-3} k^{-1}); r_{hcia} and r_{hcoa} are the resistances to heat transport (s m^{-1}); T_{ia} and T_{oa} are the temperatures of the inside air and the outside air; and, when shade cloth is wet,

$$LE_{coa} = - L A_g D_a (q_c - q_{oa})/r_{wcoa}$$

$$LE_{cia} = - L A_g D_a (q_c - q_{ia})/r_{wcia}$$

where r_{wcia} and r_{wcoa} are the resistances to water-vapor transport (s m^{-1}); q_c, q_{oa}, and q_{ia} are the specific humidities of the shade cloth, the outside air, and the inside air (kg kg^{-1}); L is the latent heat of vaporization; otherwise, q_c equals q_{oa} and q_c equals q_{ia}, and the latent-heat fluxes are zero.

The specific humidity q_{oq} is calculated from RH_{oa} by the equations in Section 4.1.5:

$$es = 0.61078 \exp[17.269\ T /(T + 237.3)]$$

$$e = RH * es(T)$$

$$q = 0.622\ e/(P - 0.378\ e)$$

As discussed in Section 4.1.5, the specific humidity of the shade cloth is described by

$$q_c = PEC\ qs(T_c) + (1 - PEC)\ q_a$$

where PEC is the active surface fraction for shade cloth which is given by

$$PEC = 1 - ß[1 - (W_c/W_{cmax})^{2/3}]$$

where W_c is the amount of liquid water on the surface of the shade cloth, W_{cmax} is the water-holding capacity of the shade cloth. When the above equation for q_c is used to calculate the moisture exchange between the cloth and the inside air, then q_a is the specific humidity of the inside air q_{ia}; when it is used to calculate the moisture exchange between the cloth and the outside air, then q_a is the specific humidity of the outside air q_{oa}. This assures that when the shade cloth is dry ($W_c = 0$), the specific humidity of the shade cloth is the same as the specific humidity of the adjacent air so that no evaporation nor storage occurs. When the cloth is wet due to rain or condensation, the wet part of the shade cloth has a saturated specific humidity at the temperature of the shade cloth. The calculation of the saturated specific humidity was given in Section 4.1.5.

The energy balance of the shade cloth is expanded as

$$(W_c c_w + C_{c,dry} V_c)\, dT_c/dt = a_c F_c (r_g Rs\ t_c t_f^2 + r_f Rs\ t_c + Rs)$$
$$+ A_c \epsilon_c [(1 - F_f) F_g \epsilon_g \sigma (T_g + 273.15)^4$$
$$+ F_f \epsilon_f \sigma (T_f + 273.15)^4 + \epsilon_s \sigma (T_s + 273.15)^4]$$
$$- 2A_c \epsilon_c \sigma (T_c + 273.15)^4 - C_a A_g (T_c - T_{ia})/r_{hcia}$$
$$- C_a A_g (T_c - T_{oa})/r_{hcoa} - L\ A_g\ D_a\ (q_c - q_{oa})/r_{wcoa}$$
$$- L\ A_g\ D_a\ (q_c - q_{ia})/r_{wcia} \qquad (4.1)$$

4.2.2 Crop-Canopy Energy Balance

As shown in Fig. 4.1, the crop-canopy energy balance is given by

$$-\Delta StH_{faf} = Rs_{cf} + Rs_{cfc} + Rs_{cfg} + Rs_{cfgf} + Rs_{cfgfc}$$
$$+ Rl_{sf} + Rl_{cf} + Rl_{gf} + Rl_{fc} + Rl_{fg} + Rl_{fs}$$
$$+ H_{fag} + H_{faia} + H_{faf} + LE_{ffa} + LE_{fag} + LE_{faia} + \Delta StLE_{faf}$$

The energy-balance terms of the crop canopy include the incoming shortwave solar radiation at the top of the canopy ($Rs_{cf} + Rs_{cfc} + Rs_{cfg}$); the reflected solar radiation from soil surface to the canopy ($Rs_{cfgf} + Rs_{cfgc}$); the longwave radiation emitted from the sky (Rl_{sf}), the shade cloth (Rl_{cf}), and the soil surface (Rl_{gf}) to the canopy; the longwave radiation emitted by the canopy downward to soil (Rl_{fg}) and upward to shade cloth (Rl_{fc}) and sky (Rl_{fs}); the sensible-heat flux to and from the soil (H_{gfa}); the sensible-heat flux to and from the inside air (H_{faia}); the sensible heat flux to the foliage to allow evaporation (H_{faf}); the latent-heat exchange between the foliage and the air in the canopy (LE_{ffa}); the latent-heat flux from the soil surface (LE_{gfa});

the latent-heat flux between the canopy air and the inside air (LE_{faia}); the sensible-heat storage in the canopy foliage, the canopy air, and the liquid water (ΔStH_{faf}); and the latent-heat storage ($\Delta StLE_{fa}$) in the canopy air.

According to the water-vapor balance of the canopy air (see Section 4.2.6 and Fig 4.2)

$$\Delta StLE_{fa} + LE_{ffa} + LE_{fag} + LE_{faia} = 0$$

The water phase change when water evaporates from the foliage converts some sensible heat into latent heat. Because in this model the crop-canopy energy balance considers the canopy as a whole and the air and foliage are not separated, although the latent-heat flux from the foliage into the canopy air is along a humidity gradient, the sensible heat is not calculable because T_f is assumed to equal the temperature of the air in the canopy T_{fa}; however, LE_{ffa} equals H_{faf} in magnitude, and so H_{faf} is quantified based on LE_{ffa}: $H_{faf} = -LE_{ffa}$.

Expanding the remaining terms in the equation with the expressions below,

$$\Delta StH_{faf} = -(D_f c_w V_f + A_g W_f c_w) dT_{fa}/dt$$

where ΔStH_{faf} is the sensible-heat storage in the canopy foliage, the canopy air, and the liquid water on the foliage (expanded according to Section 3.2.2.2); c_w is the specific heat of water; V_f is the volume of the plants per unit ground area; D_f is the density of the plants; W_f is the liquid water storage on the plants

$$Rs_{cf} + Rs_{cfc} + Rs_{cfg} = F_f a_f t_c Rs$$

$$Rs_{cfgf} + Rs_{cfgf} = F_f a_f r_g t_f t_c Rs$$

where a_f is the absorption of the canopy for shortwave radiation

$$Rl_{sf} = \epsilon_f A_f (1 - F_c) Rl_s$$

$$Rl_{cf} = \epsilon_f A_f F_c \epsilon_c \sigma (T_c + 273.15)^4$$

$$Rl_{gf} = \epsilon_f A_f F_g \epsilon_g \sigma (T_g + 273.15)^4$$

where A_f is the projected leaf area

$$Rl_{fc} + Rl_{fg} + Rl_{fs} = - 2A_f \epsilon_f \sigma (T_f + 273.15)^4$$

$$H_{fag} = - A_g C_a (T_{fa} - T_g)/r_{hgfa}$$

$$H_{faia} = - A_g C_a (T_{fa} - T_{ia})/r_{hfaia}$$

$$H_{faf} = -LE_{ffa} = -L \, PEF \, D_a \, LA(qs(T_f) - q_{fa})/r_{wffa}$$

where LA is the leaf area per unit ground area (m^2) and it has the same value as the leaf-area index; q_{fa} is the specific humidity of the air in the crop canopy; r_{wffa} is the resistance to water-vapor transfer; r_{hgfa} and r_{hfaia} are the resistances to heat transfer; PEF is a function which includes the fraction of the crop surface which is active for evaporation or condensation and the resistance to water-vapor transfer (Section 4.1.5)

$$PEF = 1 - ß[r_s/(r_s + r_{wffa})][1 - (W_f/W_{fmax})^{2/3}] \qquad (4.2)$$

If the leaf is dry ($W_f = 0$) and evaporation is occurring (ß = 1),

$$PEF = 1 - r_s/(r_s + r_{wffa})$$

$$= r_{wffa}/(r_s + r_{wffa})$$

and the equation for evaporation:

$$E_{ffa} = PEF\ D_a\ LA(qs(T_f) - q_{fa})/r_{wffa} \quad (4.3)$$

takes its usual form:

$$E_{ffa} = D_a\ LA(qs(T_f) - q_{fa})/(r_s + r_{wffa})$$

where r_s and r_{wffa} are the resistances along the path in Fig. 4.4.

When the leaf is partly wet, the effect of the stomatal resistance decreases, and evaporation comes from both the liquid water on the foliage and the plant transpiration. When the leaf is totally wet ($W_f = W_{fmax}$), and the stomata are covered, so PEF equals 1, r_s is no longer in the equation

$$E_{ffa} = D_a\ LA(qs(T_f) - q_{fa})/r_{wffa}$$

Evaporation is only from the liquid water standing on the canopy surface. If ß is equal to 0, PEF equals 1, and condensation occurs over the entire foliage.

Because stomatal resistance is not available as a function of environmental factors for potential shade-house crops such as anthuriums, an average diurnal stomatal resistance curve was developed based on the best available data. Measurements of stomatal resistance of potted *Heliconia psittacorum* L.f. Cv Common orange (S.C. Furutani, personal communication to E.A. Graser) and field-grown *Alpinia purpurata* (Vieill.) Kschum. Red ginger (D. Inouye, personal communication to E.A. Graser) showed that the plants close their stomata by mid morning. The general shape of the assumed stomatal resistance curve reflects the response of stomata to solar radiation and water uptake as well as published magnitudes

for stomatal resistance which indicated stomatal resistance may vary from about 50 to 100 s m^{-1} when stomates are wide open to very large values when tightly closed." (Rosenberg et al., 1983). A stomatal resistance of 3000 s m^{-1} is assumed for nighttime.

The heat stored in the crop canopy is given by

$$C_f V_f dT_{fa}/dt = F_f a_f (t_c Rs + r_g t_c t_f Rs) + \epsilon_f A_f [(1 - F_c) Rl_s + F_c \epsilon_c \sigma (T_c + 273.15)^4 + F_g \epsilon_g \sigma (T_g + 273.15)^4] - 2A_f \epsilon_f \sigma (T_f + 273.15)^4 - A_g C_a (T_g - T_{fa})/r_{hgfa} - L\ PEF\ D_a\ LA(qs(T_f) - q_{fa})/r_{wffa} + A_g C_a (T_{fa} - T_{ia})/r_{hfaia} \quad (4.4)$$

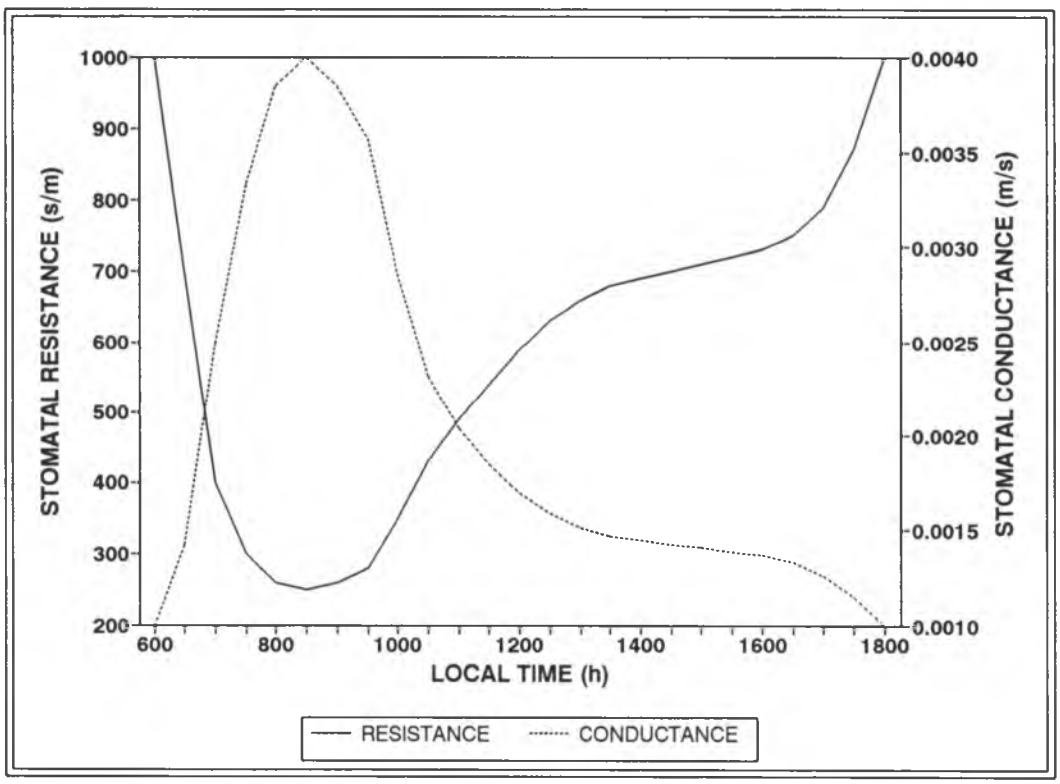

Fig. 4.8 A curve describing the assumed variation of stomatal resistance during the day. The curve is based on the unpublished measured data from several tropical crops.

4.2.3 Soil-Surface Energy Balance

As shown in Fig. 4.1, the soil-surface energy balance can be given by

$$-\Delta StH_g = Rs_{cfg} + Rs_{cfgf} + Rl_{sg} + Rl_{cg} + Rl_{fg} + Rl_{gs} + Rl_{gc} + Rl_{gf} + H_{gfa} + LE_{gfa} + G_b$$

The energy flux into the soil-surface layer includes the shortwave radiation absorbed by soil ($Rs_{cfg} + Rs_{cfgf}$); the longwave radiation from the sky (Rl_{sg}), the shade cloth (Rl_{cg}), and the crop canopy to the soil (Rl_{fg}); the longwave radiation emitted from the soil to the sky (Rl_{gs}), the shade cloth (Rl_{gc}), and the canopy (Rl_{gf}); the sensible-heat flux (H_{gfa}) and the latent-heat flux (LE_{gfa}); the heat conduction between the bottom of the surface soil layer and the underneath soil layer (G_b); and the sensible-heat storage (ΔStH_g).

Expanding these terms,

$$\Delta StH_g = -C_g A_g D_1 \, dT_g/dt$$

where C_g is heat capacity of soil; D_1 is the depth of surface soil layer

$$Rs_{cfg} + Rs_{cfgf} = (1 - r_g)t_f t_c Rs$$

$$Rl_{sg} = A_g \epsilon_g (1 - F_f)(1 - F_c) Rl_s$$

$$Rl_{cg} = A_g \epsilon_g (1 - F_f) F_c \epsilon_c \sigma (T_c + 273.15)^4$$

$$Rl_{fg} = A_g \epsilon_g F_f \epsilon_f \sigma (T_f + 273.15)^4$$

$$Rl_{gs} + Rl_{gc} + Rl_{gf} = - A_g \epsilon_g \sigma (T_g + 273.15)^4$$

$$H_{gfa} = - C_a A_g (T_g - T_{fa})/r_{hgfa}$$

where r_{hgfa} is the resistance to heat transfer between the soil surface and the air in the crop canopy.

$$LE_{gfa} = - L D_a A_g (q_g - q_{fa})/r_{wgfa}$$

where r_{wgfa} is the resistance to water-vapor transfer between the soil surface and the air in the crop canopy; q_g is the specific humidity of the soil surface. Two available methods to determine the specific humidity of the air in the surface soil will be discussed with the advantages and disadvantages of each. In the first method, the soil surface is considered to be part dry with the specific humidity of the overlying air and part wet with the specific humidity of the soil saturated at the surface-soil temperature (Section 4.1.5)

$$q_g = PEG\ qs(T_g) + (1 - PEG)q_{fa}$$

$$PEG = 1 - ß[1- (W_g/W_{gmax})^{2/3}]$$

where W_g is the amount of liquid water in the soil of the surface layer, W_{cmax} is the water holding capacity of the surface-soil layer. A disadvantage of this method is that the soil moisture is not patchy in the sense that water is on smooth surfaces and hence PEG may not work well for the soil especially with the 2/3 exponent. Deardorff (1978), who described this approach, in fact, does not treat condensation on the soil surface by this means, but adds the water to the soil liquid water storage. He points out the benefits of predicting the specific humidity based on the surface soil water content rather than the bulk soil value, so that the surface soil water content can wet up and dry out quickly as is characteristic of this interface and can affect soil evaporation.

In the second method, the specific humidity of the soil surface can be calculated from the soil water content, Θ_v, or soil liquid water storage, W_g. First the soil water potential ψ_g is determined according to the soil water characteristic curve for cinder (Fig. 4.9). Second the RH or $e_g/es(T_g)$ is calculated by (Rosenberg et al., 1983)

$$\psi_g = R\,(T_g + 273.15)/V_w \ln(e_g/es(T_g)) \qquad (4.5)$$

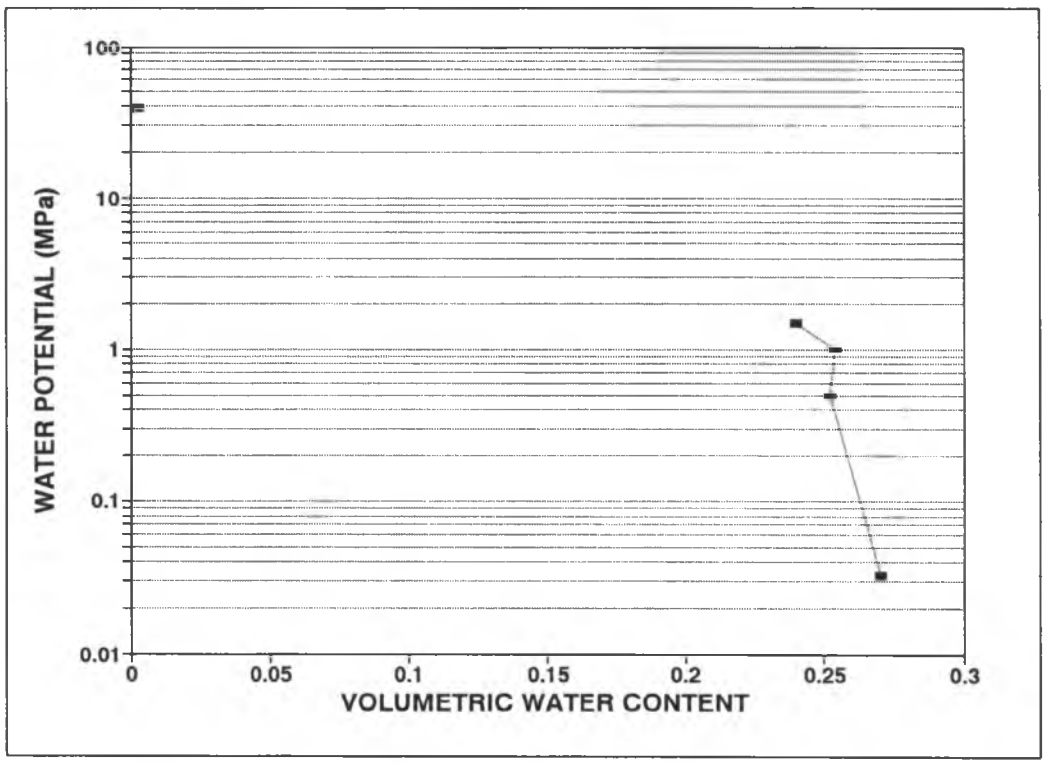

Fig. 4.9 Soil water characteristic curve for volcanic cinder. The water content at 0.5, 1.0, and 1.5 MPa water potential were measured by H. Ikawa (unpublished data). The air-dry water potential was calculated based on Equation 4.5 with a room temperature of 23.4 °C and a relative humidity of 75%. The water potential at field capacity is 0.033 MPa (Jury, 1991); the water content at field capacity was given in Section 3.2.2.3. The pressure chamber may not achieve the reported water potential in the upward-facing, cup-shaped, bubble-type pores on the upper edge of the cinder, if the water in these pores is not interconnected with the ceramic plate (micropores may not be present); the large coarse cinder also had limited contact points with the plate relative to finer textured soils.

where R is the gas constant (8.314 * 10^{-6} m^3 MPa mol^{-1} K^{-1}); V_w is the volume occupied by 1 mole of water vapor, it is 18 * 10^{-6} m^3 mol^{-1} (Campbell, 1977); ψ_g is the soil water potential in MPa; e_g and $es(T_g)$ are the vapor pressure of the air on the soil surface, which can be solved for e_g

$$e_g = es(T_g) \exp\{\psi_g V_w/[R(T_g+273.15)]\}$$

Finally e_g can be converted to q_g by (Rosenberg et al., 1983)

$$q = 0.622\ e/(P - 0.378\ e)$$

This method has the benefit of being physically based; however, the soil water characteristic curve must to be known to calculate the soil water potential and if a shade house had a different growth media (such as bagasse), the curve would be unavailable.

Two available methods for determining the soil heat flux between the surface soil and the subsoil are presented with their advantages and disadvantages. In the first method, a sine-wave approximation is used to give the soil heat flux (Campbell, 1977)

$$G_b = C_g A_{D1}(k_g\omega)^{0.5}\sin[\omega(t-t_0)+\pi/4] \qquad (4.6)$$

where C_g is the soil heat capacity; A_{D1} is the amplitude of the soil temperature wave at depth D1; k_g is the soil thermal diffusivity; ω is the angular frequency given by $2\pi/86400$ s/d; t is the time of day; t_0 is the time shift to bring the sine wave in phase with the temperature wave. The average amplitude A_{D1} is 4.12 °C based on the soil temperature data collected at a 0.005-m depth under the plant row and the soil in the shade

house from 10 January to 25 March 1992; the phase shift, t_0, to bring the sine wave in phase with the measured soil heat flux (see Fig. 4.10) is 4 h * 3600 s/h. For this cinder soil where k_s is 0.67 * 10^{-6} m^2s^{-1} and C_g is 1.5 MJ m^{-3} $°C^{-1}$ (see Section 3.2.2.3), the soil heat fluxes calculated by Equation 4.6 are compared with some measured data in Fig. 4.10. The comparison shows that a disadvantage of the approach is that it is not sensitive to day-to-day variations, for example, the temperature and water content of the soil can vary over time, but the average G_b is the same from day to day. An advantage is that, with appropriate soil constants, it gives a reliable average without detailed data on and a consideration of the subsoil.

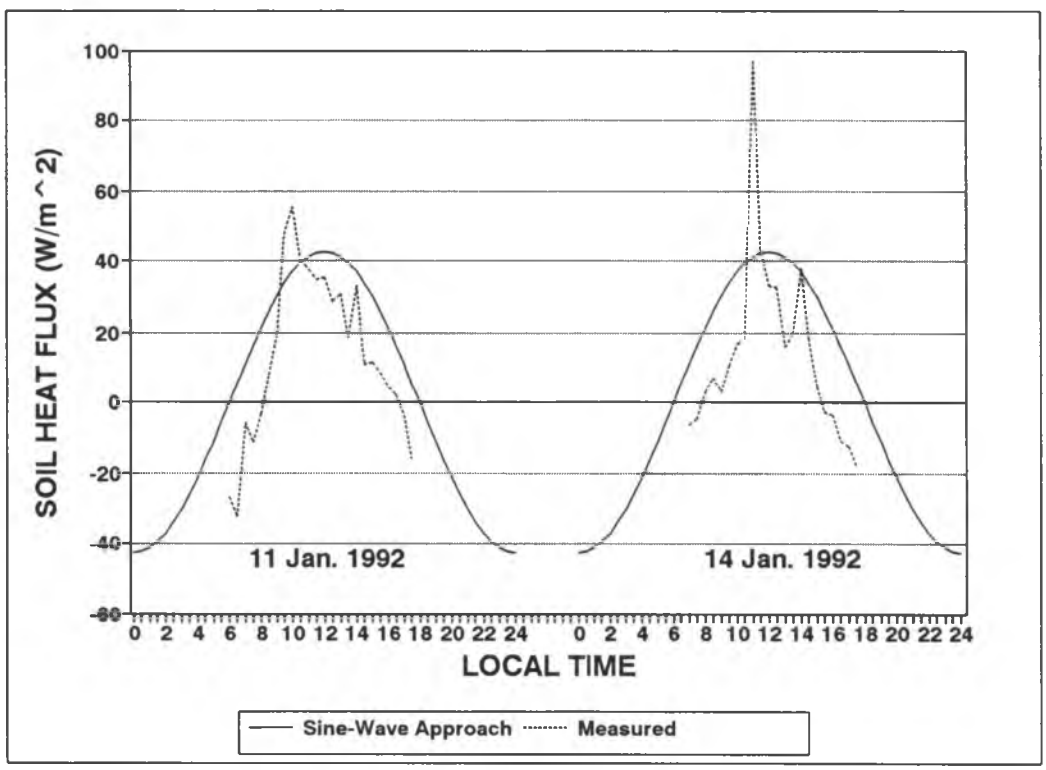

Fig. 4.10 Comparison of predicted soil heat fluxes calculated by the sine-wave approach with the measured soil heat flux. Data were collected in the shade house on 11 and 14 January 1992 on the Island of Hawaii, Hawaii.

It is surprising that the soil heat fluxes in Fig. 4.10 are larger than we expected because only a small amount of solar radiation passes into the shade house. The soil heat fluxes are about 5 to 7% of the net radiation measured above the shade house. Sellers (1965) reported that the soil heat flux varies from 5 to 15 percent of the net radiation for a crop and a grass field and 25 to 30 percent of the net radiation for a bare soil on a clear day. The soil heat flux in the shade house is near the low limit of the soil heat flux for the crop and grass field given by Sellers. A possible reason for the large soil heat fluxes is that, due to the high temperatures in the shade house and the reduced air exchange, more energy goes into the soil-heat flux than the sensible-heat flux. Another possible reason is that there may be measurement error in the soil heat flux measurement.

In the second method, the surface soil heat flux is described in terms of the temperature gradient between the surface and the subsoil according to

$$G_b = - A_g K_g (T_g - T_2)/(z_g - z_2) \qquad (4.7)$$

where T_2 is the temperature of the subsoil layer; z_g is the depth of T_g taken as the middle of the surface layer (depth, negative); z_2 is the depth of T_2 taken as the middle point of the subsoil layer; and $z_g - z_2 = 0.5\ D_2$ where D_2 is the depth of the base of the subsoil layer. D_2 is selected to be 4.67 * d where d is the damping depth so on a daily basis no heat will be lost

deeper into the soil. The method is not tested because there is no available soil temperature data available for testing it.

Two methods to determine T_2 are given. One possibility for determining the value of T_2 is by means of a relationship between the subsoil temperature and the air temperature. For example, T_2 could be assumed to be equal to the mean air temperature over the previous 24 h (Deardorff, 1978), or T_2 could be determined by a correlation between the air temperature and the soil temperature (Ikawa and Kourouma, 1985). If such a relationship is established, T_2 can be easily estimated; however, if the relationship is for an open-air location, the relationship probably is a poor predictor of the soil temperature in a shade house where solar radiation, air temperatures, and air exchange are different than for open air location. Waggoner (1959) reported that a shade house resulted in a 1.5 to 4.0 °C decrease in the temperature at the soil surface compared with outside. Another approach to determining T_2 is to predict the temperature of the subsoil layer by means of the subsoil energy balance (Deardorff, 1978). As shown in Fig. 4.11, if the soil heat flux at the bottom of the subsoil layer is negligible for the daily period due to its sufficient depth (that is, $D_2 = 4.67$ d), the subsoil temperature, T_2, which is the average temperature of the subsoil layer, depends only on the heat flux from surface soil layer into the subsoil layer. T_2 can be described by

$$C_g(D_2-D_1)A_g dT_2/dt = - G_b = K_g A_g (T_g-T_2)/(z_g - z_2)$$

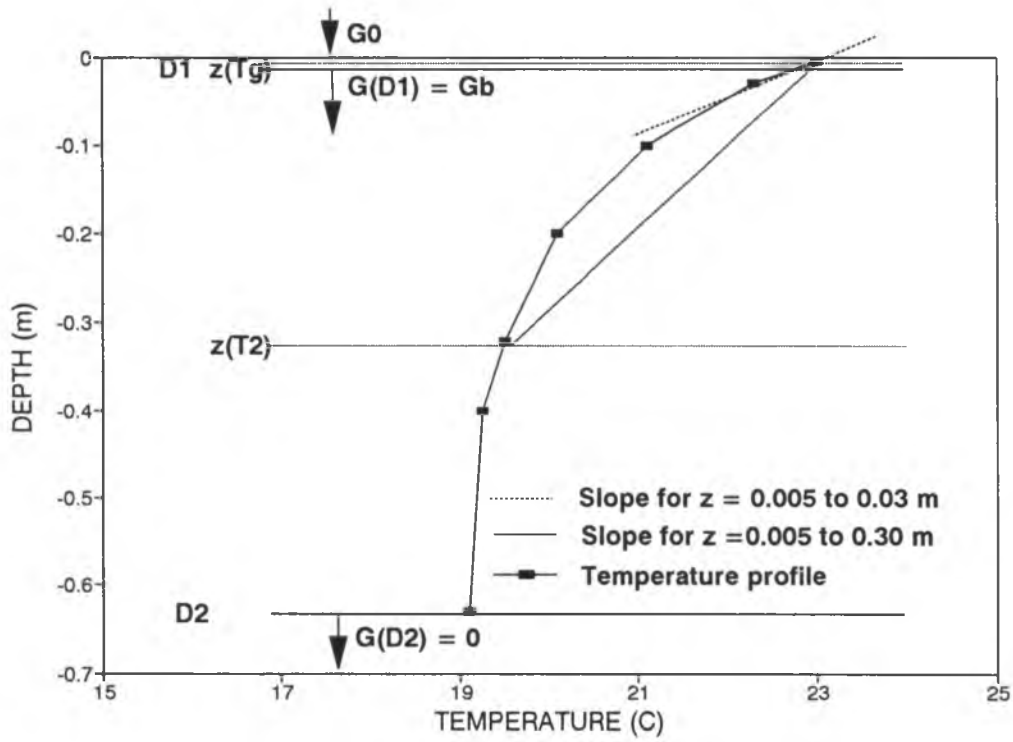

Fig. 4.11 Diagram for the two-layer soil-temperature model. The midpoint of the layers is taken as the depth with the layer-average temperature; the average temperature would actually occur above the middle of the layers. G0 is the soil heat flux into the surface soil layer at $z = 0$ m, G_b is the soil heat flux at depth $D_1 = 0.01$ m.

Together with the soil surface energy balance equation (4.8), initial values, and constants, T_g and T_2 can be predicted.

This second approach has the advantage of allowing G_b to respond day-to-day variations in T_g, but it has the disadvantage of assuming the temperature gradient is linear over a thick layer where it is clearly not linear, and of requiring the temperature of the subsoil layer T_2. There is no assurance that in the second approach to obtaining T_2, that T_2 will take a realistic value.

The energy balance equation of soil surface is given in expanded form by

$$C_g A_g D_1 \, dT_g/dt = (1 - r_g)t_c t_f Rs + A_g \epsilon_g [(1 - F_c)(1 - F_f) Rl_s + (1 - F_f) F_c \epsilon_c \sigma (T_c + 273.15)^4 + F_f \epsilon_f \sigma (T_f + 273.15)^4] - A_g \epsilon_g \sigma (T_g + 273.15)^4 - A_g C_a (T_g - T_{fa})/r_{hgfa} - L D_a A_g (q_g - q_{fa})/r_{wgfa} + G_b \quad (4.8)$$

4.2.4 Energy Balance of the Inside Air

Because air does not absorb shortwave and longwave radiation, the energy balance of the inside air will only depend on the sensible-heat and latent-heat fluxes and storage. The energy balance of the inside air, as shown in Fig. 4.1, is given by

$$-\Delta StH_{ia} = H_{iac} + H_{iafa} + H_{iaoa} + LE_{iac} + LE_{iafa} + LE_{iaoa} + \Delta StLE_{ia}$$

where H_{iac} is the sensible-heat flux between the shade cloth and the inside air; H_{iafa} represents the sensible-heat exchange between the inside air and the air in the canopy; H_{iaoa} represents the sensible-heat exchange between the inside air and the outside air; LE_{iac} is the latent-heat flux between the shade cloth and the inside air; LE_{iafa} represents the latent-heat exchange between the inside air and the air in the canopy; LE_{iaoa} represents the latent-heat exchange between the inside air and the outside air. They are described by

$$H_{iac} = - A_g C_a (T_{ia} - T_c)/r_{hcia}$$

$$H_{iafa} = - A_g C_a (T_{ia} - T_{fa})/r_{hfaia}$$

$$H_{iaoa} = - A_g C_a (T_{ia} - T_{oa})/r_{hiaoa}$$

$$LE_{cia} = - L A_g D_a (q_{ia} - q_c)/r_{wcia}$$

$$LE_{iafa} = - L A_g D_a (q_{ia} - q_{fa})/r_{wfaia}$$

$$LE_{iaoa} = - L A_g D_a (q_{ia} - q_{oa})/r_{wiaoa}$$

where r_{hiaoa} is resistance to heat transfer between the inside air and the outside air; r_{wiaoa} is resistance to water-vapor transfer between the inside air and the outside air. As discussed for the energy balance of the crop canopy, the latent-heat balance of the inside air (see Fig. 4.2 and Section 4.2.5) can be given by

$$-\Delta StLE_{ia} = LE_{iac} + LE_{iafa} + LE_{iaoa}$$

This allows the sensible-heat storage of the inside air to be simplified as

$$-\Delta StH_{ia} = H_{iac} + H_{iafa} + H_{iaoa}$$

Substituting with

$$\Delta StH_{ia} = -C_a V_{ia} \, dT_{ia}/dt$$

the sensible heat storage becomes

$$C_a V_{ia} \, dT_{ia}/dt = - A_g C_a (T_{ia} - T_c)/r_{hcia} - A_g C_a (T_{ia} - T_{fa})/r_{hfaia} - A_g C_a (T_{ia} - T_{oa})/r_{hiaoa} \quad (4.9)$$

4.2.5 Water-Vapor Balance of the Inside Air

The water-vapor content of the air inside the shade house, as seen in Fig. 4.2, depends on evaporation and condensation of liquid water from and

onto the shade cloth (E_{iac}), water-vapor exchange with the air in the canopy by the small-scale turbulence diffusion transport (E_{iafa}) and with the outside air by the large-scale gusts (E_{iaoa}), and the storage of water vapor in the air ($_{\Delta}StE_{ia}$), thus

$$-_{\Delta}StE_{ia} = E_{iac} + E_{iafa} + E_{iaoa}$$

Expanding these terms,

$$_{\Delta}StE_{ia} = -V_{ia}D_a dq_{ia}/dt$$

where V_{ia} is the volume of the inside air or $(z_{sh} - z_f)*1\ m^2$; z_{sh} and z_f are the height of the shade house and the crop canopy, respectively;

$$E_{iac} = -A_g D_a(q_{ia} - q_c)/r_{wiac}$$

$$E_{iafa} = -A_g D_a (q_{ia} - q_{fa})/r_{wfaia}$$

$$E_{iaoa} = -A_g D_a (q_{ia} - q_{oa})/r_{wiaoa}$$

The water-vapor content change over time in the shade house could be given by

$$V_{ia}D_a dq_{ia}/dt = -A_g D_a (q_{ia} - q_c)/r_{wcia} - A_g D_a (q_{fa} - q_{ia})/r_{wfaia} - A_g D_a (q_{ia} - q_{oa})/r_{wiaoa} \quad (4.10)$$

4.2.6 Water-Vapor Balance of the Air in the Crop Canopy

The water-vapor balance of the air in the crop canopy, based on Fig. 4.2, is given by

$$-_{\Delta}StE_{fa} = E_{faf} + E_{fag} + E_{faia}$$

where ΔStE_{fa} is the water-vapor storage in the canopy air; E_{fag} is the water-vapor exchange between soil surface and the air in canopy; E_{faia} is the water-vapor exchange between the inside air and the air in the crop canopy; and E_{ffa} is the water-vapor flux between the foliage and the canopy air.

Expanding these terms,

$$\Delta StE_{fa} = -V_{fa} D_a \, dq_{fa}/dt$$

where V_{fa} is the volume of the air in the crop canopy, or $z_f * 1\ m^2$; z_f is the crop height;

$$E_{ffa} = PEF\ D_a\ LA(qs(T_f) - q_{fa})/r_{wffa}$$

$$E_{fag} = - A_g D_a (q_{fa} - q_g)/r_{wgfa}$$

$$E_{faia} = - A_g D_a\ (q_{fa} - q_{ia})/r_{wfaia}$$

The expanded moisture balance of the air in the crop canopy is

$$V_{fa} D_a \, dq_{fa}/dt = D_a\ PEF\ LA(qs(T_f) - q_{fa})/r_{wffa} - A_g D_a (q_{fa} - q_g)/r_{wgfa} - A_g D_a\ (q_{fa} - q_{ia})/r_{wfaia} \qquad (4.11)$$

4.2.7 Shade-Cloth Liquid-Water Balance

According to Fig. 4.2, the liquid-water balance of the shade cloth is described by

$$W_c(t+dt) = W_c(t) + (P_c + E_{cia} + E_{coa})dt + R_c$$

where $W_c(t+dt)$ and $W_c(t)$ are the amount of liquid water (kg) on the shade cloth at times t and t + dt; dt is the time interval; P_c is the rate of rain (P) intercepted by the shade cloth; R_c is the liquid water from rain or

condensation that exceeds the water-holding capacity of the shade cloth, W_{cmax}, and drops to the crop canopy; E_{cia} and E_{coa} are the water-vapor exchange rates between the shade cloth and the inside air and the outside air, respectively. Evaporation occurs only when the shade cloth is wet from rain or dew. After q_c and q_{ia} have been determined by the simultaneous solution (Section 4.3), E_{cia} and E_{coa} are calculated from

$$E_{coa} = - A_g D_a (q_c - q_{oa})/r_{wcoa}$$

$$E_{cia} = - A_g D_a (q_c - q_{ia})/r_{wcia}$$

P_c is given by

$$P_c = A_c P$$

$$P = D_w * PPT$$

where P is the precipitation rate (kg m^{-2} s^{-1}); PPT is the precipitation rate (m s^{-1}). When $W_c(t) + (E_{cia} + E_{coa} + P_c)dt > W_{cmax}$,

$$R_c = W_{cmax} - [W_c(t) + (E_{cia} + E_{coa} + P_c)dt];$$

otherwise, $R_c = 0.0$

4.2.8 Crop-Canopy Liquid-Water Balance

The liquid-water balance of the crop canopy can be described, as shown in Fig. 4.2, by

$$W_f(t+dt) = W_f(t) + (P_f + IR_f + E_f)dt + R_c + R_f$$

where $W_f(t+dt)$ and $W_f(t)$ are the amount of liquid water (kg) on the crop canopy foliage at times $t+dt$ and t; P_f and IR_f are the rate of rain and irrigation interception by the canopy. These terms are expanded as follows:

$$P_f = P(1 - F_c)A_f$$

$$IR_f = A_f IR$$

where IR is the irrigation rate (kg m^{-2} s^{-1}).

E_f is the evaporation rate of liquid water from the canopy surface. Because E_{ffa} includes both the water evaporated from the leaf surface (E_f) and transpiration (Etr),

$$E_f = E_{ffa} - Etr$$

The difference E_{ffa} - Etr represents evaporation or condensation of liquid water from and to the canopy surface. When ß equals 1 and there is liquid water on leaves ($W_f > 0$), the liquid water will be evaporated from the canopy surface, and the transpiration will not be included. When ß equals 0, the water vapor in the air will be condensed over the entire leaf surface. After q_{fa} is determined by simultaneous solution (Section 4.3), according to Equations 4.2 and 4.3,

$$E_{ffa} = \{1 - ß[r_s/(r_s + r_{wffa})][1 - (W_f/W_{fmax})^{2/3}]\} D_a LA(qs(T_f) - q_{fa})/r_{wffa}$$

and from Deardorff (1978),

$$Etr = ß[r_{wffa}/(r_s + r_{wffa})][1 - (W_f/W_{fmax})^{2/3}] D_a LA(qs(T_f) - q_{fa})/r_{wffa}$$

E_f can be expressed as

$$E_f = \{ 1 - ß[r_s/(r_s + r_{wffa})][1 - (W_f/W_{fmax})^{2/3}]$$

$$- ß[r_{wffa}/(r_s + r_{wffa})][1 - (W_f/W_{fmax})^{2/3}]\} D_a LA(qs(T_f) - q_{fa})/r_{wffa}$$

After rearranging, E_f is given by

$$E_f = \{1 - ß[1 - (W_f/(W_{fmax})^{2/3}]\} D_a LA(qs(T_f) - q_{fa})/r_{wffa}$$

R_f is the amount of water from rain, irrigation, and condensation initially intercepted by higher surfaces running to the soil surface. When $W_f(t) + (IR_f + P_f + E_f)dt + R_c > W_{fmax}$ where W_{fmax} is the water holding capacity of the foliage

$$R_f = W_{fmax} - [W_f(t) + (IR_f + P_f + E_f)dt + R_c];$$

otherwise,

$$R_f = 0$$

4.2.9 Soil-Moisture Balance

Two approaches to the soil water balance are presented and evaluated. The most simplistic is to assume that the soil-water content remains constant over time. Most shade houses in the Hilo, Hawaii area do remain "well-watered" due to rain and/or irrigation. The second approach is to consider the terms in the soil-water balance. The water balance of the surface soil layer, as shown in Fig. 4.2, is

$$W_g(t+dt) = W_g(t) + (P_g + IR_g + E_{gfa})dt + R_f + D$$

where $W_g(t+dt)$ and $W_g(t)$ are liquid-water storage of the soil surface layer (kg) at times $t + dt$ and t; P_g and IR_g are the rate at which precipitation and

irrigation water arrive at the soil after being intercepted by the shade cloth and the crop canopy; R_f is the runoff amount; D is the drainage amount.

$$W_g = \Theta_v D_w D_1 A_g$$

where D_w is the density of water; Θ_v is volumetric water content of surface soil layer; and D_1 is the thickness of the surface soil layer.

$$P_g = P(1 - F_c)(1 - F_f)A_g$$

$$IR_g = IR(1 - F_f)A_g$$

D is the drainage deep into the soil, if the water content of the surface soil layer is greater than the water-holding capacity of the soil, W_{gmax}, where $W_{gmax} = \Theta_{vFC} D_w D_1 A_g$, that is, when

$$W_g(t) + (P_g + IR_g + E_{gfa})dt + R_f > W_{gmax}$$

$$D = W_{gmax} - [W_g(t) + (P_g + IR_g + E_{gfa})dt + R_f]$$

After q_{fa} is determined by simultaneous solution (Section 4.3), E_{gfa} is calculated according to

$$E_{gfa} = - D_a A_g (q_g - q_{fa})/r_{wgfa}$$

This soil-water balance does not consider water conduction upward from the subsoil. This omission probably works well for the cinder soil, because it is coarse and preferential flow is thought to predominate over Darcian flow, which is normal for finer textured soils. The thickness of the surface layer (see Section 4.1.2) is very important, because with this simplified approach it determines how well the soil is modeled: if the layer is too thin, excessive evaporation will reduce the water content too fast and

unreasonably high soil temperatures could result; if the layer is too thick, the (average) water content will not be changed by evaporation and condensation, and the soil temperature will be steady over time instead of corresponding to the three stages of soil drying. With an appropriate thickness and with frequent rewetting by rain and irrigation to "reset" the water content, the three stages of soil drying should be seen.

4.3 NUMERICAL SOLUTION OF SHADE-HOUSE MODEL EQUATIONS

Equations (4.1), (4.4), (4.8), (4.9), (4.10), and (4.11) (with the heat capacity or density constants moved to the other side of the equation) are first-order differential equations which describe the change over time of 6 shade-house system state variables. These equations are coupled through the energy (radiation, sensible heat, and latent energy) and water-vapor exchange between the components of the system: a change in one variable will result in changes in the others. A numerical integration method is needed to solve the equations simultaneously. The Runge-Kutta method, which is one of the most popular methods for the numerical integration of ordinary differential equation, is selected to solve the equations in the shade-house model. The Runge-Kutta method is a single-step method because it only requires knowledge of y_t to predict y_{t+dt} (Atkinson, 1988; James et al., 1977; Cheng, personal communication).

4.3.1 The Runge-Kutta Method

Assume that a dependent variable y changes over time according to the first-order differential equation below

$$dy/dt = F(t,y) \tag{4.12}$$

where dy/dt is the derivative of y over time t; F(t,y) is the expression that is the function of y and t. The solution of Equation 4.12 by means of the fourth-order Runge-Kutta method is expressed as (Atkinson, 1988; James et al., 1977)

$$y_{t+dt} = y_t + (a_1 + 2a_2 + 2a_3 + a_4)dt/6 \tag{4.13}$$

where a_1, a_2, a_3, and a_4 are the function values of F(t,y) at slightly different values of y and t

$$a_1 = F(t,y_t)$$

$$a_2 = F(t+dt/2,\ y_t + a_1dt/2)$$

$$a_3 = F(t+dt/2,\ y_t + a_2dt/2)$$

$$a_4 = F(t+dt,\ y_t + a_3dt)$$

If we know the initial value of y at time t, y at time t+dt can be obtained from Equation 4.13.

4.3.2 Application of the Runge-Kutta Method to the Shade-House Equations

The shade-house model requires six equations (4.1, 4.4, 4.8, 4.9, 4.10, and 4.11) to be solved simultaneously for six unknown variables T_c, T_{ia}, T_{fa}, T_g, q_{ia}, and q_{fa}:

$$dT_c/dt = F1(t,T_c,T_{ia},T_{fa},T_g,q_{ia},q_{fa})$$

$$dT_{ia}/dt = F2(t,T_c,T_{ia},T_{fa},T_g,q_{ia},q_{fa})$$

$$dT_{fa}/dt = F3(t,T_c,T_{ia},T_{fa},T_g,q_{ia},q_{fa})$$

$$dT_g/dt = F4(t,T_c,T_{ia},T_{fa},T_g,q_{ia},q_{fa})$$

$$dq_{ia}/dt = F5(t,T_c,T_{ia},T_{fa},T_g,q_{ia},q_{fa})$$

$$dq_{fa}/dt = F6(t,T_c,T_{ia},T_{fa},T_g,q_{ia},q_{fa})$$

where all the variables have the same meaning as was given previously. The solution of the six equations are given by a fourth-order Runge-Kutta method (James et al., 1977) as

$$T_{c\,t+dt} = T_{c\,t} + (a_1(1) + 2a_2(1) + 2a_3(1) + a_4(1))dt/6$$

$$T_{ia\,t+dt} = T_{ia\,t} + (a_1(2) + 2a_2(2) + 2a_3(2) + a_4(2))dt/6$$

$$T_{fa\,t+dt} = T_{fa\,t} + (a_1(3) + 2a_2(3) + 2a_3(3) + a_4(3))dt/6$$

$$T_{g\,t+dt} = T_{g\,t} + (a_1(4) + 2a_2(4) + 2a_3(4) + a_4(4))dt/6$$

$$q_{ia\,t+dt} = q_{ia\,t} + (a_1(5) + 2a_2(5) + 2a_3(5) + a_4(5))dt/6$$

$$q_{fa\,t+dt} = q_{fa\,t} + (a_1(6) + 2a_2(6) + 2a_3(6) + a_4(6))dt/6 \qquad (4.14)$$

where the expressions of $a_1(j)$, $a_2(j)$, $a_3(j)$, and $a_4(j)$, $j = 1$ to 6 are given by

$$a_1(j) = F_j(t,T_{c\,t},T_{ia\,t},T_{fa\,t},T_{g\,t},q_{ia\,t},q_{fa\,t})$$

$$a_2(j) = F_j(t+dt/2,\ T_{c\,t} + a_1(1)dt/2,\ T_{ia\,t} + a_1(2)dt/2,\ T_{fa\,t} + a_1(3)dt/2,$$
$$T_{g\,t} + a_1(4)dt/2,\ q_{ia\,t} + a_1(5)dt/2,\ q_{fa\,t} + a_1(6)dt/2)$$

$$a_3(j) = F_j(t+dt/2,\ T_{c\,t} + a_2(1)dt/2,\ T_{ia\,t} + a_2(2)dt/2,\ T_{fa\,t} + a_2(3)dt/2,$$
$$T_{g\,t} + a_2(4)dt/2,\ q_{ia\,t} + a_2(5)dt/2,\ q_{fa\,t} + a_2(6)dt/2)$$

$$a_4(j) = F_j(t+dt,\ T_{ct} + a_3(1)dt,\ T_{iat} + a_3(2)dt,\ T_{fat} + a_3(3)dt,$$

$$T_{gt} + a_3(4)dt,\ q_{iat} + a_3(5)dt,\ q_{fat} + a_3(6)dt)$$

4.4 STRUCTURE OF THE MICROCLIMATIC MODEL

The shade-house microclimatic model is structured as shown in Fig. 4.12. First, the physical properties of the shade cloth, the crop canopy, and the soil surface are assigned based on the experimental shade house described in Chapter 3 (Section 3.2.1), or, as available, based on data specific to the shade-house of interest.

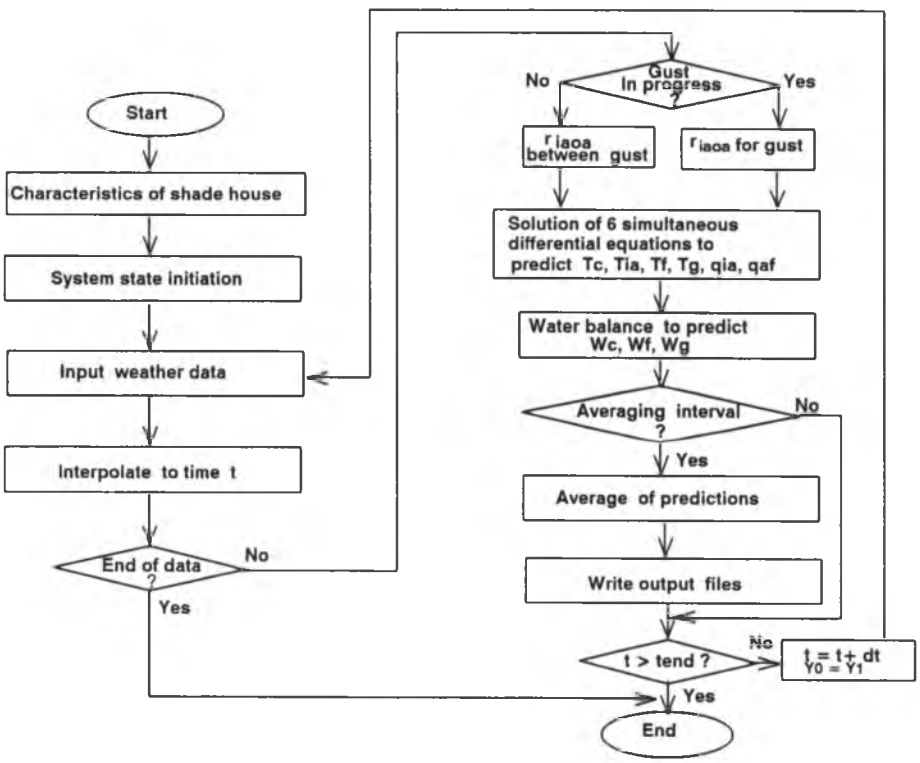

Fig. 4.12 Shade-house microclimatic model flowchart.

Next, initial conditions or values are assigned for the system-state variables: shade-cloth temperature T_c, the inside air temperature T_{ia}, the canopy air temperature T_{fa}, the soil temperature T_g, the specific humidity of the inside air q_{ia}, the specific humidity of the air in crop canopy q_{fa}, the water content of the shade cloth W_c, the water content of the canopy W_f, and the water content of the soil W_g (and possibly the subsoil temperature T_2).

The differences among the values of the system temperatures, which follow diurnal temperature cycles, are smaller in the early morning and late afternoon than in the daytime or at nighttime, because the energy balances of the system components are in transition from net energy gain to net energy loss (in the late afternoon) or the reverse (in the morning). Therefore, the best time to start the simulation model is in the early morning or late afternoon when it would be assumed

$$T_c = T_{ia} = T_{fa} = T_g = T_2 = T_{oa}$$

and

$$q_{ic} = q_{fa} = q_{oa},$$

if the weather data are available, although the model can be started at any time of the day or on any day of the year. To make the model easy to use, initial values for the system components (at $t = 0$) for the daytime and nighttime can be estimated based on the initial weather data and knowledge

of the behavior of the shade-house microclimate (Graser and Xia, 1994 and unpublished data) according to the following equations.

At night time (from 1800 to 700 h)

$$T_c = T_{oa} - 2\ °C$$

$$T_{ia} = T_{fa} = T_{oa} - 1\ °C$$

$$T_g = T_{oa} + 1\ °C$$

and, if needed,

$$T_2 = T_{oa}$$

For the day time (from 700 to 1800 h), the initial temperature of the system components are determined by both of the solar radiation and outside air temperature,

$$T_c = T_{oa} + 4\ °C\ (RS/RS_{max})$$

$$T_{ia} = T_{fa} = T_{oa} + (RS/RS_{max}) * 1\ °C$$

$$T_g = T_{oa} - 2\ °C\ (RS/RS_{max})$$

where the Rs is the solar radiation flux density, RS_{max} maximum solar radiation from the measured data.

The initial value of the specific humidity for the inside air and the air in canopy is calculated based on the assumption that the specific humidity of the inside air and the air in the canopy are 0.005 kPa less than that of the outside air

$$q_{ia} = q_{fa} = q_{oa} - 0.005\ kPa$$

where q_{oa} can be calculated from the relative humidity of the outside air RH_{oa} as described in Sections 4.1.5 and 4.2.1. The initial liquid water storage is zero for the shade cloth and crop canopy,

$$W_c = W_f = 0$$

The initial soil water content, $\Theta_v(t_0)$, is 0.259 and the initial liquid water storage for the soil, W_g, is 0.259 kg to 2.59 kg if D_1 is taken as 0.0001 m to 0.001 m (Section 3.2.2.3 and Section 4.2.9).

The time dependent data, such as the weather data and the irrigation schedule, are read from data files and the data are interpolated to the time-step of the model. A time step of 2 s is thought to be appropriate. A longer value would limit the gust durations available for calculating the large-scale gust transport resistances. These files set the simulation starting time and the simulation time period. The half-hour mean weather data are read from the weather data file, and are linearly interpolated to provide the data for use in the simulation based on the simulation time interval dt. When the weather data is completely used, the simulation is terminate; otherwise, the simulation checks if a large-scale gust is in progress and applies the Runge-Kutta method to solve the six simultaneous coupled differential equations for the system state variables T_c, T_{ia}, T_{fa}, T_g, q_{ia}, and q_{fa} (see Equation 4.14 in Section 4.3.2), which include the energy and water-vapor balance components and transport parameterization. Thus, based on the knowledge of the system state at time t (Y0 in Fig. 4.12), the temperature and moisture

of the shade-house system components are predicted at time t + dt (Y1 in Fig. 4.12) by means of the numerical integration method.

After the simulation completes the Runge-Kutta numerical integration, the liquid-water balances of the shade cloth, the crop canopy, and the soil surface are calculated. When all calculations are finished for that time, the data are recorded to an output file with the data averaged at an appropriate interval. If there are further weather data, the time is advanced one step, and the next weather data are obtained; otherwise the simulation stops.

4.5 LIST OF THE MODEL INPUTS

Following input data are needed in the microclimatic model:

dt	time step	s	2
t_0	time shift	s	4*3600
Weather data:			
RS	shortwave radiation above shade house	W m^{-2}	File
RSmean	mean solar radiation flux density curve	W m^{-2}	Fig.4.7
RS_{max}	maximum solar radiation flux density	W m^{-2}	File
T_{oa}	temperature of air outside shade house	°C	File
RH_{oa}	relative humidity of air outside shade house	%	File
PPT	precipitation rate	m s^{-1}	File
U	horizontal wind speed	m s^{-1}	File
Shade-house description:			
z_{sh}	height of the shade house	m	3.0
Shade cloth characteristics:			
$C_{c,dry}$	heat capacity of the dry shade cloth	J m^{-3} K^{-1}	0.5E6
r_c	albedo of the shade cloth	--	0.06
t_c	transmission of the shade cloth	--	0.17
V_c	volume of the shade cloth for a unit area	m^3	1.75E-5
W_{cmax}	water-holding capacity of the shade cloth	kg	0.096
ϵ_c	emissivity of the shade cloth	--	0.91

Crop canopy characteristics:			
$C_{f,dry}$	heat capacity of the foliage	J m^{-3} K^{-1}	2.7E6
LAI	leaf area index	m^2m^{-2}	1.7
r_f	albedo of the crop canopy	--	0.2
r_s	stomatal resistance	s m^{-1}	Fig. 4.8
t_f	transmission of the canopy	--	0.36
V_f	plant volume in the crop canopy	m^3	0.0033
W_{fmax}	water-holding capacity of canopy	kg	0.043
ϵ_f	emissivity of the foliage	--	0.95
z_f	height of the crop canopy	m	1.2
Soil surface characteristics:			
A_{D1}	amplitude of daily soil temperature wave	°C	4.12
C_g	heat capacity of the soil	J m^{-3} K^{-1}	Eqn.
D_1	depth of base of surface soil layer	m	0.001-0.01*
D_2	depth of base second soil layer	m	0.63
r_g	albedo of the soil surface	--	0.03
ϵ_g	emissivity of the soil surface	--	0.95
Θ_{vFC}	field capacity	m^3 m^{-3}	0.271
K_g	soil heat conductivity	J $m^{-1}K^{-1}s^{-1}$	Eqn.
k_g	soil thermal diffusivity	m^2s^{-1}	0.67E-6
Management data:			
IR	irrigation rate	kg $m^{-2}s^{-1}$	File
Constants:			
C_a	heat capacity of air	J m^{-3} K^{-1}	1200
c_w	specific heat of water	J kg^{-3} K^{-1}	4180
D_a	density of air	kg m^{-3}	1.2
D_w	density of water	kg m^{-3}	1000
L	latent heat of vaporization	J kg^{-1}	2.45E6
ϵ_s	emissivity of sky	--	1.0
σ	Stefan-Boltzman constant	W m^{-2} K^{-4}	5.67E-8

* testing is needed

CHAPTER 5
MODEL EVALUATION

As the model was developed, a lack of good approaches to or data for particular parts of modeling the shade-house system became evident. Evaluating these limitations and the error they can introduce forms a conceptual evaluation of the model. This evaluation is particularly relevant to guiding basic scientific research. A numerical evaluation indicates how well the model performs when compared with measured data. This evaluation shows how accurate the model is internally, which has relevance for scientific research, and how accurately the microclimate can be predicted, which has relevance to practical shade-house design and management. Finally, the model is evaluated to determine how well it will function in its role of allowing simulation of shade-house design and management experiments.

5.1 CONCEPTUAL EVALUATION OF THE MODEL

5.1.1 The Effect of Initial System State and Model Stability Over Time

Because the time constants of the shade cloth, the air, and the crop canopy are very small due to their small heat and moisture storage capacity, the model is not expected to be sensitive to the initial conditions, for example, the temperature, moisture, and water content of the shade cloth,

inside air, and crop canopy, if the time interval is reasonable. The soil has a large heat capacity, but, with a selected thickness of the surface layer of between 0.001 and 0.01 m, the simulation should quickly adjust from the soil water content and the temperature used for initialization to the real conditions. In addition, the values used to initialize the temperature and moisture of the system components in the model should be near the actual values because they are based on the measured outside air temperature and moisture at the starting time of the simulation.

Since predicting the system state at the time t + dt requires the previous condition at time t, it is important to consider if simulation errors in each time step will accumulate and propagate in the simulation results and if there is a time limit to the duration of simulations. Theoretically, there should be no time limit on the simulation duration since the energy and water balances for each component in the shade-house system are well developed for both day and night and the weather data provides an accurate boundary condition over time. The model coupling (feedbacks) can also prevent microclimatic conditions from reaching extreme values, for example, if one component becomes very hot, it loses more longwave energy and energy by sensible-heat convection until its temperature again is close to that of other components. In practice, the model is not perfectly developed and coupled, for example, H_{ffa} is not determined from the temperature of the

components, and one approach to G_b is imperfect and the other approach, which omits T_g, does not couple T_g to the other shade-house components.

The model's short-term usefulness is limited to some extent by the parameterization of large-scale gusts through the gust frequency, volume exchange, and resistance to exchange. These values, which are estimates of averages, cannot allow the model to accurately predict real short-term changes in the shade-house state despite the model's short time interval. Consequently, the instantaneous model predictions should not be considered real (for example, the gust frequency and volume exchange is not really constant over time; gusts are not really abrupt), but the model prediction should be considered over a 20 to 30 min period (as corresponds to the weather data).

5.1.2 Limitations in the Model Parameterizations

The parameterization of transport processes in the model is weak: the values of resistances are mere "educated guesses". When these values are too small or large, the shade-house components will be predicted to be more similar or different than they really are. Further testing of the non-local transport parameters is also needed. El-kilani (1991) said "there is a necessity for a correct separation of the different length scales and their contribution to the total transport" that is, correct parameterization of local and non-local transport. Further model development (Section 5.2.1) will

minimize these errors; other approaches such as turbulence budget closure or Lagrangian approaches to transport may offer certain advantages, but they require turbulence data as inputs which may not be available. Liquid water on the shade cloth should increase r_{iaoa}, but currently it does not; further research may be warranted.

The simple approaches to modeling the soil heat flux (Section 4.2.3) lack accuracy and/or coupling. More elaborate methods with multiple layers, which may work well for a bare soil, are not developed for a shade house using only weather data (no deep soil data) as an input and are inappropriate for this irregular unstudied "soil" underlain by broken rocks or solid rock. The sine-wave approximation may be improved by relating the amplitude of the soil-heat flux to the weather through solar radiation or outside temperature.

The simple approaches to the soil water balance (Section 4.29) should be tested with measured soil-water-content data.

The stomatal resistance for the crop (in the shade-house test case anthuriums) is not related to the weather conditions, but only time on what is thought to represent an average day, because there is an absence of data relating resistance to light, humidity, soil water content, etc. for potential crops. Consequently stomata resistance will not respond to day-to-day variability. For example, under high levels of solar radiation in the absence of water stress, the evaporation from the canopy may be underestimated,

and the temperature of the canopy may be overestimated. The stomatal resistance of potential shade-house plants needs to be studied further in the future to include weather effects.

The longwave radiation from the sky is calculated based on its estimated temperature. To estimate the apparent sky temperature accurately, the degree of cloudiness needs to be known, but these data are not measured directly at the weather station. If the sky cloudiness is erroneously estimated, for example, to be cloudy when it is clear, the calculated longwave radiation from sky will be different than the real radiation. During the daytime, the solar radiation flux density is used to identify the sky cloudiness, but, at nighttime, an approach is still needed.

The failure to model the crop temperature separately from the air temperature in the crop canopy introduced the problem of determining H_{ffa}. The approach we used left the amount of canopy cooling (ΔT) unconnected to the amount of water vapor lost (Δq). Fully separating the canopy into two components -- the plants f and the air in the plant canopy fa -- would require the energy balances of each component to be expanded independently.

5.2 NUMERICAL EVALUATION OF THE MODEL

5.2.1 Further Model Development or Calibration

Two types of data and information are available for further model development or calibration: energy balance data and turbulence characteristics information including instantaneous measurements of wind and temperature and observations of smoke. During further model development, measured energy-balance components (Section 3.2.5) would be compared with computed energy-balance components (Fig. 4.1); and transport parameterization handled by resistances would be improved by further analysis of the turbulence characteristics information (Section 3.2.4). This developmental work is only possible, due to the necessary amount of calculations involved, when the model has been coded in the form of a computer program.

Sensitivity analyses, in which variables are increased and deceased, individually or in groups, can identify which variables have a significant effect on the model results and which warrant further study and measurements.

5.2.2 Model Testing or Validation

When the model has been coded, its predictions of the shade-house condition can be compared with measurements of the shade-house conditions (Section 3.2.3) to determine the model's accuracy.

5.3 FUNCTIONAL EVALUATION OF THE MODEL

The shade-house model provides the conceptual basis for new thinking about shade-house design and management; however, it also has limitations regarding design and management of shade houses.

Long-term historical weather data need to be located for areas where the model may be used to provide an indication of the climatic variability and the resulting long-term performance of the microclimate in the shade house for which shade houses need to be designed and managed. This will be quite valuable in the management of shade houses and the selection of suitable shade-house design under the local climatic conditions.

One of the needs for the microclimatic model, mentioned in Chapter 1, is to evaluate the effect of shade-house design and management, for example, the shade-house height and the shade-cloth properties.

The transmissivity of the shade cloth has a large effect on the temperature of the inside air, the canopy, and the ground surface and possibly the water-vapor levels because it controls how much solar energy penetrates the house and it controls the exchange rate between the inside and outside air. The shade-house model is able to predict the effects of changes in cloth transmissivity if t_c, W_{cmax}, Fex, and r_{iaoa} are provided for the new cloth. The first two (t_c, W_{cmax}) can be determined as described in Chapter 3; the second two (Fex and r_{iaoa}) can be estimated for a small model

shade house with sonic anemometer data according to Section 4.1.6 and Graser and Amiro (1991).

The temperature of the shade cloth and, as a consequence, the temperature of inside air, the crop canopy, and the ground surface are modified by changing the reflectance of the shade cloth due to a reduction of the radiation absorbed by the shade cloth. The model is able to predict the effects of changes in r_c, simply by changing the value of this one variable. (Growers will notice, however, that, as r_c is increased above current levels, t_c will be increased above 0.20).

Because the height of the shade house is related to the volume of inside air, the concentration of heat, and potentially, the wind speed in shade house, changes in the height of the shade house can affect the shade-house microclimate. The model can predict the effect of changing the height of the shade house by changing the value of z_{sh} and possibly the resistances r_{hiaoa}, r_{wiaoa}, r_{hcia} and r_{wcia}.

One simplification made in this model is to assume a component-type system which is between a zero- and a one-dimensional approach. Because this shade-house model is designed only to represent the uniform area at the center of a large shade house, horizontal heat and water-vapor transport are not considered and, hence, the model cannot aid in answering many important design and management questions. This shade-house model cannot predict, for example, energy dynamics at the edges of the shade

house or in a small shade house where large temperature gradients exist and the horizontal transport of heat and moisture cannot be neglected. Practical management questions concern the extent and the magnitude of this edge effect.

Because the microclimatic model is a multiple-component model and it describes the heat and water-vapor exchange between the components, which are assumed to be uniform internally, the model cannot describe the vertical temperature and humidity profile in a shade house to the degree a fully one-dimensional model would. The temperature inversion is an important microclimatic characteristics in a shade house: it suppresses the heat and moisture exchange between inside and outside.

To take into account the horizontal heat and water-vapor exchange and to describe the vertical distribution of heat and water vapor in shade houses, a two-dimensional model will be needed. This is the next major step needed in shade-house modeling.

CHAPTER 6
SUMMARY AND CONCLUSION

6.1 THE SHADE-HOUSE MICROCLIMATIC MODEL

The microclimatic conditions at the center of a large shade house are predicted by the multiple-component shade-house microclimatic model developed here. The model is based on the energy and moisture balances of the components with both long-distance transport described by a parameterization of large-scale, non-local gusts, and local small-scale transport described in terms of the temperature and humidity gradient. Six coupled differential equations for the temperature and the water vapor content of the shade-house components are simultaneously solved numerically. In the model, the physical processes in a large shade house can be calculated quantitatively.

The microclimatic simulation model for a shade house can provide useful information on the microclimate needed for decision making regarding design and management of commercial shade houses, and for research of shade houses. This research represents the first simulation model of the microclimate in a shade house and it is presented here in full detail. It remains to code a working computer program to allow testing of the model with measured data and to make predictions to help solve practical problems. The model should have value now because of the widespread use

of shading in agriculture and horticulture and the need for research into shading.

6.2 AREAS FOR FURTHER RESEARCH

One of the purposes for development of a simulation model is to find out what aspects of the modeled system are poorly understood. As discussed in Chapter 5, a number of areas are poorly understood and need further study.

To improve this model the following areas need better approaches, knowledge, or data:

1) Parameterization of resistances between model components.

2) Prediction of soil heat flux in a shade house based on weather data.

3) Verification of the soil-water-balance approaches with soil-water data.

4) Determination of stomatal resistance as a function of environmental factors for potential crops.

5) Development of an approach to determining cloudiness at night with only weather data.

6) Investigation of the advantages and disadvantages of separating the canopy surface and air space in the model.

The development of a component-type model which can handle the horizontal exchange or a fully two-dimensional model is needed for

prediction near the edges of large houses and throughout small houses. Other types of shade houses, for example covered shade houses, also need to be modeled.

BIBLIOGRAPHY

Alabiso, M., F. Parrini, and S. Vitale. 1984. Greenhouse simulation model "ARCEL" applied to a double-layer inflated polyethylene tunnel using low temperature waste heat. Acta Horticulturea 245:356-362.

Allen, L. H., Jr. 1975. Shade-cloth microclimate of soybeans. Agron. J. 67:175-181.

Atkinson, K. E. 1988. An introduction to numerical analysis. John Wiley & Sons, Inc. New York.

Aylor, D. E., and G. S. Taylor. 1982. Aerial dispersal and drying of *Peronospora tabacina* conidia in tobacco shade tents. Proc. Natl. Acad. Sci. USA. 79:697-700.

Arinze, E. A., G.J. Schoenau, and R. W. Besant. 1984. A dynamic thermal performance simulation model of an energy conserving greenhouse with thermal storage. American Society of Agricultural Engineers. p. 508-519.

Barden, J. A., R. G. Halfacre, and D. J. Parrish. 1987. Plant science. McGraw-Hill, Inc., New York.

Campbell, G. S. 1977. An introduction to environmental biophysics. Springer Verlag, New York.

Deardorff, J. W. 1978. Efficient prediction of ground surface temperature and moisture, with inclusion of a layer of vegetation. Journal of Geophysical Research. 83:1889-1903.

Dickinson, R.E. 1983. Land surfaces, processes, and climate-surface albedos and energy balance. Advances in Geophysics, 25:305-353.

El-kilani, M. M. R. 1991. Some aspects of energy exchange processes in a plant canopy. 20th Conference on Agricultural and Forest Meteorology. p. 3-6.

Frear, W. 1906. Some notes upon the influence of the shelter tent upon temperature and moisture. Penn. Agr. Exp. Sta. Rept. 1904-5. p. 34-38.

Goudriaan, J. 1977. Crop for micrometeorology: a simulation study. Center For Agricultural Publishing and Documentation, Wageningen.

Goudriaan, J. 1989. Simulation of micrometeorology of crop, some methods and their problems, and a few results. Agric. Forest Meteorol. 47:239-258.

Graser, E. A., and B. D. Amiro. 1991. Microclimates and turbulent exchange within Hawaii shade house. 20th Conference on Agricultural and Forest Meteorology. p. 46-49.

Graser, E. A., and H. Xia. 1994a. A comparison of the microclimate in three shade enviroments. 21st Conference on Agricultural and Forest Meteorology. 7-11 March 1994, San Diego, California. p. 42-45.

Graser, E. A., and H. Xia. 1994b. (in press). A comparison of the microclimate under porous cloth, cover, and hapuu. Proc. Sixth Hawaii Anthurium Industry Conf.

Ikawa, H., and L. Kourouma. 1985. Soil temperature classes in soil taxonomy. Soil Taxonomy, Review and use in the Asian and Pacific region. FFTC Book Series No. 29. p. 121-125.

Iwakiri, S., and Z. Uchijima. 1971. Temperature regime and heat transfer in the greenhouse at the daytime. J. Agric. Meteorol., 26:196-207.

James, M. L., G. M. Smith, and J. C. Wolford. 1977. Applied numerical methods for digital computation with FORTRAN and CSMP. Harper and Row Publishers, New York.

Jenkins, E. H. 1900. Can wrapper leaf tobacco of the Sumatra type be raised in Connecticut? Conn. Agr. Exp. Sta. 24th Annual Rpt. p. 322-329.

Jury, W. A., W. R. Gardner, and W. H. Gardner. 1991. Soil physics. John Wiley & Sons, Inc., New York.

Kanemasu, E. T., M. L. Wesely, B.B. Hicks, and J.L. Heilman. 1979. Techniques for calculating energy and mass fluxes. p. 156-182. In Barfield, B. J. and J. K. Gerber. Modification of the aerial environment of plants. American Society of Agricultural Engineers, St. Joseph, Michigan.

Kimball., B. A. 1973. Simulation of the energy balance of a greenhouse. Agric. Meteorol., 11:243-260.

Martsolf, J. D., and H. A. Panofsky. 1975. A box model approach to frost protection research. HortScience 10:108-111.

Meyers, T. P., and K. T. Paw U. 1987. Modelling the plant canopy micrometeorology with higher-order closure principles. Agric. Forest Meteorol. 41:143-163.

Meyers, T. P., and K. T. Paw U. 1986. Testing of a higher order closure model for modeling airflow within and above plant canopies. Boundary Layer Meteorol. 37:297-311.

Monteith, J. L. 1973. Principles of environment physics. Edward Arnold, London.

Monteith, J. L., and M. H. Unsworth. 1990. Principles of environment physics. Edward Arnold, New York.

Norman, J. M. 1979. Modeling the complete crop canopy. p.249-277. In Barfield, B. J. and J. K. Gerber. Modification of the aerial environment of plants. American Society of Agricultural Engineers, St. Joseph, Michigan.

Norman, J. M. 1982. Simulation of microclimate. In Biometeorology in Integrated Pest Management. Academic Press, Inc., New York.

Oke, T. R. 1991. Boundary Layer Climates. Methuen, New York.

Okushima, L., S. Sase, and M. Nara. 1989. A support system for natural ventilation design of greenhouses based on computational aerodynamics. Acta Horticulturae 248:129-136.

Paw U, K. T., and L. T. Meyers. 1989. Investigations with a higher-order canopy turbulence model into mean source-sink levels and bulk canopy resistances. Agric. Forest Meteorol. 47:259-272.

Paw U, K. T., R. H. Shaw, and T. P. Meyers. 1985. Evaporation as modelled by a higher order closure scheme. p. 43-50. In Advances in Evapotranspiration. American Society of Agricultural Engineers, St. Joseph, Michigan.

Purdy, W. H. 1933. Factors influencing the growth of plants in cloth house. Proc. Amer. Soc. Hort. Sci. 30:578-579.

Raupach, M. R. 1989. A practical Lagrangian method for relating scalar concentrations to source distributions in vegetation canopies. Q. J. R. Meteorol. Soc. 115:609-632.

Raupach, M. R. 1989. Applying Lagrangian fluid mechanics to infer scalar source distributions from concentration profile in plant canopies. Agric. Forest Meteorol. 47:85-108.

Rosenberg, N. J., B. L. Blad, and S. B. Verma. 1983. Microclimate- The biological environment. John Wiley & Sons, Inc., New York.

Sellers, William D. 1965. Physical Climatology. The University of Chicago Press., Chicago.

Shantz, H. L. 1913. The effects of artificial shading on plant growth in Louisiana. USDA, Bureau of Plant Industry, Bull. 279:31.

Stathers, R. J., and W. G. Bailey. 1986. Energy receipt and partitioning in a Ginseng shade canopy and mulch environment. Agric. Forest Meteorol. 37:1-14.

Stewart, J. B. 1907. Effects of shading on soil conditions. USDA Bureau of Soils. Bull. 39:19.

Street, J. B. 1907. Effects of shade cloth on light intensity. Conn. Agr. Exp. Sta. Bull. 386:143.

Sutherland, R.A., and J.F. Bartholic. 1977. Significance of vegetation in interpretating thermal radiation from a terrestrial surface. J. Appl. Meteorol. 16:759-763.

Tanner, C.B. 1963. Basic instrumentation and measurements for plant environment and micrometeorology. Soils Bull. 6. University of Wisconsin, Madison.

Thom, A. S. 1975. Momentum, mass, and heat exchange of plant communities. p. 57-109. In Monteith, J. L. Vegetation and Atmosphere. Vol. 1. Academic Press. Inc., New York.

Udink ten Cate, A. J., and J. van de Vooren. 1984. New models for greenhouse climate control. Acta Horticulturea. 148:277-285.

Valli, V. J., and H. W. Young. 1963. Alterations of the biosphere by shading and the resulting effects on two vegetable crops. Fla. State Hort. Soc., Proc. 76:216-225.

Van Bavel, C. H. M., E. J. Sadler, and J. Damagnez. 1980. Analysis of heat and water stress of plants in greenhouses. Acta Horticulturea. 107:71-78.

Van Bavel, C. H. M., J. Damagnez, and E. J. Sadler. 1981. The fluid-roof solar greenhouse: energy budget analysis by simulation. Agric. Meteorol. 23:61-76.

van den Hurk, J. J. M. B. and D. D. Baldocchi. 1990. Random-walk models for simulating water vapor exchange within and above a soybean canopy. NOAA Technical Memorandum ERL ARL-185.

Waggoner, P. E., A. B. Pack, and W. E. Reifsnyder. 1959. The Climate of Shade: A tobacco tent and a forest stand compared to open fields. Connecticut Agric. Exp. Sta. Bull. 626.

Wilson, N. R., and R. H. Shaw. 1977. A higher order closure model for canopy flow. Journal of Applied Meteorology. 16:1197-1205.